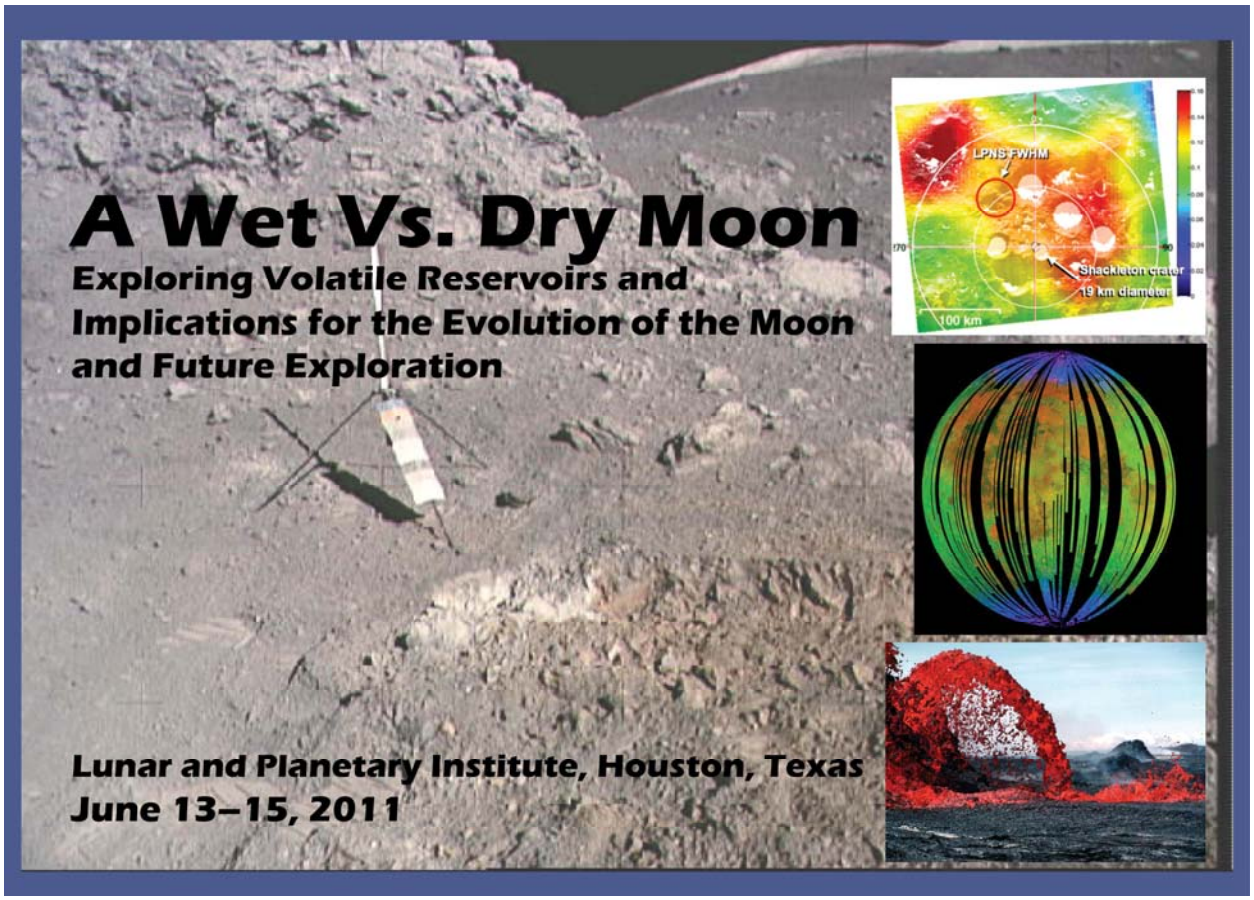

Program and Abstract Volume

LUNAR AND PLANETARY INSTITUTE

LPI Contribution No. 1621

A Wet vs. Dry Moon:
Exploring Volatile Reservoirs and Implications for the Evolution of the Moon and Future Exploration

June 13–15, 2011 • Houston, Texas

Sponsors

Curation and Analysis Planning Team for Extraterrestrial Materials (CAPTEM)
Lunar Exploration Analysis Group (LEAG)
Lunar and Planetary Institute (LPI)
NASA Lunar Science Institute (NLSI)
NASA Ralph Steckler Program

Conveners

Chip Shearer *(University of New Mexico)*
Malcolm Rutherford *(Brown University)*
Greg Schmidt *(NASA Ames Research Center)*

Scientific Organizing Committee

Don Bogard *(Lunar and Planetary Institute-NASA Johnson Space Center)*
Ben Bussey *(John Hopkins University, Advanced Physics Laboratory)*
Linda Elkins-Tanton *(Massachusetts Institute of Technology)*
Penny King *(University of New Mexico*
Gary Lofgren *(NASA Johnson Space Center)*
Francis McCubbin *(University of New Mexico)*
Carle Pieters *(Brown University)*
Paul Spudis *(Lunar and Planetary Institute)*
Edward Stolper *(California Institute of Technology)*
Richard Vondrak *(Goddard Space Flight Center)*
Diane Wooden *(NASA Ames Research Center)*

Lunar and Planetary Institute 3600 Bay Area Boulevard Houston TX 77058-1113

LPI Contribution No. 1621

Compiled in 2011 by

Meeting and Publication Services
Lunar and Planetary Institute
USRA Houston
3600 Bay Area Boulevard, Houston TX 77058-1113

Abstracts in this volume may be cited as

Author A. B. (2011) Title of abstract. In *A Wet vs. Dry Moon: Exploring Volatile Reservoirs and Implications for the Evolution of the Moon and Future Exploration,* p. XX. LPI Contribution No. 1621, Lunar and Planetary Institute, Houston.

ISSN No. 0161-5297

Preface

This volume contains abstracts that have been accepted for presentation at A Wet vs. Dry Moon: Exploring Volatile Reservoirs and Implications for the Evolution of the Moon and Future Exploration, June 13–15, 2011, Houston, Texas.

Administration and publications support for this meeting were provided by the staff of the Meeting and Publication Services Department at the Lunar and Planetary Institute.

Contents

Program

Monday, June 13, 2011
LUNAR POLAR VOLATILES: ENVIRONMENT, DISTRIBUTION, AND BEHAVIOR
8:30 a.m. Lecture Hall

Chairs: **Benjamin Bussey**
Richard Vondrak

8:30 a.m. Bussey D. B. J. * Spudis P. D.
A Review of Lunar Polar Illumination Studies Using Clementine, SMART-1, Kaguya and LRO Data **[#6038]**

8:45 a.m. Mazarico E. * Neumann G. A. Smith D. E. Zuber M. T. Torrence M. H.
Illumination Conditions of the Lunar Poles from Lunar Orbiter Laser Altimeter Data **[#6007]**

9:00 a.m. Speyerer E. J. * Robinson M. S.
Analysis of Highly Illuminated Zones Near the Lunar Poles **[#6054]**

9:15 a.m. Siegler M. A. * Bills B. G. Paige D. A.
Lunar Polar Ice and the Obliquity History of the Moon **[#6045]**

9:30 a.m. Paige D. A. * Siegler M. A. Williams J. P. [INVITED TALK]
Diviner Lunar Radiometer Observations of the North and South Polar Regions of the Moon **[#6058]**

9:45 a.m. Colaprete A. * Heldmann J. Wooden D. H. Mjaseth K. Shirley M. Marshall W. Elphic R. Hermalyn B. Schultz P. [INVITED TALK]
A Model for the Distribution of Volatiles at the LCROSS Impact Site **[#6011]**

10:00 a.m. Lawrence D. J. * [INVITED TALK]
Hydrogen on the Moon: A Summary of Lunar Prospector Neutron Measurements of Lunar Hydrogen Concentrations **[#6027]**

10:15 a.m. Elphic R. C. * Teodoro L. F. A. Eke V. R. Paige D. A. Siegler M. A. Colaprete A.
Implications for the Distribution of Water Ice and Other Volatiles from LCROSS and Lunar Orbital Data **[#6037]**

10:30 a.m. Mitrofanov I. * Litvak M. Sanin A. Golovin D. Boynton W. Chin G. Garvin J. Evans L. Harshman K. Kozyrev A. McClanahan T. Sagdeev R. Shevchenko V. Shvetsov V. Smith D. Starr R. Trombka J. Zuber M. [INVITED TALK]
LRO LEND Observations of Neutrons as Evidence for Polar Hydrogen **[#6029]**

10:45 a.m. McClanahan T. P. * Mitrofanov I. G. Boynton W. V. Droege G. Garvin J. Chin G. Starr R. D. Evans L. G. Sagdeev R. Milikh G. Smith D. E. Zuber M. T. Neumann G. Sanin A. Malakhov A. Litvak M.
Insolation Effects on Lunar Hydrogen: Correlated Observations from LEND and LOLA **[#6022]**

11:00 a.m. Spudis P. D. * Bussey D. B. J. Mini-RF Team
Mini-RF Evidence for Water Ice at the Poles of the Moon **[#6017]**

11:15 a.m. Farrell W. M. * Killen R. M. Vondrak R. R. Hurley D. M. Stubbs T. J. Delory G. T. Halekas J. S. Zimmerman M. I. Dream team L. S. I. [INVITED TALK]
Space Environmental Erosion of Polar Icy Regolith **[#6015]**

11:30 a.m. Hurley D. M. * Elphic R. C. Vondrak R. R. [INVITED TALK]
Modeling of Hydrogen Accumulation at the Lunar Poles **[#6014]**

11:45 a.m. OPEN DISCUSSION lead by Benjamin Bussey and Richard Vondrak

Monday, June 13, 2011
VOLATILES ON THE LUNAR SURFACE
1:30 p.m. Lecture Hall

Chairs: **Penny King**
Diane Wooden

1:30 p.m. Clark R. N. Pieters C. M. Green R. O. Boardman J. Petro N. E. * Buratti B. J. Cheek L. Combe J. P. Dhingra D. Goswami J. N. Head J. W. III Isaacson P. J. Klima R. Kramer G. Livo K. E. Lundeen S. Malaret E. McCord T. B. Mustard J. Nettles J. W. Runyon C. Staid M. Sunshine J. M. Taylor L. A. Thaisen K. Tompkins S. Whitten J. [INVITED TALK]
Mapping Water and Hydroxyl on the Moon as Seen by the Moon Mineralogy Mapper (M^3) **[#6047]**

1:50 p.m. Combe J.-Ph. * McCord T. B. Hayne P. O. Paige D. A.
Mapping of Lunar Volatiles: A Challenging Problem **[#6043]**

2:05 p.m. Gladstone G. R. * Retherford K. D. Stern S. A. Egan A. F. Miles P. F. Versteeg M. H. Slater D. C. Davis M. W. Parker J. Wm. Kaufmann D. E. Greathouse T. K. Steffl A. J. Mukherjee J. Horvath D. Feldman P. D. Hurley D. M. Pryor W. R. Hendrix A. R.
LRO-LAMP Measurements of Far-Ultraviolet Albedos in Permanently Shadowed Regions **[#6057]**

2:20 p.m. Bogard D. D. * [INVITED TALK]
How the Moon Makes Water: A Conceptual View **[#6003]**

2:40 p.m. Farrell W. M. * L.S.I. DREAM Team [INVITED TALK]
The Character of the Solar Wind, Surface Interactions, and Water **[#6016]**

3:00 p.m. Keller L. P. * Noble S. K. Zhang S. Christoffersen R. [INVITED TALK]
The Nature of Space Weathering Effects Recorded in Lunar Materials **[#6059]**

3:20 p.m. Ichimura A. S. * Zent A. P. Quinn R. C. Taylor L. A.
Production of OH/OD in Lunar Samples: Proton/Deuteron Bombardment **[#6053]**

3:35 p.m. Schaible M. J. * Dukes C. A. Mitchell E. H. Baragiola R. A.
Formation of OH/H_2O by 1 keV Proton Irradiation of Apollo 16 Lunar Highland Soil **[#6055]**

3:50 p.m. Baragiola R. A. * Dukes C. A.
On the Simulation of Adsorbed Water on the Moon **[#6049]**

4:05 p.m. Mitchell E. H. * Schaible M. J. Fulvio D. Dukes C. A. Baragiola R. A.
Desorption of Adsorbed Water on the Moon by Photons and Ions **[#6048]**

4:20 p.m. Cooper B. L. * Smith M. C. Gibson E. K.
Thermal Analyses of Apollo Lunar Soils Provide Evidence for Water in Permanently Shadowed Areas **[#6056]**

4:35 p.m. Anand M. * Carpenter J. ESA Topical Team-ELPM
Exploration and Evaluation of Lunar Volatiles as Potential Resource Within the ESA Lunar Lander Context **[#6013]**

4:50 p.m. OPEN DISCUSSION lead by Penny King and Diane Wooden

Monday, June 13, 2011
POSTER SESSION: EXPLORING LUNAR VOLATILE RESERVOIRS
6:00 p.m. Great Room

Starukhina L. V.
Depth of 3-Micron Lunar Absorption Bands: The Effect of Surface Brightness **[#6002]**

Sinitsyn M. P.
Microcomets as a Possible Source of Origin of the Surface Water and Hydroxyl Layer on the Moon **[#6008]**

Pugacheva S. G. Shevchenko V. V.
The Comparison Content of Hydrogen in the Region of the North Pole and South Pole of the Moon **[#6009]**

King P. L. McCutcheon W. A. Shearer C. K. Schofield C. D. M. Lee R. J. Ramsey M. S.
Progress Towards Determining the Temperature of Lunar Glass Beads **[#6012]**

Kochemasov G. G.
A Moon Origin Scenario Justifying the Perceptible Presence of Volatiles in its Body and Moon's Relief Range **[#6001]**

Gustafson J. O. Bell J. F. III Gaddis L. R. Hawke B. R. Giguere T. A. LROC Science Team
Newly Identified Potential Lunar Pyroclastic Deposits **[#6063]**

Desch S. J. Taylor G. J.
A Model of the Moon's Volatile Depletion **[#6046]**

Hurwitz D. M. Head J. W.
Implications of Volatiles Within Lunar Basalts for the Origin of Sinuous Rille Source Depressions **[#6061]**

Clark P. E. Cox R.
Lunar Polar Regions as Solar System Analogs **[#6025]**

Shearer C. K. Sharp Z. D.
Chlorine Isotope Composition of "Rusty Rock" 66095 and Apollo 16 Soil. Implications for Volatile Element Behavior on the Moon **[#6006]**

Sanin A. Mitrofanov I. Boynton W. Golovin D. Evans L. Harshman K. Kozyrev A. Malakhov A. McClanahan T. Litvak M. Milikh G. Mokrousov M. Sagdeev R. Shevchenko V. Schvetsov V. Starr R. Trombka J. Vostrukhin A.
Definition of the LEND-Derived Contours of Neutron Suppressed Region in Cabeus Crater **[#6032]**

Sagdeev R. Mitrofanov I. G. Boynton W. V. Chin G. Droege G. Evans L. G. Garvin J. Harshman K. Litvak M. L. Malakhov A. McClanahan T. P. Milikh G. M. Namkung M. Nandikotkur G. Neumann G. Sanin A. G. Starr R. D. Trombka J. I.
Fine Scale Spatial Variations of Hydrogen Presence from Neutron Counting Over Lunar NSR's **[#6035]**

Hermalyn B. Schultz P. H. Shirley M. Ennico K. Colaprete A.
Scouring the Surface: Ejecta Dynamics and the LCROSS Impact Event **[#6050]**

Droege G. F. Boynton W. V. Mitrofanov I. G.
Neutron Suppressed Regions (NSRs) Using the LRO Neutron Detector Experiment LEND **[#6062]**

Tuesday, June 14, 2011
INDIGENOUS VOLATILE RESERVOIRS
8:30 a.m. Lecture Hall

Chairs: **Francis McCubbin**
Malcolm Rutherford

8:30 a.m. Hirschmann M. * [INVITED TALK]
An Overview of Hydrous Lunar Magmatism, with an Emphasis on the Possible Role of Dissolved Molecular Hydrogen in Lunar Basalts **[#6069]**

8:50 a.m. Jones J. H. *
Lunar Volatiles: An Earth-Moon Perspective **[#6033]**

9:05 a.m. McCubbin F. M. * Shearer C. K. Jr. Elardo S. M. Sharp Z. D.
Magmatic Volatiles in Lunar Apatite: A Hexagonal Prism of Truth or a House of Cards? **[#6051]**

9:20 a.m. Treiman A. H. * Boyce J. W.
Thermochemistry of Apatite and Its Solid Solutions, Apatite-Melt Partitioning, and Implications for the Moon **[#6068]**

9:35 a.m. Boyce J. W. * [INVITED TALK]
Analysis of Volatiles in Apatite: Implications for Quantitative Hygrometry **[#6065]**

9:55 a.m. Nekvasil H. *
New Constraints on the Relative Abundances of Water, F, and Cl in Parental Magmas of KREEP-Bearing Lithologies — Taking Degassing into Account **[#6052]**

10:10 a.m. Liu Y. * Taylor L. A.
Water and Cl in Lunar Basalts: Solubility and Degassing of OH-Cl in Basaltic Magma **[#6030]**

10:25 a.m. Hauri E. H. * Weinreich T. Saal A. E. Rutherford M. C. Van Orman J. A. [INVITED TALK]
Evidence for High Volatile Abundances in Lunar Melt Inclusions **[#6036]**

10:45 a.m. Saal A. E. * Hauri E. H. Rutherford M. J. Van Orman J. A. [INVITED TALK]
The Volatile Contents and D/H Ratios of the Lunar Picritic Glasses **[#6034]**

11:05 a.m. Greenwood J. P. * Itoh S. Sakamoto N. Warren P. H. Dyar M. D.
Taylor L. A. Yurimoto H. [INVITED TALK]
Water in the Moon: Evidence from Hydrogen Isotope Compositions of Lunar Apatite **[#6028]**

11:25 a.m. Monecke T. Andrews-Hanna J. C. * Hinton R. W. Warren P. H. Kempe U. Gotze J.
The Lanthanide Tetrad Effect in Lunar Granites: Evidence for the Occurrence of Water on the Moon? **[#6066]**

11:40 a.m. OPEN DISCUSSION lead by Francis McCubbin and Malcolm Rutherford

Tuesday, June 14, 2011
ROLE OF VOLATILES IN FUNDAMENTAL LUNAR PROCESSES
1:30 p.m. Lecture Hall

Chairs: **Peter Schultz**
John Jones

1:30 p.m. Taylor G. J. * [INVITED TALK]
Water in the Moon: Implications for Lunar Formation and Geochemical Evolution **[#6039]**

1:55 p.m. Stevenson D. J. * [INVITED TALK]
What Do Origin Models Tell Us About Lunar Volatile Depletion **[#6026]**

2:20 p.m. Elkins-Tanton L. T. * Grove T. L.
Water in the Lunar Magma Ocean **[#6024]**

2:40 p.m. Wetzel D. T. * Rutherford M. J. Jacobsen S. D. Hauri E. H. Saal A. E.
Carbon Solubility in Lunar Magmas **[#6040]**

3:00 p.m. Rutherford M. J. * Wetzel D. Hauri E. H. Saal A. E.
Origin and Composition of Lunar Volcanic Gas: The Picritic Glass Model **[#6010]**

3:20 p.m. Ustunisik G. * Nekvasil H. Lindsley D. H.
Experimental Determination of Degassing Paths of Volatiles from Lunar Magmas: New Insights from Time Studies **[#6018]**

3:40 p.m. Shearer C. K. * Burger P. V. Guan Y. Papike J. J. Sutton S. R.
Volatile Element Transport in the Lunar Crust **[#6005]**

4:00 p.m. Schultz P. H. *
Delayed Release and Delivery of Volatiles to Polar Reservoirs **[#6020]**

4:20 p.m. Wooden D. H. * Colaprete A. Heldmann J. L. Retherford K. D. Killen R. M. Elphic R. Ennico K.
Discovery of Heavy Atoms in the Exosphere Above the Permanently Shadowed Region in Cabeus **[#6067]**

4:40 p.m. Teodoro L. F. A. * Elphic R. C. Eke V. R. Siegler M. Schorghofer N.
Constraining Models of Water Migration in the Lunar Subsurface **[#6064]**

4:55 p.m. OPEN DISCUSSION lead by Peter Schultz and John Jones

Wednesday, June 15, 2011
EXPLORATION AND UTILIZATION OF LUNAR VOLATILES
8:30 a.m. Lecture Hall

Chairs: **Charles Shearer**
Greg Schmidt

8:30 a.m. Lofgren G. E. * [INVITED TALK]
Special, Unopened Lunar Samples: Another Way to Study Lunar Volatiles **[#6041]**

8:55 a.m. Shearer C. K. * Neal C. R.
A Consortium to Study "Special" Lunar Samples. Exploring Volatile Reservoirs on the Moon Now and Preparing for Future Lunar Exploration **[#6021]**

9:10 a.m. Calaway M. J. * Allen C. C.
Cold and Cryogenic Curation of Lunar Volatile Samples Returned to Earth **[#6004]**

9:25 a.m. Litvak M. L. * Mitrofanov I. G. Sanin A. B. Boynton W. V. Chin G. Garvin J. B. Golovin D. V. Evans L. G. Harshman K. Kozyrev A. S. Malakhov A. V. McClanahan T. Milikh G. Mokrousov M. I. Sagdeev R. Z. Shevchenko V. V. Shvetsov V. N. Smith D. E. Starr R. Tretyakov V. I. Trombka J. Varenikov A. B. Vostrukhin A. A. Zuber M. T.
Properties of Moon PSRs from LEND/LRO Data **[#6044]**

9:40 a.m. Plescia J. B. * [INVITED TALK]
Lunar Robotic Exploration Objectives in the Next Decade **[#6019]**

10:05 a.m. Quinn J. W. * Larson W. E. Sanders G. B. Baird R. S. Colaprete A. Picard M.
RESOLVE — A Payload to Groundtruth the Presence of Volatiles on the Moon **[#6023]**

10"20 a.m. Gibson E. K. * Pillinger C. T. McKay D. S. Waugh L. J.
Volatile Analyzer for Lunar Polar Missions **[#6031]**

10:35 a.m. Sanders G. B. * Larson W. E. [INVITED TALK]
The Impact of Lunar Polar Volatiles on In-Situ Resource Utilization **[#6060]**

11:00 a.m. Harris R. S. * Schultz P. H.
The Potential of Impact Melts as a Lunar Water Reservoir **[#6042]**

11:15 a.m. OPEN DISCUSSION lead by Charles Shearer and Greg Schmidt

EXPLORATION AND EVALUATION OF LUNAR VOLATILES AS POTENTIAL RESOURCE WITHIN THE ESA LUNAR LANDER CONTEXT. M. Anand[1,2], J. Carpenter[3] and the ESA Topical Team on the Exploitation of Local Planetary Materials (TT-ELPM)*, [1]Centre for Earth, Planetary, Space and Astronomical Research (CEPSAR), The Open University, Walton Hall, Milton Keynes, MK7 6AA, UK (m.anand@open.ac.uk), [2]Department of Mineralogy, The Natural History Museum, London, SW7 5BD, UK, [3]European Space Agency, ESA-ESTEC, Keplerlaan 1, 2201 AZ Noordwijk , The Netherlands.

The European Space Agency (ESA) Topical Team on Exploitation of Local Planetary Materials (TT-ELPM) is investigating the viability of lunar volatiles as a potential resource for future exploration activities and the possible application of the ESA Lunar Lander [1,2] to help address unknowns on the abundance and distribution of volatiles on the Moon. The ESA Lunar Lander is a mission currently being investigated within the Human Space Flight Directorate of ESA, as a precursor mission to future exploration of the Moon. A candidate payload for the mission will measure lunar volatiles *in-situ*. We report on the findings of the Topical Team to date, in terms of the potential applications of lunar volatiles for exploration, the unknowns associated with the composition, abundance, distribution and extraction of those volatiles and the potential of the ESA Lunar Lander to address some of these issues.

Additional information: The members of the TT-ELPM are: **Mahesh Anand**, The Open University, UK; **Marianne Balat-Pichelin,** PROMES-CNRS, France; **Claudio Bruno,** University of Rome, Italy; **Ian Crawford**, Birkbeck College, University of London, UK; **Vincent Eke,** Durham University, UK; **Ralf Jaumann,** DLR, Germany; **Caroline Lange,** DLR, Germany; **Wim van Westrenen,** VU University Amsterdam, The Netherlands.

References: [1] J.D. Carpenter et al., Objectives and payload for human exploration preparation on ESA's first Lunar Lander, Proc. IAC, Prague, September 2010, IAC-10.A3.2B.9. **[2]** A. Pradier et al., The First European Lunar Lander and the ESA DLR approach to its development, Proc. IAC, Prague, September 2010, IAC-10.A3.2B.8.

ON THE SIMULATION OF ADSORBED WATER ON THE MOON. Raúl A. Baragiola and Catherine A. Dukes, University of Virginia, Laboratory for Atomic and Surface Physics, Thornton Hall, Charlottesville, VA 22904. E-mails: raul@virginia.edu, cdukes@virginia.edu.

Introduction: Water can be formed by combining implanted solar wind protons with oxygen in lunar soil. The question of how *likely* this effect is was renewed by recent observations of ~3 μm structure in infrared spectra of three different spacecraft [1-3]. The fact that such structures were not observed by previous studies using Galileo and Clementine [4] remains unexplained.

Recent experiments: In our laboratory, careful *in situ* studies of proton irradiation of minerals [5] found no evidence for the amounts of water required to explain the 2009 reports. Baragiola and Dukes [6] suggested that the origin of global surface water could be ejecta from the ice in polar cold traps evidenced by LCROSS [7]. Water molecules released by meteoritic or ionic impact, or thermal desorption, will hop across the lunar surface by surface-exosphere diffusion assisted by photodesorption and sputtering, in a non-random walk affected by temperature and solar exposure. A similar idea was advanced independently by Farrell et al [8]. In addition, surface water may originate from sub-surface water deposited by accumulated cometary impacts [6, 9].

Notes on laboratory simulations: There are many differences between laboratory mineral or rock samples and lunar soil, the question is which ones are relevant to the processes of water formation and retention. A very important property of lunar soil is that grain have been denatured by solar wind irradiation in a surface region corresponding to the depth of penetration, transforming the samples into amorphous glasses with significant oxygen depletion and formation of nanoscopic metallic Fe [10]. This occurs on lunar rocks and grains, producing amorphous surface layers with different composition from that of the underlying soil.

To mimic mature lunar soil in the laboratory, the best samples are those containing mafic silicates that have been heavily irradiated with solar wind ions [6]. Alternatively, it is possible to coat the surface with vapor from laser ablation of minerals, to simulate deposits produced by ejecta of meteorite bombardment. Loeffler et al [11] have shown that coatings from laser ablation of olivine are amorphous and contain metallic iron nanoparticles.

Both the oxygen deficit and the presence of metallic iron can affect water formation and retention. Lunar soil is moderately porous (m^2/g), and this can cause two main effects: (i) reduce sputtering yield by 30-70% due to redeposition of ejecta, and (ii) increase the area available for adsorption and of volatiles.

Returned samples and lunar simulants: Artificial lunar simulants are designed to reproduce bulk properties but they should not be used when the fidelity to surface properties is important. That is the case for several surface sensitivite processes such as water adsorption, electrostatic charging, desorption and sputtering, where the state of the topmost monolayer is crucial. Even the best simulant will have its surface contaminated by exposure to laboratory air, which deposits hydrocarbons and water, and possibly other tightly bound molecules. Such molecules cannot typically be removed by heating alone, at least without at the same time radically altering the sample. Gentle exposure to low energy plasmas can efficiently remove contaminants [12]. More energetic protons and helium ions can clean the surface but also alter it by amorphization, ion implantation and preferential sputtering.

The alternative to use directly lunar soil is not without caveats. Although actual lunar grains have been processed by the solar wind, exposure to atmospheric contaminants will produce drastic changes in surface chemistry. Exposure to water even in 'dry' environments is likely sufficient to partially replenish the surface oxygen. In addition, water reacts with radiation damaged surfaces, altering surface composition, as seen in the exceptionally fast depletion of Mg from irradiated olivine after immersion in water, or even after exposure to atmospheric humidity [13]. Strong cation depletion has recently been observed in simulations of space weathering in forsterite, augite, albite and anorthoclase [14].

Research supported by NASA Cosmochemistry Program.

References:

[1] Clark, R.N. (2009) *Science* 326, 562. [2] Sunshine, J. M. et al. (2009) *Science* 326, 565. [3] Pieters, C.M. et al. (2009) *Science* 326, 568. [4] Lucey, P. et al. *Rev. Min. Geochem.* 60 (2006) 83. [5] Burke, D.J. et al (2011) *Icarus* 211, 1082. [6] Colapetre, A. et al. (2010) *Science* 220, 463. [7] Baragiola, R. A., Dukes, C.A. (2011) *42nd LPSC,* 2477. [8] Farrell, W.M. et al (2011) *42nd LPSC*, 1770. [9] Sinitsyn, M.P. (2011) *42nd LPSC*, 1236. [10] Loeffler, M.J. et al (2009) *JGR* 114, E03003. [11] Loeffler, M.J. et al (2008) *Icarus* 196, 285. [12] Dukes, C.A., Baragiola, R.A. (2009) *Surf. Interf. Anal.* 42, 40. [13] Cantando, E. et al. (2008) *JGR* 113, E09011. [14] Dukes, C.A., Baragiola, R.A. (2011) *Mat. Res. Bull.,* in press.

HOW THE MOON MAKES WATER: A CONCEPTUAL VIEW.

Donald D. Bogard, Formerly NASA-JSC and LPI (retired). donbogard@comcast.net

Material surfaces can readily be chemically activated by various processes that break chemical bonds, such as physical breaking and irradiation by charged particles or high-energy photons. The typical Si-O bond is ~450 kjoule/mole, or ~2.4 ev/bond, which is substantially below the electron ionization energy of either element. In many silicates, the Si-O bond length is ~0.16 μm, and the lunar surface erosion rate produced by micro-particle impacts is ~10^{-9} m/yr, or a few Si-O bonds/yr. Thus both surface erosion and impact breaking can produce active surfaces. In addition, solar wind protons, with an energy of ~1 keV and a flux at the Moon of ~3 x10^{8} atoms/cm^2-sec, are capable of breaking all Si-O bonds on a surface in a time period of less than a year. Thus the solar wind may activate surfaces on a rate comparable to that produce by surface erosion. Further, the flux of UV photons on the lunar surface is ~10^{15} photon/cm^2-s, far greater than the solar wind H flux. A UV photon with 300 nm wavelength has an energy of ~4 ev, or slightly above the Si-O bond energy. Thus, whereas far UV and X-ray photons are capable of breaking Si-O bonds, visible light is not. All of the above mechanisms likely contribute to producing chemically activated material surfaces on the Moon.

When such broken bonds are produced, there are limits to the degree they can be reformed internally through bond distortion. Such chemically activated surfaces can be strongly reactive toward other atoms brought into contact, and through chemi-sorption they can produce bonding whose strength approaches those of normal silicate bonds, or up to ~400 kjoule/mole. This chemi-sorption bonding occurs only in a monolayer and can have covalent or ionic character. In the lunar environment there are few volatile species that can quickly neutralize these chemically active surfaces, and so they persist. Such chemically active surfaces do not persist on Earth, both because physical breaking to form new surfaces is the only common way to generate them (the atmosphere stops solar H and UV photons) and because the terrestrial environment has volatiles to quickly neutralize such active surfaces. For example, to neutralize active surfaces on 10 g of regolith consisting of grains of 10 μm diameter, probably would require only ~20 cm^3 of terrestrial air at 50% humidity and STP, considering only chemi-sorption by water. It has proven to be difficult to generate such active surfaces in laboratory experiments and to preserve them long enough so as to measure their chemical activation properties.

The lunar surface is continually bombarded by solar wind H, and this H is capable of interacting with unsatisfied O bonds at material surfaces to produce an O-H bond. This process may be the most probable way in which unsatisfied O surface bonds are satisfied. The Deep Impact flyby of the Moon in June, 2009 spectrally detected the 2.8 μm O-H adsorption feature at middle latitudes on the Moon, where water ice cannot exist (Sunshine et al., 2009). Such O-H surface bonding may also incorporate through chemi-sorption a second H atom to produce a proto H_2O atom, which might be then released into the lunar atmosphere. However, such a process occurring repeatedly on a silicate surface would tend to deplete that surface in O and produce a charge imbalance that would retard the process. Nevertheless, continual generation of new chemically active material surfaces and their reaction with solar wind H is probably a continuous process by which the Moon produces water.

ANALYSIS OF VOLATILES IN APATITE: IMPLICATIONS FOR QUANTITATIVE HYGROMETRY.
J.W. Boyce[1,2], [1]Division of Geological and Planetary Sciences, Caltech (1200 E. California Blvd. Pasadena, CA 91125. jwboyce@caltech.edu), [2]Department of Earth and Space Sciences, UCLA (Los Angeles, CA 90095-1567).

Introduction: In order to begin quantifying H in a host melt, rock, or planetary body based on measurements of H in apatite (H_{AP}), one must be able to make precise and accurate measurements of H_{AP} at a spatial scale of a few to tens of μm.

Quantitative Analysis by Electron Microprobe: The practice of estimating H_{AP} by measuring F and Cl using the electron probe (EPMA) is still employed. A recent study of best practices for measuring F and Cl in apatite by EPMA [1] indicates that the most reliable data result from the combination of defocused beams (10x10μm) with large rastered areas (30x30μm), on crystals with their c-axis perpendicular to the electron beam. Such analyses require large crystals and still result in significant uncertainties (σ) in F and Cl, and thus H_{AP}. Even these best protocols yield large σ(F) and σ(Cl) for crystals not oriented with the electron beam perpendicular to the c-axis of the crystal (Fig. 1). The σ(F) and σ(Cl) must then be propagated into σH_{AP}, resulting in σ(H_{AP}) of 10^2-10^4 ppm (Fig. 1). For melt-apatite partitioning of H [2,3], where small grains were analyzed, σ(H_{AP}) could easily exceed 100%, leading to a non-trivial σ in partitioning.

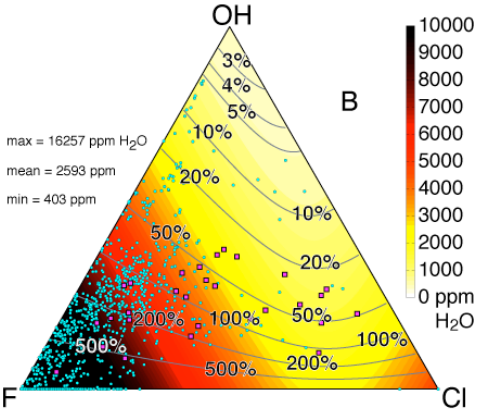

Fig.1: Uncertainties in hydrogen estimates shown in absolute ppm (color scale, as H_2O) and % (contours) for best EPMA protocols of [1], but worst orientation (c-axis parallel to electron beam). All calculated as two standard deviations of the mean. Cyan circles are natural apatite data from GEOROC, squares are synthetics from [2,3] used to define partitioning relationships.

Quantitative Analysis by SIMS: SIMS is a better method for determining H_{AP} , as it requires less than ~20x20μm areas for quantitative analysis of volatiles. However, such efforts are limited by the paucity of adequate standards: the σ of the standards and calibration are largely responsible for σ(H_{AP}) > 15% [4,5] derived from "conventional" calibrations (CC).

I report an advance in the measurement of H, F, and Cl in apatite that eliminates the need for homogeneous, well-characterized standards by using measured ratios to solve an inverse problem that yields calibration slopes for each element. This "inverse calibration" (IC) model assumes that measured intensities are linearly correlated with concentrations for all elements in all measured samples (*m* in Eq. 1), and that F+Cl+OH=100% occupancy (right hand side of Eq. 1). These assumptions appear to be justified at the resolution of SIMS measurements. The slopes (*m*) are the only unknowns, with the measured ratios (*R*) and masses (*M*) held constant. For N ≥ 3 linearly independent analyses we can solve the system of equations.

$$\frac{m_{OH}R_{OH}}{M_{OH}} + \frac{m_F R_F}{M_F} + \frac{m_{Cl}R_{Cl}}{M_{Cl}} = 1 \quad \textbf{Equation 1}$$

IC has been tested on a well-characterized apatites (F. McCubbin and colleagues), and reproduces their H, F, and Cl to within the typical 6-12% σ (Fig. 2). IC is further improved by adding additional apatites of different H, F, and Cl, even "unknown" apatites: In doing so, IC reproduces CC-derived H concentrations on Durango apatite to within <1%, F within 3%, and Cl within 1%. In all cases, IC yields individual σ that are smaller than those of CC by a factor of 2-18. Eliminating the need for homogeneous, well-characterized standards will allow more labs to generate more accurate and precise H_{AP}.

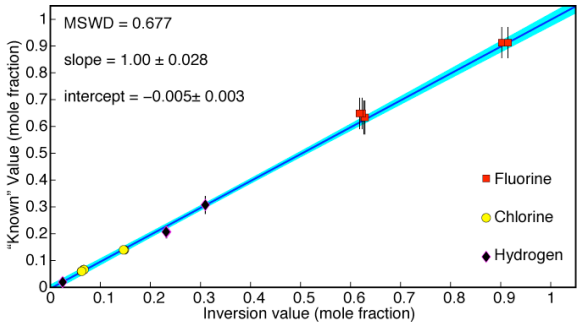

Fig.2: Comparison of H, F, and Cl values (as mole fractions) derived from CC and IC methods. Slope = 1 and small intercept indicates good agreement for all elements.

References: [1] Goldoff, B. et al., *AGU* (2010). [2] Mathez, E. & J. Webster, *GCA* (2005). [3] Webster, J.D. et al., *GCA* (2009). [4] McCubbin et al. *PNAS* (2010). [5] Greenwood et al., *Nature Geosci*, (2011).

A REVIEW OF LUNAR POLAR ILLUMINATION STUDIES USING CLEMENTINE, SMART-1, KAGUYA, & LRO DATA. D. B. J. Bussey[1], P. D. Spudis[2], [1]The Johns Hopkins University Applied Physics Laboratory, Laurel MD USA, ben.bussey@jhuapl.edu, [2]Lunar and Planetary Institute, Houston TX USA.

Introduction: The lunar poles are of great interest for both scientific and operational reasons. The discovery of permanently shadowed regions inside craters close to the poles, which are prime candidates for locations of deposits of water ice [1-6], has important ramifications for a human return to the Moon. Similarly, regions that receive near-constant solar illumination are possible sites for future lunar bases. Not only do these areas permit operations in a relatively benign thermal environment, but also a lunar base could be supported by solar photovoltaics without the need of additional power sources.

The Moon's spin axis is nearly perpendicular to the ecliptic plane, with an inclination of 1.5° from the vertical. A consequence of this is that the Sun will always appear close to the horizon near the poles, as the Moon slowly rotates on its axis every 708 hours (about 29 Earth days). Thus, topographically high and low points in the vicinity of the poles are potentially permanently illuminated or shad- owed, respectively [1-3]. Data from several missions have illuminated these relations:

Clementine: Our first comprehensive look at the Moon's polar illumination conditions came from the Clementine mission. Clementine, launched in January 1994, mapped the Moon in a near polar orbit for a period of 71 days. In doing so, it provided the first digital data set with which to analyse the lunar poles at medium-high resolution (250-500 m/pixel) with contiguous, consistent coverage. These data were collected during winter for the southern hemisphere. Using these data we produced the first quantitative illumination maps for both poles [7,8] (Fig 1).

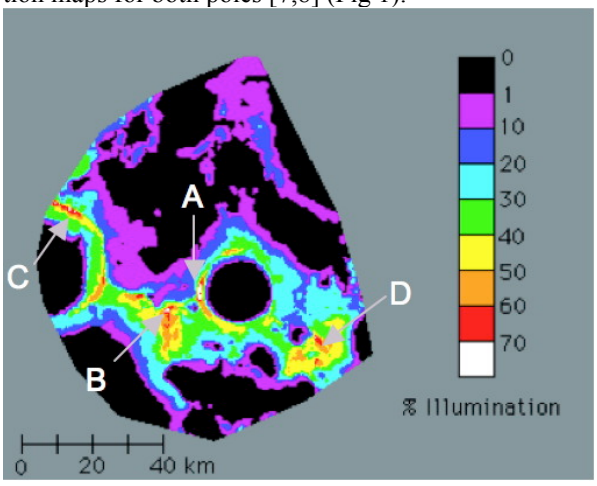

Figure 1. Quantitative south polar illumination map for a winter day, from [7].

These maps show the percentage of time that a point on the surface is illuminated during a lunar day. Key results for the south pole were: a) Identification of the locations that receive the most sunlight; b) None of these locations were permanently illuminated; c) Two locations close to the rim of Shackleton were collectively almost permanently illuminated. Key results for the north pole include indentification of places near the rim of Peary that were illuminated for an entire summer day, as well as locations of permanently shadowed craters on the floor of Peary crater.

SMART-1: The AMIE camera on SMART-1 provided additional information on the polar illumination conditions. It's main advantage over the Clementine data were that it acquired images over an entire year. Analysis of these data showed that "Point B" from the Clementine study is illuminated during an entire day in summer [9].

KAGUYA: JAXA's Kaguya spacecraft returned the first laser-derived topographic data of sufficient fidelity to be useful for illumination studies. Comparison between simulations and images with identical illumination conditions showed that the KAGUYA topography can be used to generate precise lighting predictions. We used these data to analyse the polar lighting conditions over an entire year [10]. Key results include:- 1. the areas that receive the most illumination are the same locations as we found in the Clementine and SMART-1 study, 2. Several locations are continuously illuminated for several months, centered around mid-summer, 3. Mapping out the frequency and duration of all the shadowed periods for these key locations. HDTV images of the poles from Kaguya confirm the findings from LALT and images.

LRO: The LOLA instrument on LRO is providing higher-resoltion topography of the polar regions. We have used these data to further characterize the illumination conditions in the polar regions. One aspect we are studying is the needed height of a mast to reducing the duration of shadowed periods.

References: [1] Watson et al., JGR, 1961, [2] Arnold, JGR, 1979, [3] Ingersoll et al., Icarus, 1992, [4] Shoemaker et al., Science, 1994, [5] Nozette et al., Science, 1996, [6] Feldman et al., Science, 1998, [7] Bussey et al., GRL 1999, [8] Bussey et al., Nature 2005. [9] Bussey et al., LPSC XXXIX, 2008, [10] Bussey et al., Icarus 2011, [11] Quinn et al., LPSC XXXII, 2011.

COLD AND CRYOGENIC CURATION OF LUNAR VOLATILE SAMPLES RETURNED TO EARTH.

M. J. Calaway[1] and C. C. Allen[2], [1] Jacobs Technology (ESCG) at NASA Johnson Space Center, Astromaterials Acquisition and Curation Office, Houston, TX 77058 (michael.calaway@nasa.gov), [2] NASA Johnson Space Center, Astromaterials Acquisition and Curation Office, Houston, TX 77058 (carlton.c.allen@nasa.gov).

Introduction: The study of volatile compounds and volatile elements, such as H, He, C, N, O, H_2O, CH_4, SO_2, CO, CO_2, NH_3, HCN, etc., are commonly used for constraining evolutionary processes on planets, satellites, and asteroids, as well as formulating models of solar system formation. For Lunar science, the recent evidence of regolith and rocks containing small amounts of OH^- and/or H_2O has renewed scientific interest into the study of lunar volatiles [1, 2]. Future lunar sample return missions will include the study of volatiles as a high priority.

Comet particles from the Stardust mission, asteroid particles from Hayabusa, meteorites, and subsurface lunar samples all occupied subfreezing environments prior to collection. Valuable geochemical information on volatiles is often lost when these samples are allowed to reach ambient temperatures on Earth. The ability to store, document, subdivide, and transport extraterrestrial geologic samples while maintaining below freezing or cryogenic temperatures is required for the complete scientific study of such samples, as well as future samples from a wide range of solar system bodies.

Lunar Temperatures: Recent Lunar Reconnaissance Orbiter (LRO) Diviner radiometer observations have shown that cold traps in the polar regions of the moon have temperatures as low as 38 K [3]. Diviner data also estimates that the lunar surface (in the top 2 cm), daytime temperatures range from about 180 to 300 K and 60 to 120 K in semi-shaded areas [3]. Nighttime observations show an estimated temperature range from 38 to 90 K, where 38 K is in permanently shadowed craters [3]. Therefore, volatiles in regolith samples that would be collected and returned to Earth might need to be maintained at extremely low temperatures to fully preserve their scientific integrity.

Curation at 250 K: Subsurface lunar regolith samples collected and preserved at 250 K could contain ice and solar wind derived volatiles. Returning such samples from the lunar surface could require having the sample return capsule outfitted with several sample containers situated inside a freezer that would survive a reentry. Curation at 250 K on Earth could require that the samples be handled inside an insulated glovebox with an inert gas environment. An alternative option would be a glovebox placed inside a walk-in freezer [4]. Storage of the samples would be in commercial freezers with redundant systems.

Curation at 40 K: Samples from extremely cold environments, including the lunar polar cold traps, could require curation at temperatures as low as 40 K. For cryogenic samples returning to Earth, a combination of passive cooling during cruise and active cooling during and after reentry might be required. Once on Earth, the sample return container could be placed into a helium shroud cryopump vacuum chamber. Cryocontainment would be maintained through delivery to a cryogenic chamber in the curation facility. This 40 K thermal vacuum chamber would include cameras and robotic manipulators for preliminary examination, subdivision of samples, and specialized sample allocation containers for shipment to laboratories. Cryogenic curation is feasible with current technologies developed for the superconductor industry. However, significant research and development costs would be required to tailor these technologies to the task of sample return and long term curation of lunar volatile samples at 40 K.

Future Cold / Cryo Curation: With over four decades of scientific investigation, the Apollo sample collection has given the science community the ability to study lunar materials with highly precise measurements made in multiple laboratories. High-resolution studies of lunar volatiles will require a sample return mission where cold or cryogenic curation preserves the scientific integrity of these fragile samples.

References: [1] Pieters, C.M. et al. (2009) Science, 326(5952): 568-572. [2] Anand, M. (2011) Earth, Moon, and Planets, 107(1): 65-73. [3] Paige, D.A. et al. (2010) Science, 330(6003): 479-482. [4] Herd, C.D.K. et al. (2011) The Importance of Solar System Sample Return Missions to the Future of Planetary Science Workshop, Abstract# 5029.

The Lunar Polar Regions as Solar System Analogs. P.E. Clark[1], R. Cox[2], [1]Catholic University of America@NASA/GSFC, Code 695, Greenbelt, MD 20771, Pamela.E.Clark@NASA.gov; [2]Flexure Engineering Inc.

Introduction: The lunar polar regions are ready made laboratories for studying surface chemistry and processes and testing technology necessary to support such scientific activity throughout the solar system.

Lunar Surface Processes and Conditions: The temperature of a smooth surface (without shadowing) at the poles would range from about 50K to about 300K [1]. However, the polar regions experience lower sun angles, and have rugged topography, and a bombardment saturated terrain which includes boulder populations. This creates a large variety of 'microniches' with degrees of illumination (during a diurnal cycle) varying from constantly illuminated (so-called 'points of eternal light', with temperature nearly constant at the upper end of that range) to permanently shadowed (with temperature nearly constant at or below 40K. Only half a meter below the surface, temperatures are a nearly constant average of surface temperatures above. These microclimates could be extremely local niches: beneath a rock or on a slope with an overhang above it, or more extensive, as in permanently shadowed craters. Studying grain surface chemistry induced interaction or lack of interaction due to shielding from fields, particles, dust, solar wind, and exosphere, would provide insights into space weathering processes affecting most of the (regolith covered, bombardment dominated) surfaces in the solar system. Grain surface chemistry with hydrogen and hydrides, as will as silicate surface chemistry involving 'volatile incompatibles' (to silicate matrix) cations could provide clues as to volatile origin (interior, meteoritic, solar wind, or trapped exosphere). These microclimates could also stand in as analogs for a variety of solar system environments with distinctive chemical interactions enabled under the conditions within selected microniches.

The Moon as Surface Condition and/or Temperature Analog for many targets: As illustrated in the table [2], surface conditions on a variety of targets, including NEOs, Mercury (lower range), and icy moons, overlap with those on the lunar surface. Temperature ranges for the outer planets and Mars fall within temperature ranges on the Moon. The nature of and extent to which surface constituents are involved in surface and subsurface processes depends on their volatilities, and thus on effective surface temperatures and illumination on atmosphereless bodies [2,3]. This means the lunar surface could act as a testbed, either as as a chemistry laboratory for surface processes in the solar system, or as a proving ground for technologies that reduce resource consumption while improving capability (e.g., ultra low temperature ultra low power electonics), resulting in higher value and lower cost exploration of the entire solar system.

References: [1] Clark P.E. et al (2011) AIP Conference Proceedings, SPESIF (in press); [2] Zhang J.A. and Paige D. A. (2009) GRL, 36, L16203, doi:10.1029/2009GL038614; [3] Paige D. (2010), Science, 330, 479, DOI: 10.1126/science.1187726.

Target	Processes	Temperature Range
Moon	grain surface chemistry. space weathering. bombardment of silicate surface. volatiles, exosphere processes	<40 – 400K
NEOs	grain surface chemistry, space weathering. bombardment, for silicate surface but with higher volatile, organic, metallic iron	<40 – 350K
Mercury	grain surface chemistry, space weathering. Bombardment for silicate surface, with higher volatile content including water (discrete ice layer) and sulfur	<40 – 650K
Mars	bombardment plus volcano–tectonic activity for silicate surface with seasonal volatile atmosphere, polar deposit circulation, subsurface hydrothermal processes, wind (dust), volatiles as erosional agents. sulfur chemistry	135 – 325K
Outer Planets	water, methanol, ammonia, formaldehyde, carbon dioxide, hydrogen sulfide, sulfur dioxide chemistry	80 – 175K Jupiter 30 – 150K Saturn 60 – 70K Uranus 50–55K Neptune
Icy Moons	grain surface chemistry, space weathering, bombardment (for atmosphereless), volatiles ionization, organic and sulfur chemistries	<40 – 100K
Molecular Clouds	grain surface chemistry involving hydrogen and hydrides.	<90K

MAPPING WATER AND HYDROXYL ON THE MOON AS SEEN BY THE MOON MINERALOGY MAPPER (M^3).

Roger N. Clark[1], Carlé M. Pieters[2], Robert O. Green[3], Joe Boardman[4], Noah E. Petro[7], Bonnie J. Buratti[3], L. Cheek[2], J. P. Combe[6], D. Dhingra[2], J. N. Goswami[5], James W. Head III[2], Peter J. Isaacson[2], R. Klima[8], G. Kramer[16], K. Eric. Livo[1], S. Lundeen[3], E. Malaret[12], Thomas B. McCord[6], J. Mustard[2], Jeff W. Nettles[2], C. Runyon[13], M. Staid[14], Jessica M. Sunshine[8], Larry A. Taylor[9], K. Thaisen[9], S. Tompkins[15], J. Whitten[2], [1]USGS Denver, 80225 (rclark@usgs.gov), [2]Dept. Geological Sciences, Brown University, Providence, RI, [3]JPL, Pasadena, CA, [4]AIGLLC Boulder, CO, [5]PRL/ISRO, Ahmedabad, India, [6]BFC, Winthrop, WA, [7]NASA Goddard, [8]U. Maryland, [9]U. Tennessee, [12]Applied Coherent Technology Corp., VA, [13]College of Charleston, Charleston, SC, [14]Planetary Sciences Institute, Tucson, AZ, [15]Defense Advanced Research Projects Agency, Arlington, VA, [16]LPI, Houston, TX.

Introduction: In the recent discovery of water and hydroxyl on the Moon [1, 2, 3], near-infrared lunar spectra were shown to contain absorptions due to adsorbed water and hydroxyl.

We studied the shapes and positions of water and hydroxyl absorptions in the M^3 data set using both global mode (85-spectral channels) and target mode (full spatial and spectral resolution) data. Some thermal emission was removed according to [4].

Results: Water and hydroxyl absorptions were analyzed for position and shape using the methods described in [5]. Figure 1 is based on the broad water plus hydroxyl absorption that starts around 2.6 µm and extending to 3 µm. The color code captures the diversity of the shape of the absorption. There are linear downturns from ~2.6 to 3-µm, concave curves, stair-step shapes and variations in those themes. The shapes are partially influenced by the strength of relatively narrower hydroxyl absorptions that occur from about 2.7 to beyond 2.8 microns. Different absorption shapes appear to be associated with diverse geologic units. Some fresh craters show exposed water and hydroxyl absorptions, while other nearby craters show none. Similarly, some older craters exhibit water and hydroxyl, while others do not. Large regions, such as around Orientale, appear water and hydroxyl rich, while others, such as South Pole Aiken Basin, appear water and hydroxyl poor. Mare surfaces also appear to contain less water than the surrounding highlands.

These results point to amazing geologic diversity across the Moon, resulting from complex geologic processes that could involve endogenic water as well as interaction with the solar wind.

References:

[1] Clark, R. (2009) Science **326**, 562-564.
[2] Sunshine *et al.* (2009) Science **326**, 565-568.
[3] Pieters *et al.* (2009) Science **326**, 568-572.
[4] Clark *et al.*, (2011) JGR, In Press.
[5] Clark *et al.*, (2003) JGR **108**, 5-1 to 5-44.

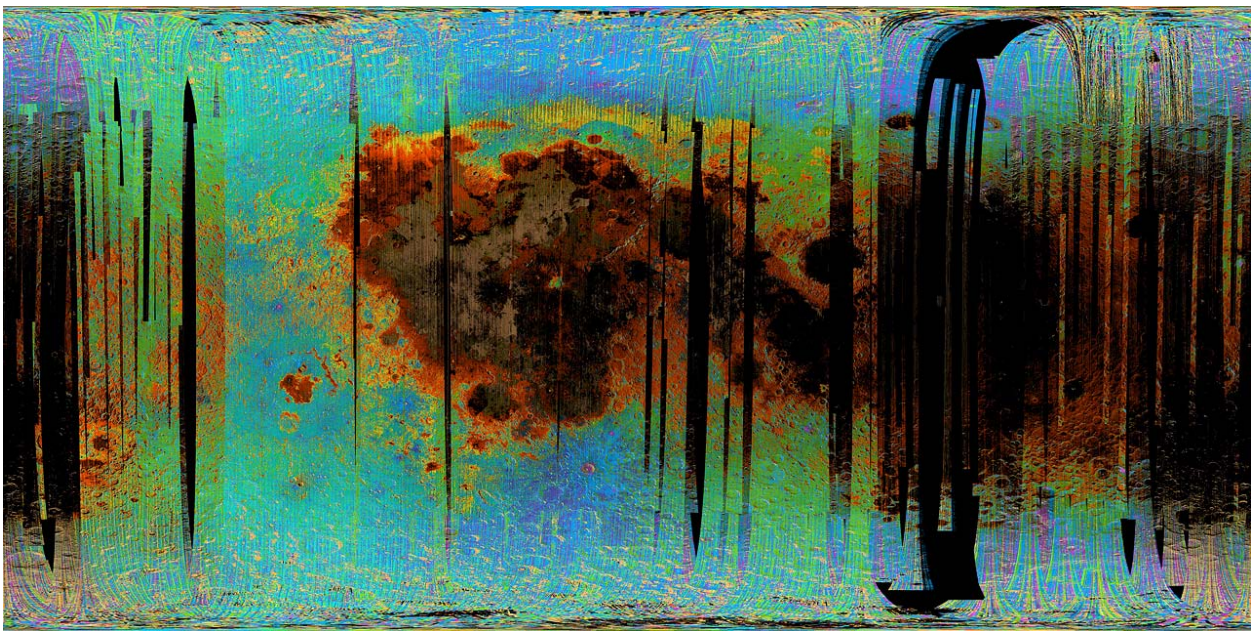

Figure 1. Water on the moon in a simple cylindrical projection. Different colors indicate different shapes for the 3-µm water absorption. The shape is influenced by the presence of narrower hydroxyl absorptions and how water molecules are bound to the minerals and glasses in the rocks and soils.

A Model for the Distribution of Volatiles at the LCROSS Impact Site. A. Colaprete[1], J. Heldmann[1], D. H. Wooden[1], K. Mjaseth[1], M. Shirley[1], W. Marshall[1], R. Elphic[1], B. Hermalyn[2], P. Schultz[2], [1]NASA Ames Research Center, Moffett Field, Anthony.colaprete-1@nasa.gov, [2]Brown University, Department of Geological Sciences, Providence, RI.

Introduction: Using the spent Centaur booster as an impactor, the Lunar Crater Observation and Sensing Satellite (LCROSS) mission sampled one spot within the South Pole crater Cabeus by lifting material from shadow and into sunlight. The LCROSS Shepherding Spacecraft (SSC) flew four minutes behind the impacting Centaur making measurements of the impact, debris clouds, and resulting crater [1]. At the same time, measurements were made by instruments onboard the Lunar Reconnaissance Orbiter (LRO), including the Lyman Alpha Mapping Project (LAMP) spectrometer at impact and the Diviner Lunar Radiometer (DLR) approximately 90 seconds after impact [2,3]. These various observation platforms provided a number of unique and complimentary measurements of the impact. This paper presents an attempt to piece together the conglomerate of observations into a single model for the surface conditions at the LCROSS impact site. In particular, the model addresses the distribution and form of the various volatiles, including water, observed in the LCROSS impact event.

LCROSS Impact Location: The LCROSS Centaur impacted into an area in the crater Cabeus which has been in permanent shadow for the more than one Gyr4]. The impact site was selected based on a variety of criteria, including the presence of hydrogen, temperatures, height to sun illumination, and slopes. Leading up to the final impact target selection, LRO data was used to understand these parameters with nearly continuous updates coming from the LRO instrument teams. The two most important criteria were hydrogen concentrations and height to sun illumination.

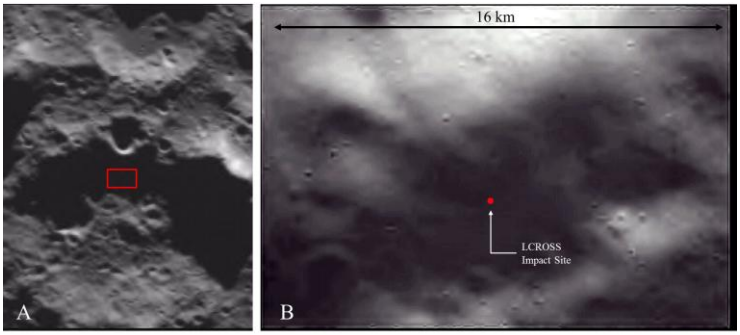

Figure 1. Images taken from a NIR Camera #2 on the LCROSS Shepherding Spacraft at an altitude of approximately 145 km (panel A) and 43 km (panel B) above the surface of Cabeus. The area is in permanent shadow and illumination is the result of light reflected/scattered off adjacent terrain (sun is to the upper left, while the inner walls of small craters in panel B indicate illumination from the bottom of the image).

The LCROSS impact site, imaged by the LCROSS NIR camera and registered to LOLA DEMs [5, 6], was in a depression that would have provided extra shadowing from secondary scattering from surround terrain. It is in these "double-shadowed" areas that temperatures are theoretically coldest (Figure 1).

Characteristics of the Impact and Impact Site: The impact resulted in a two-component ejecta curtain: a high angle plume which has been associated with the low density of the impactor, and the canonical "low angle" curtain, which, while similar to traditional natural impacts, was also modulated by the density of the impactor [5]. Based on the nature of the NIR and visible impact flashes the impact site appears to be relatively low density (porosities >70%) [5]. While the impact generated relatively cool and localized debris (T~1000-1200 K), a variety of vapors were released at impact (including CO and H_2) [2]. Other vapor components (e.g., Na) appear only after the first dust is seen via scattering of sunlight, suggesting some of the volatile components were intimately entrained in the soil/ice mixture [5]. Water ice grains were observed in the ejecta at early times (Impact +20 sec), and again at later times (Impact+230 sec). This observation suggests that these grains were at least part of the high angle ejecta cloud and most likely also in the nominal angle ejecta component [1,7,8]. Increases in water vapor with time after impact suggest exposed water at the impact site. The cold temperatures within the Centaur crater (as observed by the NIR and as observed by Diviner) indicate a possible ice rich soil [1, 3]. Combined, these observations help constrain the types and distribution of volatiles at the LCROSS impact site. This paper will present a summary of the observations and an evaluation of various models for the distribution and form of volatiles at the LCROSS impact site.

[1] Colaprete et al., (2010), *Science*, **330**, 463-468. [2] Gladstone et al., (2010), *Science*, **330**, 472-476. [3] Hayne et al., (2010), *Science*, **330**, 477-479. [4] Paige et al., (2010) *Science*, **330**, 479-482. [5] Schultz et al., (2010), Science, 330, 468-472. [6] Marshall et al., (2011), *PSS*, In Press. [7] Colaprete et al, 2011, 42nd LPSC , abs# 2037. [8] Hermalyn et al.(2011), Wet vs. Dry Moon Workshop, LPI.

MAPPING OF LUNAR VOLATILES: A CHALLENGING PROBLEM. J.-Ph. Combe[1], T. B. McCord[1], P. O. Hayne[2] and D. A. Paige[3]. [1]Bear Fight Institute, 22 Fiddler's Road, Winthrop, WA, USA. [2]Caltech, Pasadena, CA. [3]UCLA, Los Angeles, CA. (Contact: jean-philippe_combe @ bearfightinstitute.com),

Introduction: Uncertainties in the interpretation of spectral signatures of volatiles.

Background: Spectral signatures of hydroxyl and/or water molecules have been observed at 2.8 and 3 µm by the Moon Mineralogy Mapper (M^3) onboard the Chandrayaan-1 spacecraft [1-3], and confirmed by the Epoxi mission [4] and Cassini Visual and Infrared Mapping Spectrometer (VIMS) [5]. If those volatiles are endogenic, their identification would have implications for the understanding of lunar interior geological proceses. If OH and/or H_2O result of surficial processes, they are likely related to the space environment and surface properties of the Moon, one hypothesis being the interaction of solar wind particles with minerals of the lunar soil [2].

Problem: Measurements of the position, strength and shape of the absorption bands are essential for the interpretation of the type of volatile, its distribution, and depedence on lunar physical properties. However, these measurements have significant uncertainties [2]. Thermal emission contributes significantly to the lunar radiance in the 3-µm region above 250 K [6, 7]: It fills and distorts the absorption bands of volatiles, and it is correlated to illumination (latitude, local slope, surface roughness and time of day), surface albedo and composition [2, 8]. The accuracy of thermal removal based on reflectance spectra [6, 7] is affected by the broad 2-µm band of pyroxenes and the presence of the 3-µm band of volatiles. Photometric properties of the lunar soils have also significant spectral effects.

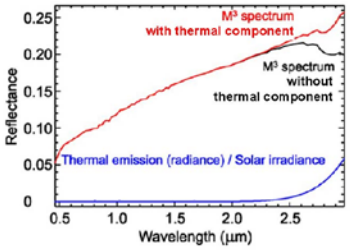

Figure 1:. Example of M^3 spectrum with and without thermal emission in it, for surface temperature of 350 K.

The main objectives in our study are 1) the interpretation of the OH-bearing composition, which is based on the position of the bands, 2) quantifying the components, which is partly related to the depth of the bands, 3) monitoring temporal variations of the volatile distribution, which is a way to determine if the volatiles are endogenic or at the topmost surface, and 4) determining the association of various types of volatiles to different mineralogical compositions, which may provide insights on geological processes, or how the minerals interact with solar wind particles. We are first focusing on thermal emission removal because it has the strongest effects on the absorption bands.

Spectral analysis and results: Thermal emissionn removal and monitoring temporal variations.

We use M^3 reflectance spectra with thermal emission correction based on the data themselves [6, 7, 8]. We use also brightness temperature measured by the Diviner Lunar Radiometer Experiment [9] on Lunar Reconaissance Orbiter (LRO), where data are available at the same lunar local time of day than M^3 observations. Both methods so far lead to an incomplete thermal emission removal [8]. Qualitatively, the variability of the 3-µm band depth observed as function of the composition after incomplete removal of the thermal contribution is sensitive to the actual dependence to the composition. Quantitatively, this dependence is likely underestimated. The band shape estimate of the 3-µm absorption band is sensitive to the diversity of volatiles. However, since the thermal emission is not completely corrected, and since this incompleteness varies from place to place, and also between observations of the same scene under different geometries of illumination, it is not yet possible to reach firm conclusions. Variations with time of day seem also to indicate an increase of the 3-µm absorption band depth when the sun is lower above the horizon. However, thermal removal uncertainties are also higher when shadows are mixed in the scene. We are currently working on improving the temperature modeling from Diviner data in order to account for surface roughness, and therefore reduce some of the uncertainties.

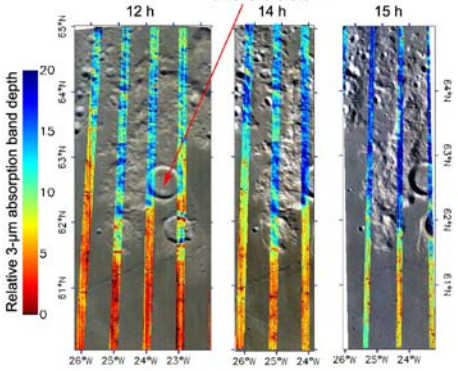

Figure 2: 3-µm absorption band depth near Fontenelle Crater D (red arrow) for three times of day after thermal removal using Diviner brightness temperature measurements at 8 µm.

References: [1] Pieters et al., Science 326, 2009. [2] McCord et al., JGR, in press. [3] Clark et al. JGR, in press. [4] Sunshine et al., Science 326, 2009. [5] Clark, Science 326, 2009. [6] Clark et al., Icarus 40, 1979. [7] Clark et al. submitted to JGR. [8] Combe et al., LPSC abstract 2573. [9] Paige et al. Science 330, 2010.

THERMAL ANALYSES OF APOLLO LUNAR SOILS PROVIDE EVIDENCE FOR WATER IN PERMANENTLY SHADOWED AREAS. B.L.Cooper[1] M.C. Smith[2] and E.K.. Gibson[3], [1] Jacobs ESCG (bonnie.l.cooper@nasa.gov), [2] East Tennessee State University (smithmc2@gmail.com), [3] NASA Johnson Space Center.

Introduction: Thermally-evolved-gas analyses were performed on the Apollo lunar soils shortly after their return to Earth [1-8]. The analyses revealed the presence of water evolving at temperatures above 200°C. Of particular interest are samples that were collected from permanently-shadowed locations (e.g., under a boulder) with a second sample collected in nearby sunlight, and pairs in which one was taken from the top of a trench, and the second was taken at the base of the trench, where the temperature would have been -10 to -20°C prior to the disturbance [9]. These samples include 63340/63500, 69941/69961, and 76240/76280.

At the time that this research was first reported, the idea of hydrated minerals on the lunar surface was somewhat novel. Nevertheless, goethite was observed in lunar breccias from Apollo 14 [10], and it was shown that goethite, hematite and magnetite could originate in an equilibrium assemblage of lunar rocks [11].

Current Effort: We have begun a re-analysis of the thermally-evolved-gas data which was preserved in paper format, converting the data into a spreadsheet in which the onset temperature of each peak is recorded. The lunar data are then compared to terrestrial samples that were measured in the same instrument and at the same pressure ($2x10^{-6}$ torr). Comparing the data with thermal gas release curves taken at ambient pressure would introduce an error, because the onset temperature decreases as pressure is lowered [12]. Gas released at temperatures below 150°C at $2x10^{-6}$ torr were shown by [3-5] to result from adsorbed terrestrial water, but volatiles above that temperature are likely to be an inherent component of the sample.

First Results: In the figure, we compare the water curve for permanently shadowed soil 63340 with that of a sample from a nearby sunlit area, 63500. The curves are overlaid to show the larger amount of water that was released from the sample that was in permanent shadow.

Conclusion: Evidence exists in the Apollo sample collection for the retention of water and other volatiles from permanently shadowed areas near the lunar equator, where temperatures are much higher (-20C) than in the permanently shadowed regions near the poles. Both cometary water and water from hydrated samples are seen, which supports the idea that these volatiles will be found in greater abundance at lower temperatures near the poles.

References:

[1] Moore, C.B., et al., (1970) *Science, 167*, 495. [2] Gibson, E.K. and Hubbard, N.J. (1972) *Proc. Third Lunar Sci. Conf.*, 2003-2014. [3] Gibson, E.K., Jr. and Moore, G.W. (1972) *The Apollo 15 Lunar Samples*. 307-310. [4] Gibson, E.K., Jr. and Moore, G.W. (1972) *Proc. Third Lunar Sci. Conf.*, 2029-2040. [5] Gibson, E.K. and Moore, G.W., (1973) *Science, 179*, 858-861. [6] Chang, S., et al. (1974) *Proc. 5th Lunar Sci. Conf.*, 1785-1800. [7] Gibson, E.K., Jr., (1975) *Moon, 13*, 321-326. [8] Gibson, E.K., Jr. and Andrawes, F.K. (1978) *Planetary Water and Polar Processes, Proc. 2nd Colloquium*. 2. [9] Keihm, S. and Langseth Jr, M. (1973) *Lunar & Planet. Sci. Conf. 4th*, 455-456. [10] Agrell, S., et al. (1972) *Lunar Sci. III*. 7. [11] Williams, R.J. and Gibson, E.K., (1972) *Earth and Planetary Science Letters, 17*, 84. [12] Kotra, R.K., et al., (1982) *Icarus, 51*, 593-605.

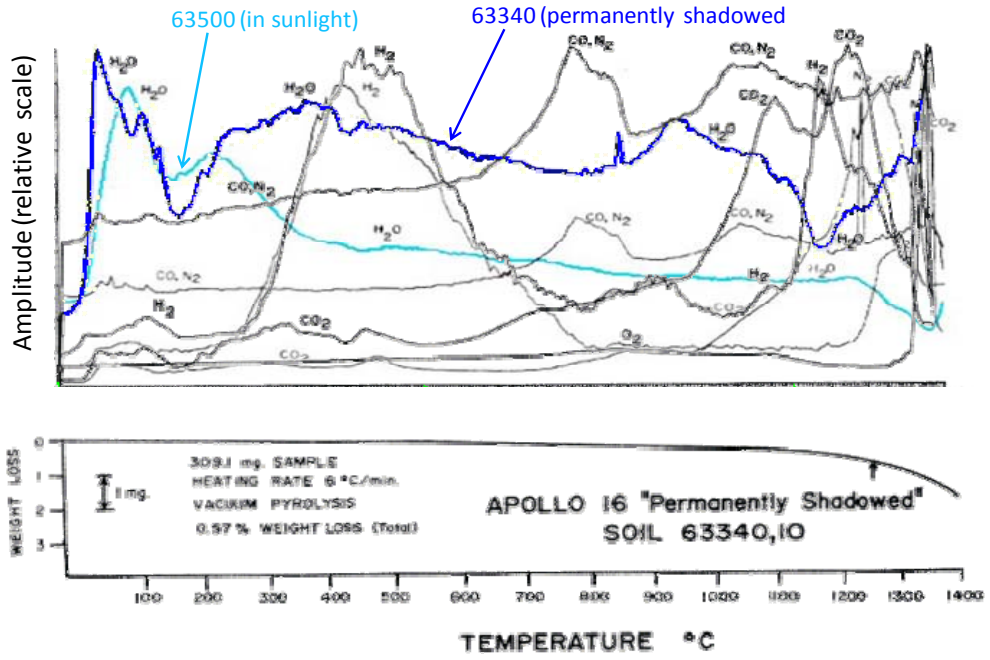

A MODEL OF THE MOON'S VOLATILE DEPLETION. **Steven J. Desch**[1] and **G. Jeff Taylor**[2]. [1]School of Earth and Space Exploration, Arizona State University, PO Box 871404 Tempe, AZ 85287. [2]Hawaii Institute for Geophysics and Planetology, Univ. of Hawaii, Honolulu, HI. (steve.desch@asu.edu) .

The Moon is widely accepted to have formed from a proto-lunar disk, formed after the impact of a Mars-sized planetary embryo with the Earth [1]. The disk material derived 20% from the Earth's mantle, and 80% from the impactor's mantle [2,3], which probably was similar to Earth's. During the disk's existence, material is hypothesized to have exchanged between the Earth and disk, to explain the remarkably similar oxygen isotopic composition of the Earth and Moon [4]. In this picture, volatiles should have exchanged as well, so the Moon may be expected to have formed with the terrestrial abundances of H_2O ($\approx$ 500 ppm; [5]) and Na ($\approx$ 2500 ppm; [6]). In fact, the Moon is depleted in these and other volatiles. Recent analyses of lunar samples suggest a bulk lunar abundance of H_2O in the range 0.1 - 30 ppm [7-10]; to fix numbers we consider an abundance of 10 ppm. Our aim is to quantify the loss of volatiles during the protolunar disk stage, to explain why the Moon is depleted in volatiles.

All volatile loss must be by hydrodynamic escape. Loss of 500 ppm of H_2O from an area $\sim 50\pi R_\oplus^2$, in $< 10^2$ yr, implies fluxes $> 3 \times 10^{16}$ cm^{-2} s^{-1}, for which the crossover mass [11] is $\sim 10^7$ amu. Therefore gases are lost according to their proportions in a disk atmosphere above and below the magma disk. Our model calculates how much of each volatile (such as H_2O) is dissolved in the magma (with mass fraction x_s) in each disk annulus, and how much is in the disk atmosphere (with partial pressure P_{H2O}). For example, $x_s = (6\times10^{-7})(P_{H2O}/1\,\mathrm{dyn\,cm^{-2}})^{0.54}$ [12], and typically $1-15\%$ of the H_2O is dissolved in the magma. We calculate the rate of hydrodyanmic escape of these (orbiting) gases from the disk-Earth system, accounting for the fact that the gas has high temperature T and has varying mean molecular weight. An important result is that the mean molecular weight is typically $\sim$ 20 amu unless $T > 2800$ K, when rock vapor dominates (assuming $X_{Fa} = 0.09$ and the vapor pressure of [13]). At low densities, we find, thermal dissociation of H_2O and thermal ionization of Na and K, can lower the mean molecular weight. We account for hydrodynamic loss deeper than the exosphere by using the variation of mass loss with Knudsen number derived by [14] based on molecular Monte Carlo simulations. Gases in the atmosphere are not bound to the Moon after it forms, which will thus accrete only those volatiles dissolved in the magma.

We consider a $\sim 2\,M_L$ disk from $1\,R_\oplus$ to $5\,R_\oplus$ that then viscously spreads as described by [1]. Viscous heating maintains high temperatures iuntil the surface density drops because of the disk spreading. Temperatures ~ 2100 K, consistent with solidifcation of rock and possibly the triggering of the Moon's formation, are reached at the Roche limit $2.9\,R_\oplus$ after about 20 years, and the Moon may form quickly after that. In Figure 1 we show the total disk mass beyond $2.9\,R_\oplus$, as well as the total mass of H_2O dissolved in the magma beyond $2.9\,R_\oplus$, as functions of time. At 20 years, the total mass to be swept up is $\approx 1.0\,M_L$, and the bulk water content is $\approx$ 10 ppm, thus potentially explaining the depletion of water in the Moon.

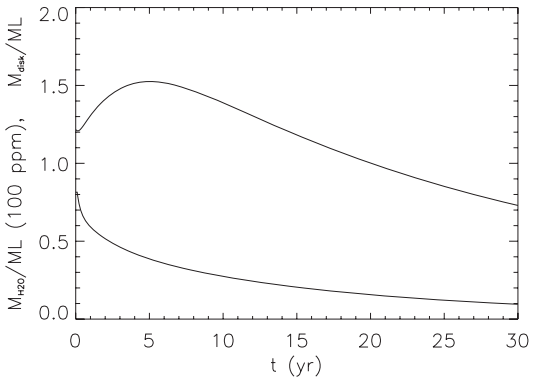

References: [1] Stevenson, D, AREPS 15, 271, 1987. [2] Canup, R, Icarus 168, 433, 2004. [3] Canup, R, Icarus 196, 518, 2008. [4] Pahlevan, K & Stevenson, D, EPSL 262, 438, 2007. [5] Mottl, M, et al. ChemErde 67, 253, 2007. [6] McDonough, W, & Sun S-s, Chem Geol 120, 223, 1995. [7] Saal, A et al. Nature 454, 192, 2008. [8] McCubbin, F, et al., PNAS 1006677107, 2010. [9] Sharp, Z, et al. 2010, Science 10.1126/science.1192606. [10] Greenwood, J, et al., Nature Geoscience 10.1038/NGEO1050. [11] Hunten, D, Pepin, R, & Walker, J, Icarus 69, 532, 1987. [12] Fricker, P & Reynolds, R, Icarus 9, 221, 1966. [13] Nagahara, H, et al. GCA 58, 1951, 1994. [14] Volkov, A, et al. arXiv1009.5110, 2010

NEUTRON SUPPRESSED REGIONS (NSRs) USING THE LRO NEUTRON DETECTOR EXPERIMENT LEND. G. F. Droege[1], W. V. Boynton[1], I. G. Mitrofanov[2], and the LEND team. [1]The University of Arizona, Tucson, AZ USA, gdroege@lpl.arizona.edu, [2]Institute for Space Research, 117997 Moscow, Russia, imitrofa@space.ru

Introduction: The Clementine mission initially suggested that deposits of water ice might exist in the permanently shadowed regions (PSRs) near the lunar south pole [1]. Subsequent data were taken by the Lunar Prospector Neutron Spectrometer (LPNS), revealing suppression of epithermal neutrons at the poles above 70° latitude, interpreted to indicate enhancement of hydrogen, predominantly within PSR areas [2].

Here we present data from the Lunar Exploration Neutron Detector (LEND) instrument onboard the NASA Lunar Reconnaissance Orbiter (LRO) that provides further context and statistics for interpreting and defining the neutron suppressed regions (NSRs).

Methods: A map of the epithermal neutron counting rate was made by binning the LEND counts from the four collimated epithermal neutron detectors using HEALPix [3] bins of 1.7 km. The maps are smoothed by a Gaussian filter. Uncertainty maps based on counting statistics were made and smoothed by the same filter.

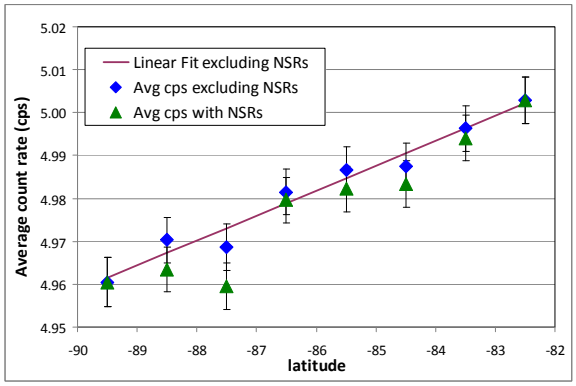

Fig1. Average count rate of collimated epithermal neutrons in one-degree latitude bands.

Areas of enhanced hydrogen content are found by looking for regions of lower-than-normal epithermal counting rates. To do this we first made a difference map by determining the average epithermal neutron counting rate as a function of latitude in one-degree latitude bands between -82° and -90° (fig 1). A general decrease in count rate (increase in H content) is observed toward the pole. A preliminary difference map was made by subtracting these latitude-dependent count rates from the smoothed map. The resultant map is similar to that shown in figure 2, but before we generated the final difference map, we re-made the latitude-dependent count rate plot excluding the HEALPix bins that had values lower than -0.05 on the preliminary difference map. A linear fit to these values (fig. 1) was made and was used to generate the final difference map (fig 2.)

Results: It can be seen that there are two very large neutron suppression regions (NSRs) that correspond to the Cabeaus and Shoemaker craters as originally noted in [4]. Contours have been added at the -0.04 cps level to help define the spatial extent of these NSRs.

Discussion: As noted elsewhere [5], the NSRs are not closely related to the PSRs. The NSR at Shoemaker does follow the outline of the local PSR, but the one at Cabeus is substantially larger than the Cabeaus PSR. Many other PSRs show no evidence of any neutron suppression.

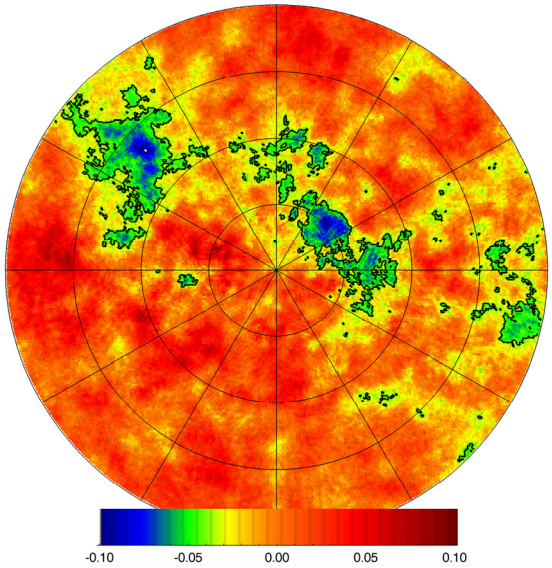

Fig2. South polar map of count rate differences from 82°S. The contour is at -0.04 cps. All values < -0.04 cps are significant at the 3σ level or greater.

Another interesting observation is the general increase in background H content with latitude. Since it is unreasonable to argue that the influx of H is any greater in the polar regions than elsewhere, this relationship argues for a general mobility of H with a greater deposition and retention due to lower temperatures with closer proximity to the pole.

References: [1] P. D. Spudis *et al.*, *Solar Syst. Res.* 32, 17 (1998). [2] W. C. Feldman *et al.*, *Science* 281, 1496 (1998). [3] Hierarchical Equal Area isoLatitude Pixelization, http://healpix.jpl.nasa.gov. [4] I.G. Mitrofanov, *et al.* (2010) *Science*, 330, 483–486. [5] Mitrofanov *et al.*, This volume, (2011)

WATER IN THE LUNAR MAGMA OCEAN. L. T. Elkins-Tanton[1] and T. L. Grove[1], [1]Massachusetts Institute of Technology, Cambridge MA (ltelkins@mit.edu, tlgrove@mit.edu).

Introduction: Lunar sample suites indicate fractional crystallization of a lunar magma ocean (*1-6*). The last dregs of the magma ocean, the ur-KREEP, would have been highly enriched in incompatible elements, including any water or hydroxyl; this simple observation forms a base for this study.

After fractional solidification and gravitational solid-state cumulate overturn, secondary melting of cumulate source regions produced mare basalts and picritic glasses. Here we present results from modeling fractional solidification of a lunar magma ocean with traces of water, and thermodynamic calculations of oxygen, hydroxyl, water, and iron metal co-existence, as found in many lunar samples.

Models: Compositions of mineral phases are calculated in equilibrium with the magma ocean liquid composition at each fractionation step using experimentally-determined partition coefficients for water; a full model description is given in (*7*).

Results and discussion: To recreate the inferred melting source region water contents from (*8, 9*) (100 to 700 ppm) through a fractionally solidifying magma ocean, the bulk magma ocean must have contained at least 100 ppm with a high fraction of retained interstitial melt in the cumulates, or, more likely, over 1000 ppm water with a smaller retained melt fraction. The smaller hypothesized melting source region water contents of (*10-12*) (10 ppb to 10 ppm) can be created with a bulk magma ocean with 100 ppm water or less.

Magma oceans that began with 100 ppm or more of water would likely produce KREEP with water concentrations in the weight percent abundance range (Table 1). Further, if KREEP originally resided at the base of the anorthosite flotation crust, it would have formed at a pressure around 2 kbar, sufficient for water saturation near 5 wt% (*13*). Thus degassing is not a sufficient explanation for drying KREEP.

The existence of water or hydroxyl in magma implies this reaction relationship $H_2 + ½\ O_2 \Leftrightarrow H_2O$, which is controlled by an equilibrium constant K; see (*14*). Maintaining a magma with 1 wt% water at an f_{O2} below the iron-wüstite buffer requires hydrogen fugacity between 1 and 100 bars. At low f_{O2} and high magmatic temperature, f_{H2} has to be equal to or greater than f_{H2O}. At low f_{O2} and low magmatic temperature, f_{H2} can be as much as two orders of magnitude less than f_{H2O} but never less than about 0.1 bar on the Moon. We therefore conclude that significant water contents in magmas are unlikely on the low-gravity Moon.

Conclusions: We conclude that (1) KREEP signature and water should be positively correlated if the water was processed through the original magma ocean, and (2) producing a picritic glass source region with water consistent with the results of Saal et al. (*8*) creates KREEP too wet to be consistent with lunar petrology. We further suggest that the measurements made in lunar samples are largely explained by hydrogen rather than hydroxyl or water. Additionally, water may have been delivered to the lunar shallow mantle by later impacts, and non-water volatiles may have been degassed from the lunar magma ocean and trapped in the lunar conductive lid, providing a later driving mechanism for fire fountains.

Initial water content of magma ocean [ppm]	Water in KREEP (final 2 vol% of magma ocean) [wt%]
1000	~4.7
100	~0.5
10	~0.05

Table 1. KREEP water contents resulting from magma ocean fractional solidification with 1% retained interstitial melt.

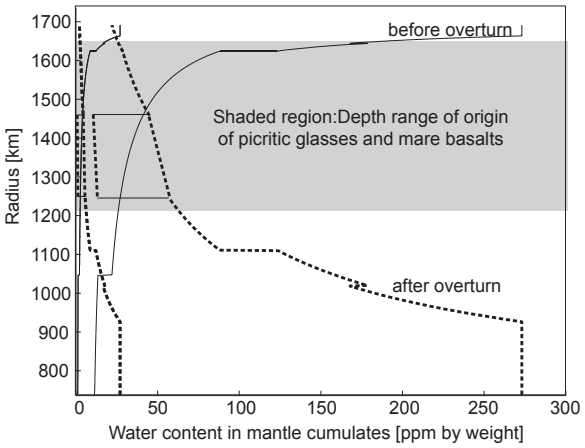

Figure 1. Effect of initial bulk magma ocean water on cumulate mantle composition. 100 and 1000 bulk ppm water, with 1% retained melt.. Depth range of picritic glasses and mare basalts from experiments referenced in (*15*).

References: [1.] Wood, *LSC* **1**, 965 (1970). [2.] Smith, *LSC* **1**, 897 (1970). [3.] Solomon, *LSC* **8**, 583 (1977). [4.] Warren, *Ann. Rev. Earth Planet. Sci.* **13**, 201 (1985). [5.] Snyder, *GCA* **56**, 3809 (1992). [6.] Hess, *EPSL* **134**, 501 (1995). [7.] Elkins-Tanton, *EPSL* **304**, 326 (2011). [8.] Saal, *Nature* **454**, 193 (2008). [9.] Boyce, *Nature* **466**, 466 (2010). [10.] McCubbin, *PNAS* **107**, 11223 (2010). [11.] Greenwood, *LPSC* **41**, 2439. [12.] Sharp, *Science* **329**, 1050 (2010). [13.] Médard, *CMP* **155**, 417 (2008). [14.] Elkins-Tanton, *EPSL* **submitted**, (2011). [15.] Elkins-Tanton, *EPSL* **222**, 17 (2004).

IMPLICATIONS FOR THE DISTRIBUTION OF WATER ICE AND OTHER VOLATILES FROM LCROSS AND LUNAR ORBITAL DATA. R. C. Elphic[1], L. F. A. Teodoro[2], V. R. Eke[3], David A Paige[4], Matthew A Siegler[4], A. Colaprete[1], [1]Planetary Systems Branch, NASA Ames Research Center, Moffett Field, CA, USA. [2]BAER Institute, NASA Ames Research Center, Moffett Field, CA, USA, [3]Institute for Computational Cosmology, Physics Department, Durham University, Durham, UK, [4]Earth and Space Sciences, UCLA, Los Angeles, CA, USA.

Introduction: The LCROSS impact occurred within Cabeus crater (84.9°S, 35.5°W), where the Lunar Prospector Neutron Spectrometer (LPNS) mapped the highest inferred hydrogen abundance on the Moon [1]. Image reconstruction work [2,3] suggests an abundance of ~1 wt% WEH, if confined to the area of permanent shadow. However, the LCROSS impact yielded total water estimates, ice plus vapor, of between 3 and 10 wt% [4]. LRO/Diviner data/modeling reveal that shallow subsurface temperatures $\leq$100K prevail over extensive areas outside strict permanent shadow [5]. Ice-bearing regolith could conceivably exist within a few tens of centimeters of the surface in such permafrost regions. If placed in the relatively limited Cabeus permanently shadow region (PSR), a uniform regolith mixture of 5 wt% water-equivalent hydrogen (WEH) based on LCROSS would create measurably lower epithermal neutron count rates than are actually seen in orbital data; 17.9±0.08 ct/s instead of the 18.20±0.08 ct/s. If such an ice mixture is present in the areally more extensive permafrost region, the disagreement with orbital data is even greater.

It is likely that volatiles are inhomogeneously distributed, due to both impact processes and emplacement history. Here we examine two possibilities that may bring consistency to the orbital and LCROSS measurements.

Inhomogeneous lateral distribution: Consider the extreme case of a bimodal distribution within the crater – patches of relatively dry and relatively icy regolith. Such a model may seem overly simplistic, were it not for the case that LCROSS impacted a doubly-shadowed region with the Cabeus PSR [6]. The evolution of cold-trapped volatiles may be controlled in part by such double-shadowing. In this case the epithermal leakage flux seen from orbit is a mixture of two different values, weighted according to fractional areas. One possibility is that ~40% of the PSR area may be "icy", the remainder dry (implanted solar wind levels of <0.1 wt% WEH). However, if the whole area of permafrost is considered, then as little as 20% of the area will be as "wet" as the LCROSS results (and LCROSS was lucky).

Inhomogeneous depth distribution: For inhomogeneous mixtures, the leakage flux of thermal and epithermal neutrons depends on both depth of burial of an icy layer and its ice abundance. For a given regolith composition, the combination of epithermal and thermal leakage fluxes imply a burial depth and ice abundance. Therefore, for the Cabeus PSR, the pixon reconstruction values for the epithermal flux defines a range of burial depths and ice abundances. The ambiguity is resolved by a reconstruction of the thermal+epithermal flux. There can be significant uncertainties, however, due mainly to variations in iron abundance in the anorthositic regolith. Even small variations in FeO (2 – 6 wt%) can have a significant impact on thermal neutron leakage flux. We use the Lunar Prospector Gamma Ray Spectrometer results for FeO to gauge the thermal neutron dependence on soil composition. With this effect removed, it is possible to estimate both the burial depth of an icy layer and its WEH abundance. The two measurements require one additional assumption: the upper layer is dry and has a prescribed WEH abundance comparable to returned lunar samples. Nevertheless, plausible thermal neutron values in the PSR, while uncertain, include the LCROSS abundances under 50-100 cm of dry soil.

Conclusion: The discrepancy between LCROSS water-equivalent hydrogen abundances of between 5 and 10 wt%, and the inferred orbital homogeneous abundances of 0.2 to 1 wt% can be resolved. It is physically realistic to expect that lateral and/or depth variations in volatile abundances occur, and a reasonable range of these values leads to agreement. Between 20% and 40% of the Cabeus floor may be "icy", or alternatively a 5-10 wt% "icy" layer exists between 50 and 100 cm beneath a layer of dry regolith within the PSR. But volatile abundances of 5 wt% or more, distributed uniformly and homogeneously throughout the Cabeus PSR do not agree with orbital measurements.

References: [1] Feldman, W. C. et al. (2001) *J.Geophys.Res., 106,* 23,231. [2] Eke, V. et al., (2009), *Icarus 200,* p 12. [3] Teodoro, L., et al., (2010), *Geophys. Res. Lett., 37,* L12. 201. [4] Colaprete, A et al. (2010) *Science*, *330*, 463-468. [5] Paige, D. A. et al. (2010) *Science, 330*, 479-482. [6] Colaprete, A., et al. (2011), *this conference.*

THE CHARACTER OF THE SOLAR WIND, SURFACE INTERACTIONS, AND WATER. W. M. Farrell[1,2] and the DREAM Lunar Science Institute, [1]NASA/Goddard SFC, Greenbelt MD (William.M.Farrell@nasa.gov), [2]NASA Lunar Science Institute, Ames RC, Moffett Field, CA.

We discuss the key characteristics of the proton-rich solar wind and describe how it may interact with the lunar surface. We suggest that solar wind can be both a source and loss of water/OH related volatiles, and review models showing both possibilities.

Energy from the Sun in the form of radiation and solar wind plasma are in constant interaction with the lunar surface. As such, there is a solar-lunar energy connection, where solar energy and matter are continually bombarding the lunar surface, acting at the largest scale to erode the surface at 0.2 Angstroms per year via ion sputtering [1]. Figure 1 illustrates this dynamically coupled Sun-Moon system.

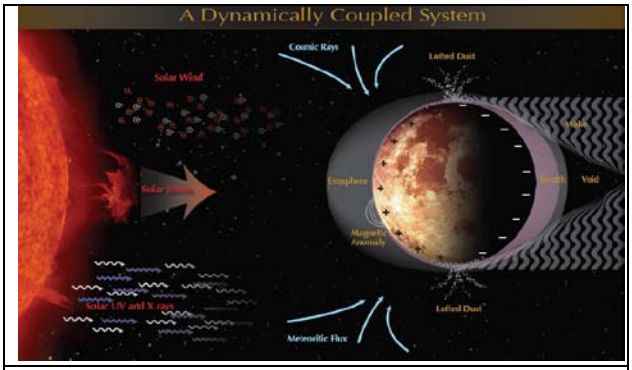

The solar-lunar energy coupling via solar radiation, solar wind plasma, and episodic solar storms

The Solar Wind Plasma. The Sun emits a plasma from its corona called the solar wind. At 1 AU, this wind has a nominal density of 5 ions per cubic centimeter, a temperature of ~ 10^5K, and a flow speed of 400 km/sec. However, this solar wind is highly variable with densities & temperatures capable of changing by a factor of 5 and flow speeds by a factor of 2.

Solar Storms. The solar wind energy can become extraordinarily intense during a solar storm and associated coronal mass ejection (CME). A CME is a regional mass of plasma being ejected from the sun at high speeds (super-Alfvenic speeds). The driver gas typically has a collisionless shock ahead of it. This driver gas can also be 10-15 times denser than the nominal solar wind and contain a greater concentration of the heavy, highly-charged He^{++} than nominal solar wind.

Plasma/Surface Interactions. There are a number of ways the plasma interacts with the surface. First, there is an electrical connection. Plasma and photo-electron currents must all be balanced at the surface. As such, the lunar surface will become charged to create that current balance. On the photo-electron driven dayside, the surface charges positive but on the nightside charges strongly negative in association with the trailing plasma void [2,3].

Second, there is an interaction in the form of a sputtering loss of regolith atoms via solar wind ions. In sputtering, incoming energetic ions transfer kinetic energy to the bound surface atoms, releasing surface material back into the space environment. There are really three types of sputtering [4]: momentum exchange, ionization, and chemical, and we will review all three and show examples of each class. There is also ion sputtering from the surface, where a solar wind ion releases an ion refractory species (like Si or Fe) [5].

Third, the solar wind electrons can act to release material via electron stimulated desorption processes [4]. At the heart of this process is a chemical interaction where the energetic electron alters the existing potential state of the surface-bound atom interaction. For example, a volatile loosely bound to the regolith could be affected by the chemical interaction of the solar wind electron of a few eV [6]. As we demonstrate, a challenge in understanding the electron interaction is the transition from the classical plasma physics picture to the quantum solid state picture.

The Water Paradox. Ironically, solar wind can be considered both a source and a loss for surficial water. Source mechanisms include the recombinative desorption process [6] and manufacturing via impact vaporization [7]. In this former case, solar wind protons incident with the surface take an O from the silica and form OH; the OHs then merging to create and release water. In the latter, a build-up of solar wind implanted hydrogen in the surface may be transformed to water using the energy in impact vaporization. However, water losses from sputtering should ever-present (especially on the dayside). As such, any water buildup must also be tempered by solar wind ion sputtering losses. We will provide an example from a polar crater model [8].

References: [1] Stern S. A., Rev. Geophys., 37, 453, 1999; [2] Manka, R. H., in Photon and Particle Interactions with surfaces in space, ed R. J. L. Grard, Reidel Pub., 1973; [3] Halekas J. S. et al., Planet. Space Sci., in press, doi:10.1016/j.pss.2010.08.0112011; [4] Johnson, R. E., Energetic Charged Particle Interactions with Atmospheres and Surfaces, Springer-Verlag, 1990; [5] Elphic, R. C. et al., Geophys. Res. Lett., 18, 2165, 1991; [6] Dyar, M. D., et al., Icarus, 208, 425, 2010; [7] Vondrak, R. R. and D. H. Crider, Am. Sci., 91, 322; [8] Farrell W. M. et al., J. Geophys. Res. 115, E03004, 2010

Space Environmental Erosion of Polar Icy Regolith. W. M. Farrell[1,5], R. M. Killen[1,5], R. R. Vondrak[1,5], D. M. Hurley[2,5], T.J. Stubbs[1,3,5], G. T. Delory[4,5], J. S. Halekas[4,5], M. I. Zimmerman[1,5] and the DREAM Lunar Science Institute, [1]NASA/Goddard SFC, Greenbelt MD (William.M.Farrell@nasa.gov), [2]Johns Hopkins/Applied Physics Laboratory, [3]Univ. of Maryland Baltimore County, [4]Univ. of California, Berkeley, [5]NASA Lunar Science Institute, Ames RC, Moffett Field, CA.

While regions at the floors of permanently shadowed polar craters are isolated from direct sunlight, these regions are still exposed to the harsh space environment, including the interplanetary Lyman-α background, meteoric impacts, and obstacle-affected solar wind.

We demonstrate that each of these processes can act to erode the polar icy regolith located at or near the surface along the crater floor. The Lyman-α background can remove/erode the icy-regolith via photon-stimulated desorption [1], meteoric impacts can vaporize the regolith [2], and redirected solar wind ions can sputter the ice-regolith mix [3].

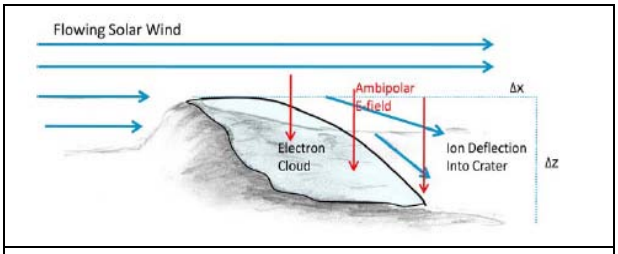

Deflected solar wind ion inflow into a lunar polar crater, redirected by ambipolar processes (from [3])

As an example we shall examine in detail the inflow of solar wind ions and electrons into polar craters. One might expect such ions to flow horizontally over the crater top (see Figure). However, we find that plasma ambipolar processes act to deflect passing ions into the craters [3]. We examine this plasma process and determine the ion flux as a function of position across a notional crater floor. We demonstrate that inflowing solar wind ions can indeed create sputtering along the crater floor, effectively eroding the surface. Erosion time scales from sputtering will be presented.

We shall also consider the effect of impact vaporization on buried icy-regolith regions. There will also be a discussion of solar wind electrons that enter into the PSR, demonstrating that these also have the ability free surface-bound atoms via electron stimulated desorption processes [1].

References: [1] Thrower J. D. et al., J. Vac. Sci. Technol., A 28, 799, 2010. [2] Cintala, M. J., J. Geophys. Res., 97, 947, 1992. [3] Farrell W. M. et al., J. Geophys. Res. 115, E03004, 2010.

Volatile Analyzer for Lunar Polar Missions. Everett.K. Gibson[1], Colin T. Pillinger[2], David S. McKay[1], and Lester J. Waugh[3]. [1]KR, NASA-JSC, Houston, TX 77058, [2]PSSRI, The Open University, Milton Keynes, MK7 6AA, UK, [3]EADS Astrium, Stevenage, UK. everett.k.gibson@nasa.gov

One of the major questions remaining for the future exploration of the Moon by humans concerns the presence of volatiles on our nearest neighbor in space. Observational studies, and investigations involving returned lunar samples and using robotic spacecraft infer the existence of volatile compounds particularly water [1]. It seems very likely that a volatile component will be concentrated at the poles in circumstances where low-temperatures exist to provide cryogenic traps. However, the full inventory of species, their concentration and their origin and sources are unknown. Of particular importance is whether abundances are sufficient to act as a resource of consumables for future lunar expeditions especially if a long-term base involving humans is to be established.

To address some of these issues requires a lander designed specifically for operation at a high-lunar latitude. A vital part of the payload needs to be a volatile analyzer such as the Gas Analysis Package specifically designed for identification quantification of volatile substances and collecting information which will allow the origin of these volatiles to be identified [1]. The equipment included, particularly the gas analyzer, must be capable of operation in the extreme environmental conditions to be encountered. No accurate information yet exists regarding volatile concentration even for sites closer to the lunar equator (because of contamination). In this respect it will be important to understand (and thus limit) contamination of the lunar surface by extraneous material contributed from a variety of sources. The only data for the concentrations of volatiles at the poles comes from orbiting spacecraft and whilst the levels at high latitudes may be greater than at the equator, the volatile analyzer package under consideration will be designed to operate at the highest specifications possible and in a way that does not compromise the data.

Various space agencies are considering a lunar landing mission near the end of this decade. Hopefully, those missions will include a lunar water and volatile resource analyzer. A team from NASA-JSC, The Open University, EADs Astrium and other industrial, educational and international scientific colleagues have been studying the design for a water and volatile analyzer using the heritage from the Gas Analysis Package of Beagle 2 and the Lunar Beagle concept instrument [2]. The purpose of the study was to produce a preliminary design for a package to characterize water and volatiles during the lunar landing mission provisionally scheduled for launch by the end of the decade. The design took into consideration the problems created by contamination and was compatible with all mission and environmental constraints.

The analysis instrument under study would provide information on the measurement of the number density and composition of both neutrals and ions in the lunar exosphere. Whilst the measurement of neutrals are doubtless important and insightful (e.g. answering questions such as the efficiency of cryogenic trapping of individual species, efficiency during the fourteen day lunar night (and their release during the temperature rise associated with the dawning of the lunar day). The long term monitoring of the lunar exophere is important to understand because of increased human presence on this delicate environment.

The instrument package under consideration would also include the capability to collect samples in the vicinity of the lander. Surface and sub-surface samples would be collected utilizing a device such as a lunar mole [2]. The samples would be characterized via XRF, Mossbauer and optical spectroscopy prior to water and volatile analysis. Techniques developed for the Beagle 2's Gas Analysis Package [2] will be used for "processing" the sample prior to releasing the water and volatiles by heating. Identification of the released volatiles will be made via mass spectrometry along with measurements of the volatiles abundances and isotopic compositions.

Hopefully, the volatile analyzer package can be selected for a future lunar lander and additional vital information can be provided to the scientific and engineering community on the state and role of water and volatiles on the Moon.

References: [1] Gibson E.K., Pillinger C.T. and Waugh L.J. (2010) Lunar Beagle and Lunar Astrobiology, *Earth, Moon and Planets*, 107, 25-42. [2] Gibson, E.K., Pillinger C.T. and Waugh L.J. (2009) *Beagle 2 The Moon Concept Study*, NASA-JSC, 125 pgs.

LRO-LAMP MEASUREMENTS OF FAR-ULTRAVIOLET ALBEDOS IN PERMANENTLY SHADOWED REGIONS. G. R. Gladstone[1], K. D. Retherford[1], S. A. Stern[2], A. F. Egan[2], P. F. Miles[1], M. H. Versteeg[1], D. C. Slater[1], M. W. Davis[1], J. Wm. Parker[2], D. E. Kaufmann[2], T. K. Greathouse[1], A. J. Steffl[2], J. Mukherjee[1], D. Horvath[1], P. D. Feldman[3], D. M. Hurley[4], W. R. Pryor[5], and A. R. Hendrix[6], [1]Southwest Research Institute, 6220 Culebra Rd., San Antonio, TX 78238, [2]Southwest Research Institute, 1050 Walnut St., Boulder, CO 80302, [3]Johns Hopkins University, 3400 N. Charles St., Baltimore, MD 21218, [4]Johns Hopkins University Applied Physics Laboratory, 11100 Johns Hopkins Rd., Laurel, MD 20723, [5]Central Arizona University, [6]Jet Propulsion Laboratory, Pasadena, CA.

Introduction: The Lyman Alpha Mapping Project (LAMP) [1] is a far-ultraviolet (FUV) imaging spectrograph on NASA's Lunar Reconnaissance Orbiter (LRO) mission [2]. During LRO's nominal mission for NASA's Exploration Systems Mission Directorate (ESMD), i.e., during 9/15/2009–9/14/2010, the LAMP instrument observed FUV brightnesses on the nightside of the Moon to search for indications of water frost and other surface volatiles in permanently shadowed regions (PSRs) near each pole. LAMP accomplished this by measuring the signal reflected from the nightside lunar surface and in PSRs using interplanetary medium (IPM) Lyα and FUV starlight as light sources. Both these light sources provide fairly uniform, faint illumination and were estimated using model fits of SOHO/SWAN data for the IPM Lyα illumination and IUE data for stellar fluxes (plus LOLA topography for sky visibility) in order to convert the LAMP-observed brightnesses into albedos.

Observations: LRO's polar orbit provides for repeated observations of PSRs, enabling accumulation of the faint reflected UV signal with the photon-counting LAMP instrument. The LAMP instrument covers an FUV passband of 57-196 nm, and its 6°×0.3° slit is nominally pointed at the nadir.

At LAMP's sensitivity the nightside count rate due to reflected IPM Lyα light is ~200-300 counts/s over the entire slit, which from ~50-km altitude amounts to >150 counts/km^2 from each ~5-km wide orbit swath. The background count rate is very low (~20 counts/s), so the signal-to-noise ratio (SNR) for a Lyα albedo map is approximately the square root of the number of counts per bin, e.g., >10 in polar regions for 240-m bins.

Results: The Lyα albedos of PSRs are quite variable, as shown in Figure 1. Most PSRs (e.g., Haworth, Shoemaker, Faustini) are considerably less reflective at Lyα wavelengths (A~0.03) than are their surroundings (A~0.04). However, some PSRs (e.g., Shackleton, and a similar-sized crater on the southern rim of Nobile) are no less reflective than their surroundings. The lower albedo regions are roughly correlated with the coldest regions reported in Diviner temperature maps.

In this presentation we will investigate some possible causes of this albedo darkening at Lyα wavelengths, e.g. the presence of UV-absorbing volatiles at the surface and/or changes in surface properties (e.g., roughness) at these interesting locations. Note that because of the (nearly) uniform illumination by the IPM Lyα, the LAMP surface albedos are directly related to the single-scattering albedo (ω_o) of the surfaces particles [3], with ω_o~4A.

References:

[1] Gladstone, G. R. et al. (2010) *Space Sci. Rev.*, *150*, 161-181. [2] Chin, G. et al. (2007) *Space Sci. Rev.*, *129* 391-419. [3] Hapke B. (1993) *Theory of Reflectance and Emittance Spectroscopy*, Cambridge, 455 pp. [4] Mazarico, E. et al. (2011), Icarus, 211, 1066-1081.

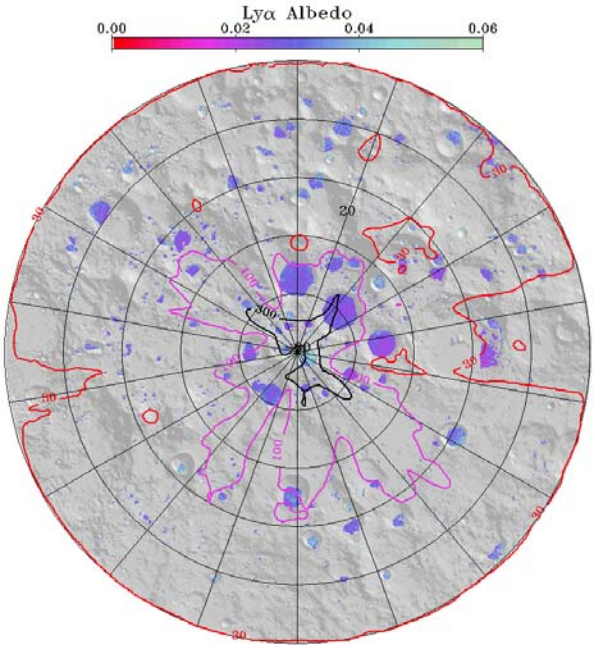

Fig. 1. LAMP nightside Lyα albedos of LOLA-determined PSRs [4] near the south pole, overplotted on a shaded relief map of a LOLA 240m DEM. Both data sets are from the nominal ESMD mission. The contours show accumulated LAMP counts in counts/240-m pixel, which is approximately SNR^2. Note the considerable variation in PSR albedo.

WATER IN THE MOON: EVIDENCE FROM HYDROGEN ISOTOPE COMPOSITIONS OF LUNAR APATITE. J. P. Greenwood[1], S. Itoh[2], N. Sakamoto[2], P. H. Warren[3], M. D. Dyar[4], L. A. Taylor[5] and H. Yurimoto[2], [1]Dept. of Earth & Environmental Sciences, Wesleyan University, Middletown, CT 06459 USA, [2]Natural History Sciences, Hokkaido University, Sapporo 060-0810 Japan, [3]Dept. of Earth & Space Sciences, UCLA, Los Angeles, CA 90095 USA, [4]Dept. of Astronomy, Mount Holyoke College, S. Hadley MA 01075 USA, [5]Dept. of Earth & Planetary Sciences, University of Tennessee, Knoxville, TN 37996 USA.

Introduction: Since the discovery of trace amounts of water in lunar fire-fountain glasses in 2008 [1], several groups have more recently reported on the existence of copious amounts of water in lunar apatite [2-5], with maximum values of 6050 ppm determined from mare basalt 12039 apatite [5]. Modeling of these results to determine the original content of water in the lunar mantle is fraught with difficulties and unknowns in key parameters [2,3]. We have recently reported the first D/H measurements of lunar water from ion microprobe measurements of D/H in apatite from Apollo rock samples [5]. Here we summarize and discuss key results of our research.

Results and discussion: Results of our ion microprobe spot analyses of H_2O and D/H of lunar apatite are shown in Fig. 1. A histogram of our D/H results are shown in Fig. 2.

D/H of the Moon. The mean and standard deviation of δD analyses of mare basalts 10044, 12039, and 75055 are +681±132‰ (n=27) (Fig. 2). That the D/H of these 3 mare basalts from different landing sites should be so similar argues that the mare source region is also similarly elevated in D/H.

The δD of apatite from an intrusive highlands alkali anorthosite clast (14305,303) is also elevated relative to Earth (δD=+238±72‰; +341±53‰), but less so than mare basalts 10044, 12039, and 75055. The elevated D/H for this intrusive sample seems to rule out assimilation of regolith material (derived from comets or asteroids) by the extrusive mare lavas to explain the elevated D/H of the Moon.

Degassing of H_2. The mean and standard deviation of δD of pigeonite basalt 12039,43 are +698±61‰ (n=9). This is almost identical to the mean δD of 12039,42 (mean δD=+689±180‰ (n=13) [5]), but with much less variability. We have analyzed 13 apatite grains in 12039, and these grains exhibit a 6-fold change in water content and almost no change in D/H. This argues strongly against a model of degassing of H_2 from lunar magmas with Earth-like D/H *during apatite crystallization* to explain the elevated D/H of 12039 apatite. Our results do not rule out degassing of H_2 *prior to apatite crystallization* to explain elevated D/H of mare basalts.

References: [1] Saal A. E. et al. (2008) *Nature 454,* 192-196. [2] McCubbin F. et al. (2010) *PNAS 107,* 11223 [3] Boyce J. et al. (2010) *Nature 466*, 466. [4] McCubbin F. et al. (2010) *Am. Min. 95* 1141 [5] Greenwood J. P. et al. (2011) *Nature Geosci.* doi:10.1038/NGEO1050.

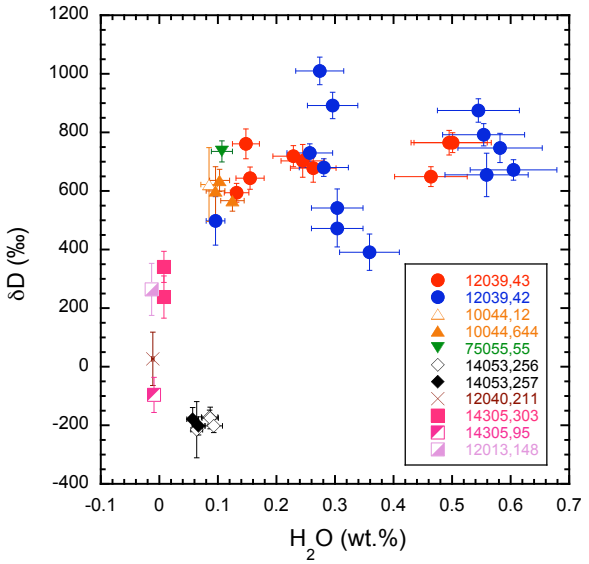

Figure 1. δD vs. H_2O (wt.%) plot of apatite from lunar samples collected during the Apollo programme.

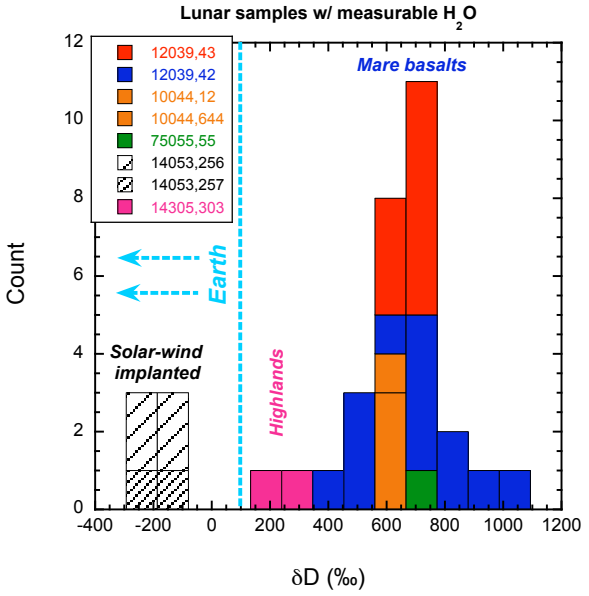

Figure 2. Histogram of δD analyses of lunar samples with measurable water.

NEWLY IDENTIFIED POTENTIAL LUNAR PYROCLASTIC DEPOSITS. J.O. Gustafson[1], J.F. Bell III[2,3], L.R. Gaddis[4], B.R. Hawke[5], T.A. Giguere[6] and the LROC Science Team. [1]Dept. Earth & Atmospheric Sciences, Cornell University, Ithaca, NY 14853; [2]Astronomy Dept., Cornell University, Ithaca, NY 14853; [3]School of Earth and Space Exploration, Arizona State University, Tempe, AZ 85281; [4]Astrogeology Program, U.S. Geological Survey, Flagstaff, AZ 86001; [5]Hawaii Institute of Geophysics and Planetology, University of Hawaii, Honolulu, HI 96822; [6]Intergraph Corporation, Kapolei, HI 96707.

Introduction and Background: Pyroclastic deposits have been recognized all across the Moon, identified by their low albedo, smooth texture, and mantling relationship to underlying features [1-3]. Localized pyroclastic deposits (LPDs) have been interpreted to form by the explosive release of pressure resulting from degassing of shallow magma intrusions [4]. Characterizing the frequency and distribution of such deposits will help constrain estimates of the concentration and distribution of volatile constituents in the lunar crust. At least 55 potential LPDs have been identified during previous studies (e.g. [5]). Lunar Reconnaissance Orbiter (LRO) camera data [6] are being used to search for dark mantle deposits of potential pyroclastic origin that have not been previously catalogued.

Methods: We examined LROC WAC and NAC images for dark deposits with morphologic indicators of pyroclastic origin, such as:

- mantle and subdue subjacent terrain
- exhibit diffuse margins
- do not embay adjacent topographic lows
- associated with rilles or possible vents

Results and Discussion: We have identified approximately 15 candidate deposits that we consider to be of "possible" or "probable" pyroclastic origin. "Possible" deposits generally have low albedo, lack sharp margins, and exhibit some evidence of mantling the local topography. In addition to these features, "probable" deposits typically either exhibit strong evidence of mantling or are associated with possible vents.

These potential newly identified pyroclastic deposits are located primarily on the near side, in both the highlands and the maria. The most common setting is either highlands adjacent to maria or within basalt-flooded highlands craters (Fig. 1). The deposits are usually found in areas exhibiting other evidence of volcanic activity (e.g. effusive deposits, rilles, domes, or possible vent structures). Suspected vents often appear as irregular depressions 1-2 km wide and 2-5 km long, although in some cases individual vents may be contained within larger depressions of possible tectonic origin. Two "probable" locations are the dark-halo craters and associated deposits within farside craters Anderson E&F (Fig. 2).

Fig. 1 - Previously cataloged locations of pyroclastic deposits and additional candidate locations

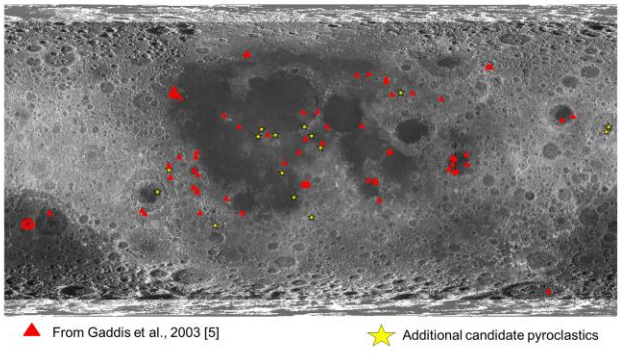

Conclusions and Future Work: An examination of LROC images has indicated that there are potential localized lunar pyroclastic deposits that have not been cataloged in previous surveys, most likely due to their small size or subtle features. Consistent with previous studies, they are concentrated on the near side, typically near the margins of basins and in floor-fractured craters. However, our survey has located probable LPDs within Anderson E&F on the lunar farside that are distant from previously known deposits. Cataloging deposits such as these is important for understanding the number and distribution of these volatile-driven pyroclastic eruptions.

Fig. 2 – Probable pyroclastic deposits in Anderson E&F

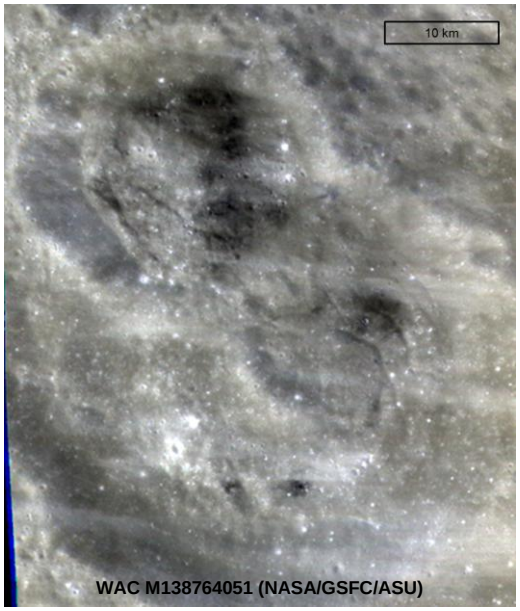

References: [1] Head J.W. III (1974) *PLSC 5th*, 207-222. [2] Gaddis L.R. *et al*. (1985) *Icarus* 61, 461-488. [3] Hawke B.R. *et al*. (1989) *PLPSC 19th*, 255-268. [4] Head J.W. and Wilson L. (1979) *PLPSC 10th*, 2861-2897. [5] Gaddis L.R. *et al*. (2003) *Icarus* 161, 262-280. [6] Robinson M.S. *et al*. (2010) *Space Sci. Rev*. 150 (1-4), 81-124.

THE POTENTIAL OF IMPACT MELTS AS A LUNAR WATER RESERVOIR. R. S. Harris[1,2] and P. H. Schultz[2], [1]Department of Geosciences, Georgia State University, Atlanta, GA 30302 (rsharris@gsu.edu), [2]Department of Geological Sciences, Brown University, Providence, RI 02912 (peter_schultz@brown.edu).

Summary: The possible role of cometary and/or asteroidal impacts in the delivery of water to the lunar environment has been widely recognized (e.g., [1-3]). However, most water retention models focus on the eventual fate of the vapor phase released from the impactors during hypervelocity collisions. We propose that significant concentrations of water, and perhaps other volatiles, can be trapped more directly as dissolved species in impact melts. The resulting water-rich glasses subsequently can be buried and assimilated into lunar magmas, while surviving fragments in the regolith and fresh ejecta can slowly release OH^- and H_2O to the surface [2]. We provide geologic and experimental evidence supporting the plausibility of this concept, and we suggest that lunar impact glasses should be scrutinized with the same attention presently applied to the reanalysis of volcanic ejecta in order to assess their contribution to the Moon's water budget.

Hydrous Impact Melts in Nature and Experiments: We previously have reported (e.g., [4, 5]) the preservation of hydrous melts in natural glasses produced by impacts into wet loess on the Pampean plain of Argentina (Fig. 1). We have measured water concentrations as high as ~20 wt% using multiple techniques including μT-FTIR, μR-FTIR, and SIMS. Similar experimental melts were produced at the NASA Ames Vertical Gun Range (AVGR) by firing Pyrex® projectiles into water-saturated pumice targets. Both high pressures and rapid quench rates appear to play a role in their formation.

If target volatiles can be entrained in an impact melt, volatiles originating from certain portions of the impactor should be available to trapping, as well. In order to investigate this process experimentally, we fired simulated comets and wet asteroids into dry pumice targets at the AVGR. The "comets" are water-filled hollow aluminum spheres, and the "asteroids" are fashioned from serpentinite. These collisions produce amalgamated melts of target and projectile material. Two interesting observations have been made in our preliminary analyses. The "comet" impacts produce some yellowish, filamentous materials reminiscent of the hydrous inclusions shown in Fig. 1. The melted target materials also appear to contain abundant clay-like phases (either absent or far less concentrated in the pre-impact pumice). We currently are analyzing these experimental melt breccias to determine their compositions and water contents. Phyllosilicate production either during or as an immediate disintegration of wet melts could be an additional way to sequester volatile species in lunar soils and breccias.

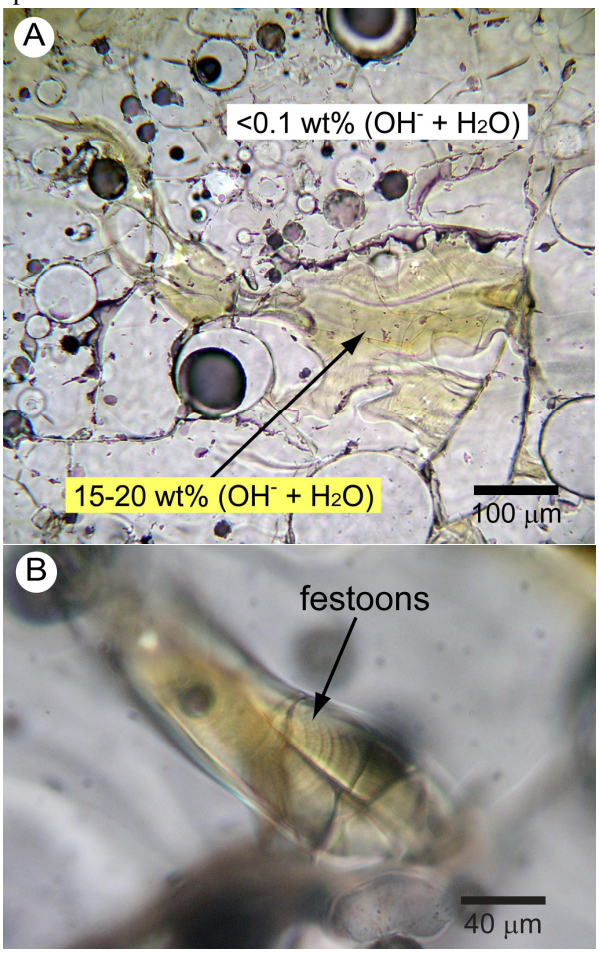

Figure 1. Plane-polarized light (PPL) photomicrographs of terrestrial impact glasses formed by melting water-rich regolith. A) Hydrous yellow glass inclusion in 425 ka impact glass from Centinela del Mar, Argentina. The encasing clear glass is essentially anhydrous. B) Ropy hydrous inclusion in 9.21 Ma impact melt breccia from Chasicó, Argentina.

References: [1] Ong L. et al. (2010) *Icarus, 207*, 578-589. [2] Schultz P. H. et al. (2010) *Science, 330,* 468-472. [3] Greenwood J. P. et al. (2011) *Nature Geoscience, 4*, 79-82. [4] Harris R. S. and Schultz P. H. (2005) *Meteoritics & Planet. Sci., 40,* A63. [5] Harris R. S. et al. (2007) *LPI Contr. No. 1360*, 8051.

Acknowledgements: This work was funded in part by NASA PGGP Grant NNX08AM45G to PHS. Additional support was provided to RSH by the Mary-Hill and Bevan M. French Fund for Impact Geology. We appreciate the continued advice and assistance of P. L. King (UNM).

EVIDENCE FOR HIGH VOLATILE ABUNDANCES IN LUNAR MELT INCLUSIONS. E. H. Hauri[1], T. Weinreich[2], A. E. Saal[2], M. C. Rutherford[2], and J. A. Van Orman[2], [1]Department of Terrestrial Magnetism, Carnegie Institution of Washington, Washington DC 20015 (ehauri@ciw.edu), [2]Department of Geological Sciences, Brown University, Providence, RI 02912, [3] Department of Geological Sciences, Case Western Reserve University, Cleveland, OH 44106

Introduction: Melt inclusions have been used for decades to determine pre-eruptive volatile contents of terrestrial magmas from subduction zones, hotspots and mid-ocean ridges [1], as well as volatile contents of Martian magmas [2]. Using standard petrographic methods, Edwin Roedder and Paul Weiblen were the first to identify silicate melt inclusions trapped within lunar minerals, ranging in size from 1μm up to 400μm, and they would go on to identify and melt inclusions in samples returned from all of the Apollo and Luna missions [3 and refs therein]. Many of these early-described melt inclusions were analyzed for major elements by microprobe, and though only a minority of the melt inclusions were trapped in early-crystallizing minerals such as olivine, it is clear from Roedder's data that most of the range in TiO_2 content observed in mare basalts and picritic pyroclastic glasses is reflected in the composition of silicate melt inclusions. This observation indicates that lunar melt inclusions preserve much of the range of magma compositions that are thought to have been erupted on the Moon's surface.

The Gas Phase in Lunar Melt Inclusions: For the purposes of studying the abundances of volatile elements in primitive lunar magmas, a key observation that can be gleaned from the early work on lunar melt inclusions is that they often contained a vapor bubble co-existing with glass ± daughter minerals within the inclusion cavity. The volume fraction of the inclusion cavity occupied by these vapor bubbles ranges from 1% up to 20%. These vapor bubbles could be syngenetic (trapped together with the inclusion), and/or they could be shrinkage bubbles that exsolved during differential shrinkage of melt within the inclusion during cooling of the host crystal; high volume fractions of vapor favor a syngenetic origin for some vapor bubbles. In either case, the presence of vapor bubbles in silicate melt inclusions from the Moon, including those trapped in olivine, is direct evidence that lunar magmas contained significant amounts of volatile elements that partition into a vapor phase at magmatic temperatures, and that lunar magmas likely reached vapor saturation at some point in their eruptive evolution. The importance of this observation was noted by Roedder & Weiblen in their very first study of lunar melt inclusions [4], but its significance has grown in light of new data indicating the presence of magmatic water in primitive lunar magmas, and extrapolation of low measured H_2O contents to provide estimates of pre-eruptive water concentrations [5].

Implications for Volatiles in Lunar Magmas: The amount of gas contained in a melt inclusion vapor bubble can be estimated from the ideal gas equation (PV=nRT), given measurements of the vapor saturation pressure within the inclusion cavity, the volume of the vapor bubble, and an assumption about the vapor trapping temperature (commonly assumed to be the glass transition temperature). If one assumes an origin as a shrinkage bubble, then this gas can be added back into the volume of melt to arrive at an estimate of the magma's volatile content at the time of trapping. This method is commonly used in studies of terrestrial melt inclusions, and is facilitated by measurement of volatiles whose pressure-dependence is well known, such as CO_2 and H_2O [6], to provide a measure of the vapor saturation pressure within the melt inclusion. Unfortunately, for lunar melt inclusions, low fO_2 does not favor the formation of CO_2 vapor, and so even if we knew the C and H_2O contents of glass within a lunar melt inclusion, the uncertainty about C speciation in the melt and its pressure-dependent solubility hinders any educated estimate at the vapor saturation pressure prevailing within lunar melt inclusion vapor bubbles.

Nevertheless, some simple calculations are instructive. If we assume a melt inclusion pressure of 100 bars, equivalent to a depth of only 300 meters below the lunar surface, and add the vapor phase back into the melt inclusion, vapor volume fractions of 1% to 20% result in ideal gas abundances in the melt that range from 685 to 13,200 ppm on a molar basis. This would translate into mass abundances of 60-1200 ppm C for a pure carbon vapor, or H_2O abundances of 90 to 1800 ppm H_2O for pure water vapor. These abundances are higher than directly measured in primitive lunar glasses, but overlap the range of pre-eruptive water contents extrapolated from picritic glass diffusion profiles [5].

References: [1] Hauri E. H. et al. (2002) *Chem Geol, 183,* 1–4. [2] Leshin-Watson L. et al. (1994) *Science, 265,* 86-89. [3] Roedder E. and Weiblen P. (1977) *LPS XVII,* 1767–1783. [4] Roedder E. and Weiblen P. (1970) *LPS I,* 801–837. [5] Saal A. E. et al. (2008) *Nature, 454*, 192-195. [6] Dixon J. E. et al. (1995) *J Petrol, 36,* 1607-1631.

SCOURING THE SURFACE: EJECTA DYNAMICS AND THE LCROSS IMPACT EVENT B. Hermalyn[1], P. H. Schultz[1], M. Shirley[2], K. Ennico[2], and A. Colaprete[2] [1]Brown University, Providence, RI 02912-1846 (Brendan_Hermalyn@brown.edu), [2]NASA Ames Research Center, Moffett Field, CA 94035

Introduction and Background: The Lunar CRater Observation and Sensing Satellite mission (LCROSS) utilized the spent upper stage of a rocket as a kinetic impactor to launch material from a permanently shadowed region (PSR) within Cabeus crater above the sunlight horizon [1]. A suite of nine instruments onboard the LCROSS shepherding spacecraft (SSc) made measurements of the sunlit ejecta and released volatiles[1, 2]. By integrating the observations from multiple instruments (including those onboard LRO [3, 4]), a time-resolved evolution of the cratering event can be constructed. While the combined observations establish the presence of volatiles, interpretation of the source region and conditions in the PSR from these data is highly dependent on the specific mechanics of the impact (e.g., the high weight percent of species reported in [3]). Here we present the results of a series of impact experiments designed to explore the LCROSS event using both high-speed cameras and LCROSS engineering units.

LCROSS Impact: The impact was a unique cratering event due to the low density and geometry of the hollow Centaur and the relatively low impact speed (2.5km/s). In addition, the ejecta needed to reach the 833m sunlight horizon from the permanently-shadowed floor of Cabeus, placing a high velocity requirement for any material reaching sunlight. In contrast to the standard "inverted lampshade" ejecta curtain, the visible camera (VIS) revealed a relatively symmetric cloud (Fig. 1a). A continued presence of volatiles (and integrated intensity over pre-impact background) in the spectrometer measurements persisted for almost 4 minutes after impact[1].

Experimental Studies and Analysis: Prior to impact, several independent studies predicted the ejecta dynamics of the impact event (e.g., [5, 6, 7]. In this study, a series of impact experiments was performed at NASA Ames Vertical Gun Range to explore the unique characteristics relevant to the LCROSS event. Both high-speed equipment and LCROSS engineering instruments (identical to flight hardware) were used to record the experiments, allowing direct comparison to the mission data. These studies revealed: 1) an early-time, low-angle departure from dimensionally-predicted ejecta models 2) shallower coupling and excavation depths in regolith-like target materials 3) the emergence of a high-angle, high-speed plume that remains aloft well past the end of crater growth (Fig. 1b) and 4) the non-homogenous distribution of heated projectile/target material emplaced by impact. A ballistics analysis of the two-component ejecta curtain scaled from experiments matches the spectrometer and VIS camera measurements of the impact event when convolved with the instruments' fields of view. The LCROSS thermal measurements are more consistent with frictionally-heated target and projectile material dispersed in clumps around the newly-formed crater than a homogeneous layer of heated material.

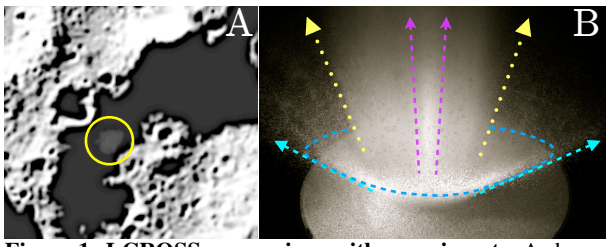

Figure 1: LCROSS comparison with experiments. A shows ejecta (circled in yellow) in LCROSS image reaching sunlight a few seconds after the impact into Cabeus. B is an oblique view of an experiment demonstrating low-angle (blue dashed) and high-angle (dotted yellow) ejecta components. A near-vertical portion of the plume is prominant (magenta).

Conclusions: The unique conditions of the LCROSS impact created a two-component ejecta plume (e.g., Fig. 1) which sampled to different depths in the subsurface: the usual inverted lampshade "low-angle" component and a high speed, high-angle plume. Extrapolations from experimental studies match the VIS data and the light curves in the spectrometers. The impact caused only small amounts of vaporization or shock heating. Warm material is emplaced at early times by sparse ejecta launched at high speeds and heterogeneously around the crater at late times, rather than a simple homogenous "warm" blanket. The crater itself was probably cooled quite rapidly, leaving only localized areas surrounding frictionally-heated portions of the crushed Centaur impactors thermally emitting. Additionally, the ballistic return of sunlight-warmed ejecta surrounding the crater may lead to a significant increase in the surficial source region for volatiles measured in by the LCROSS spectrometers. These results have implications for the spatial distribution of volatiles in the shadows of Cabeus.

References:

[1] Colaprete, A.,*et al.* (2010) *Science 330*(6003).
[2] Schultz, P.H., *et al.* (2010) *Science 330*(6003).
[3] Gladstone, G.R.,*et al.* (2010) *Science 330*(6003).
[4] Hayne, P.O.,*et al.* (2010) *Science 330*(6003).
[5] Schultz, P.H. (2006) *LPI Contributions 1327*.
[6] Korycansky, D.G., *et al.* (2009) *MAPS 44*(4).
[7] Hermalyn, B., *et al.* (2010) *LPSC* vol. 41,2095.

An Overview of Hydrous Lunar Magmatism, with an Emphasis on the Possible Role of Dissolved Molecular Hydrogen in Lunar Basalts.

Marc Hirschmann Department of Geology and Geophysics, University of Minnesota

The increasing pace of observations of endogenous H_2O in high temperature lunar materials represents an exciting challenge to understanding of a range of important processes associated with the origin and differentiation of the Moon. Measurements of lunar materials combined with appropriate models and experimental partition coefficients will presumably document a range of H_2O concentrations in lunar magmatic products and their reservoirs. As I am not engaged in any of these measurements, my purpose is to take a larger perspective on how small to modest H_2O concentrations in lunar magmas may influence our understanding of lunar processes and petrogenesis.

Modest concentrations of H_2O in the lunar interior will undoubtedly influence understanding of delivery and retention of volatiles in the early Earth-Moon system. To date, the largest H_2O concentrations that have been considered in the lunar interior by Saal et al. (2009) that at least some lunar basalt source regions have H_2O concentrations similar to the terrestrial oceanic mantle. Such high concentrations are not easily reconciled with the strong depletions of other volatile elements (Ag, Zn, Sn, In, Br, Cd, Bi, Tl) in lunar basalts, which are 50 X lower than MORB (Wolf and Anders, 1980). If the comparatively high concentrations inferred by Saal et al. (2009) are robust, then either most lunar H_2O must be from a highly fractionated (cometary?) source or the behavior of a wide range of volatiles in lunar petrogenesis require reexamination.

The relatively modest concentrations of H_2O apparent in lunar basalts will likely have relatively little effect on their petrogenesis, except that they may account in part for the vesiculation and eruption dynamics. As is true for MORB, source concentrations as high as 100 ppm H_2O will have modest influence on the region from which small degree (< 1%) melts can be extracted, but little effect on larger degree partial melt source regions. Only modest influences on the major element compositions of basalts is expected, except that effective mean melt fractions will be reduced by extraction of significant hydrous small degree partial melts.

One important consideration is that the comparatively reduced conditions in the lunar interior dictate that much of the dissolved hydrous magmatic component is likely molecular hydrogen rather than H_2O or hydroxyl. Preliminary solubility measurements of molecular H_2 under reduced conditions made at the University of Minnesota (Ardia et al. in prep), analyzed by both FTIR and SIMS, indicate appreciable H_2 solubilities. Combining these results with established dependences of H_2O (OH) solubility on H_2O fugacity, T, and P allows estimation of the relative concentrations of different dissolved hydrous species. For example, at conditions of 1 GPa and 1400 °C and an oxygen fugacity similar to 1.5 log units below iron wustite, as much as 2/3 of the hydrogen, on a molecular basis, can be H_2 rather than H_2O. However, relative proportions of hydrogen and hydroxyl are highly sensitive to oxygen fugacities, absolute concentrations, and pressure. In particular, whereas concentratons of OH vary with the square root of H_2O fugacity, those of dissolved H_2 vary with the H_2 fugacity. Thus, there is a strong possibility of redox reactions between dissolved species on decompression, with magmas driven to more reduced conditions.

MODELING OF HYDROGEN ACCUMULATION AT THE LUNAR POLES. D. M. Hurley[1], R. C. Elphic[2], and R. R. Vondrak[3], [1]Johns Hopkins University Applied Physics Laboraroty (11100 Johns Hopkins Rd., Laurel, MD 20723), [2]NASA Ames Research Center, [3]NASA Goddard Space Flight Center.

Introduction: As evidence mounts establishing the presence of volatiles in permanently shadowed regions of the Moon [1-6], work continues to understand the distribution of those volatiles within the regolith. Are they homogeneous? If not, what is the lateral and depth distribution?

Modeling of space weathering processes on volatile deposits in permanently shadowed regions suggests that there is a time dependent spatial scale for which to expect coherence of a volatile deposit [7-10]. Comparing these predictions from modeling to limits placed on the distribution from the incoming data, one can place limits on the sources and timing of volatile emplacement in lunar permanently shadowed regions. We present modeling results and set benchmarks for the observations.

Space Weathering Model: The model follows the distribution of volatiles with depth in several vertical columns of material. The set of columns of material is separated by different lateral spacing. The volatiles in each column are tracked simultaneously as processes acting on the material modify the abundances.

The model is a Monte Carlo simulation that selects a distribution of impactors to bombard the area of simulation from the crater size-distribution function [11]. The impacts modify the material to a depth determined by the crater shape and the position of the crater center relative to the column. Impacts deposit ejecta in some areas and excavate material from other areas. This process alters the height of the surface, removes volatiles, and redistributes a reduced amount of volatiles. In between discrete impacts, the model computes the evolution in the top layers from steady processes. These include smaller impacts from micrometeoroids, exposure losses to UV and sublimation, diffusion, and delivery of new volatiles.

Performing many runs with different seeds to the random number generator, the output produces a range of final distributions. By averaging over the many runs, the model calculates the expectation values for the distribution of volatiles in a volume of lunar regolith as a function of time.

Interpretations: Starting with various assumptions of the initial distribution of volatiles, we follow the time evolution of pre-existing volatile deposits. Using many Monte Carlo runs, the expectation values for several parameters can be computed: e.g., retention rate, depth of deposit, correlation length. These parameters vary as a function of time, initial conditions, and assumptions about the delivery and loss in between larger impactors. We show the results for the evolution of an ice layer and for the steady accumulation of volatiles in permanent shadow. Using the expectation values, we place limits on how recently an ice layer could be emplaced and be detectable by remote sensing techniques, e.g., radar, neutron spectroscopy, and FUV reflectance.

After the LCROSS impact experiment into Cabeus, data now exist on the liberation of volatiles due to an impact into a permanently shadowed region [5, 12]. We discuss the implications these new results have on the modeling done here. Furthermore, these simulations reflect related processes in effect at the planet Mercury. The similarities to Mercury are discussed. Based on the retention rates calculated here, we also extrapolate to the influx of volatiles to the Moon.

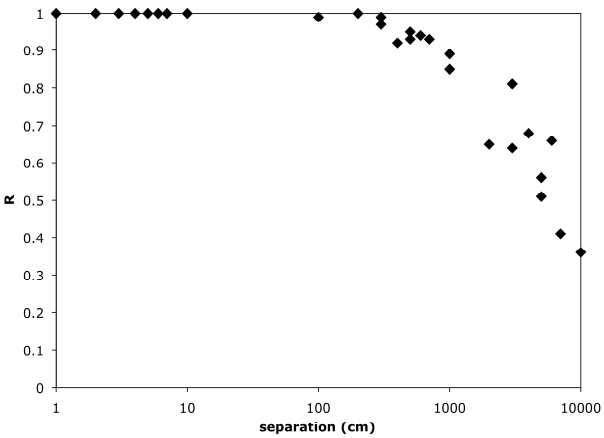

Figure 1. As a function of the lateral separtion of two columns of regolith, the correlation coefficient is shown for the amount of regolith cover emplaced in 100 Myr.

References: [1] Watson K. et al. (1961) *JGR* 66, 3033. [2] Arnold, J. (1979) *JGR 84*, 5695. [3] Feldman W. et al. (1998) *Science 281*, 1496. [4] Bussey B. et al. (2010) *AGU Fall Meeting*, P34A-07. [5] Colaprete A. et al. (2010) *Science 330*, 463. [6] Gladstone, R. et al. (2010) *Science 330*, 472. [7] Arnold J. (1975) *LPSC VI,* 2375. [8] Crider D. and Vondrak R. (2003) *JGR 108*, 5079. [9] Crider D. and Vondrak R. (2003) *ASR 31*, 2293. [10] Crider D. et al. (2006) *Adv. in Geosci. 3*, 93. [11] Neukum G and Dietzel H. (1971) *PSL 12*, 59. [12] Schultz P. et al. (2010) *Science 330*, 468.

IMPLICATIONS OF VOLATILES WITHIN LUNAR BASALTS FOR THE ORIGIN OF SINUOUS RILLE SOURCE DEPRESSIONS. D. M. Hurwitz[1] and J. W. Head, [1]Brown University, 324 Brook Street, Providence, RI 02906; debra_hurwitz@brown.edu.

Introduction: Observations of pyroclastic materials in dark mantle deposits (DMDs) have led to the interpretation that explosive volcanism occurred early in lunar history [1-5]. These explosive eruptions were driven by the exsolution of various volatile species [6-9] and in some cases resulted in the formation of unique geologic features, such as source depressions of sinuous rilles [10,11].

New high-resolution image (Lunar Reconnaissance Orbiter Wide and Narrow Angle Cameras, LROC WAC and NAC) and topography (Lunar Orbiter Laser Altimeter, LOLA) data are used to investigate the morphologies of the source depressions of several lunar sinuous rilles with associated pyroclastic deposits. Details in morphology, such as depression shape and width, the continuity of subsurface layers, and peripheral deposits, are investigated to look for evidence of explosive activity and to explore the origin of the source depressions and the associated sinuous channel.

Lunar Pyroclastic Eruptions:

Geochemical evidence for volatile content. Substantial research has been completed in investigating the volatile content of lunar basalts, both from laboratory measurements of returned glass samples [6-8] and from remote observations of lunar surface deposits [12-14]. Initial investigations of Apollo green and orange glasses found volatile-rich coatings that contained Zn, Pb, Cu, S, F, and Cl, among other volatile species. Advances in ion mass spectrometry have led to increased accuracy in measurements of volatile abundances in the cores of lunar glasses, with the most significant volatile species including S, H_2O, F, Cl, and CO_2 [8]. These more detailed analyses lead to the interpretation that lunar magmas contained more volatiles than previously expected, indicating that the Earth-Moon system either retained significant amounts of volatiles after initial formation or that volatile-rich material accreted to both the Earth and Moon shortly after formation but prior to 4.3 Gyr [8].

In addition to laboratory investigations, observations of volatiles on the lunar surface have been made using visible to near-infrared wavelength spectra collected by Earth-based telescopes [3,5,12], Clementine [13] and the Moon Mineralogy Mapper aboard Chandrayaan-1 [14,15]. Pyroclastic materials are observed within DMDs and are characterized by the presence of a significant Fe^{2+}-bearing component consistent with volcanic glasses [3,5,12].

Theory of explosive eruptions. The occurrence of pyroclastic DMDs have been attributed to eruptions similar to terrestrial Hawaiian-style eruptions [1,2]. Magma was likely generated either from a volatile-rich source deep in the lunar mantle [16] or by recycling and remelting a dense, ilmenite-rich layer in the lunar mantle [17]. While the magma was subjected to larger pressures deep in the lunar interior, the volatile elements remained dissolved, but as the magma rose to the lunar surface and pressure decreased, the gas exsolved and formed a foam that accelerated magma ascent until it erupts explosively at the lunar surface [6,18]. Eruption velocities may have been as high as 50 – 100 m/s [9], resulting in a dispersion of pyroclastic materials that cover an area 6x larger than expected for similar terrestrial eruptions due to lower lunar gravity [5]. Such high eruption velocities likely influenced the formation of the vent, and ponding of lava near the eruption source in some cases resulted in the formation of the depressions surrounding the eruption vent [10].

Observations: LROC WAC and NAC images and LOLA topography data are used to observe morphologies of source depressions of sinuous rilles. Observations of both elongate (i.e., Rima Hadley) and circular (i.e., Rima Prinz) source depressions will be investigated as will sources for sinuous rilles that are associated with pyroclastic deposits (i.e., Rimae Hadley and Bode) and that are not associated with pyroclastic deposits (i.e., Rima Prinz) to compare morphologies of sources with interpreted pyroclastic and effusive volcanic eruption origins.

References: [1] Head J. W. and Wilson, L. (1979) *Proc. LPS X*, 2861-2897. [2] Wilson, L. and Head, J. W. (1981) *JGR*, *86*, 2971-3001. [3] Gaddis, L. R. et al. (1985) *Icarus, 61*, 461-489. [4] Coombs, C. R. et al. (1987) *LPS XVIII*, 197-198. [5] Hawke, B. R. et al. (1989) *Proc. LPS XIV*, 255-268. [6] Meyer, C. et al. (1975) *Proc. LPS VI*, 1673-1699. [7] Butler, P. Jr. (1978) *Proc. LPS IX*, 1459-1471. [8] Saal, A. E. et al. (2008) *Nature Letters*, *454*, 192-195. [9] Rutherford, M. J. and Papale, P. (2009) *Geology*, *37*, 219-222. [10] Wilson, L. and Head, J. W. (1980) *LPS XI*, 1260-1262. [11] Coombs, C. R. et al. (1990) *Proc. LPS XX*, 195-206. [12] Lucey, P. G. et al. (1984) *LPS XV*, 495-496. [13] Gaddis, L. R. et al., *Icarus, 161*, 262-280. [14] Pieters, C. M. et al. (2009) *Science*, *23*, 568-572. [15] Clark, R. N. (2009) *Science, 23*, 562-564. [16] Shearer, C. K. et al. (2006) in *New Views of the Moon. Reviews in Mineral. And Geochem., 60*, 365-518. [17] Hess, P. C. and Parmentier E. M. (1995) *Earth Planet. Sci. Lett.*, *134*, 501-514. [18] Wilson, L. and Head, J. W. (2003) *GRL, 30*, 1605.

PRODUCTION OF OH/OD IN LUNAR SAMPLES: PROTON/DEUTERON BOMBARDMENT

A. S. Ichimura[1], A. P. Zent[2], R. C. Quinn[3], L. A. Taylor[4], [1]Department of Chemistry and Biochemistry, San Francisco State University, 1600 Holloway Avenue, San Francisco, CA 94132, ichimura@sfsu.edu, [2]MS 245-3, NASA Ames Research Center, Moffett Field, CA 94035 aaron.zent@nasa.gov, [3]MS 239-4, NASA Ames Research Center, Moffett Field, CA 94035 richard.c.quinn@nasa.gov, [4]Department of Earth and Planetary Sciences, University of Tennessee, Knoxville, TN 37996-1410, lataylor@utk.edu.

Introduction: The Moon Mineralogy Mapper (M^3) on Chandrayaan-1 recently detected IR absorption features in the 2.8 to 3.0 micron range on the surface of the Moon [1]. Corroborating evidence of the spectral absorptions [2,3] and independent identification of polar ice [4] has confirmed that a population of OH, and possibly H_2O, is present in or on particle grains at the lunar surface. In this laboratory study, we sought to test the hypothesis that the ~3 µm signal observed by spectral reflectance remote sensing has its origins in the solar wind [5]. Infrared spectra were acquired from lunar specimens exposed to hydrogen and deuterium ion beams. In particular, the 2.5 - 5.4 µm region corresponding to hydroxyl and deuteroxyl bands was investigated. Although a number of studies have used terrestrial minerals [6] and glasses [5] to carry out ion-implantation experiments and subsequent IR measurements, none have used Apollo lunar soils. The use of lunar soils as targets for implantation provides spectroscopic evidence for the viability of the solar wind hypothesis and enables qualitative comparisons to spectra acquired by remote sensing.

Experimental: Two lunar specimens were used in this study, a mare soil, Apollo 17 (70051), and a plagioclase-rich highland soil, Apollo 16 (62241). Ilmenite powder was also used for implantation experiments. Dehydroxylation/dehydration of the specimens was accomplished by heating them to 500^0C at a pressure of $2x10^{-4}$ Pa for two hours. Ion implantation was accomplished using the etching gun of a Gatan PECS 682 coater-etcher system. In serparate experiments, lunar soils were exposed to $^1H_2^+$ and D_2^+ ion beams with an energy of 2.3 keV, 80-109 µA, and a pressure of 0.03-0.05 Pa for up to three hours. After each hour of exposure, the specimen was removed from the instrument, shaken to expose fresh surface, and the implantation resumed. Samples were immediately transferred to the dry environment of the FTIR for measurent. Spectra were acquired using a Nicolet 4700 FTIR with 4 cm^{-1} resolution and 256 scans.

Results: Figure 1 shows reflectance spectra for the Apollo 16 highland soil reported as the ratio of R/R_0. The specimen heated under vacuum served as the reference, R_0. The effect of high temperature is to dehydroxylate the lunar soil as shown by the broad band at 2.94 µm (3404 cm^{-1}) (Fig. 1, black) of the specimen before any treatment. Exposure of a heated sample to hydrogen or deuterium ion beams produces absorptions at 2.96 (Fig. 1, blue) and 3.92 µm (Fig. 1, red), respectively. The isotope shift of the OH fundamental vibrational stretching frequency from 3520 cm^{-1} to 2600 cm^{-1} during D^+ exposure shows that ion implantation was successful and not due to reaction of the highland soil surface with water vapor during sample transfer between instruments. The IR signals are attributed to hydroxyl and deuteroxyl groups that formed during reaction of H^+ and D^+ with silicates in vapor deposited rims [7]. Comparison of the OH band position and shape in Figure 1 to data acquired by EPOXI [2] are similar suggesting that the bands detected by remote sensing have their origin in the solar wind.

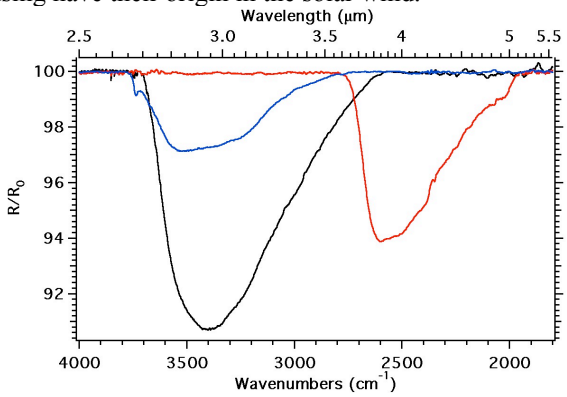

Figure 1. Diffuse reflectance spectra of the Apollo 16 sample before (black), after 500^oC and exposure to the D_2^+ (red) and H_2^+ ion beams (blue).

After intitial measurements, the Apollo 16, 17, and ilmenite specimens were stored under ambient conditions for several months. During this period, a OH signal grew in and the OD signal decreased. IR spectra acquired as a function of storage time will be presented and discussed. IR data acquired in this study will be compared to spectral libraries.

References: [1] Pieters C. M. *et al*. (2009) *Science,* **326**, 568 -572. [2] Sunshine, J. M. (2009) *Science*, **326**, 565 – 568. [3] Clark, R. N., (2009) *Science*, **326**, 562 – 564. [4] Colaprete, A. (2010) *Science,* **330**, 463-468. [5] Zeller, E. B., et al. (1966*) J. Geophys. Res.* **71**(20), 4855-4860. [6] Siskind, B.., et al. (1977) *J. Vac. Sci. Technol*. **14**(1), 537-542. [7] McCord, T. M., et al. (2011), *J. Geophys. Res., in press*.

LUNAR VOLATILES: AN EARTH-MOON PERSPECTIVE. J.H. Jones, KR, NASA/JSC, Houston, TX 77058. john.h.jones@nasa.gov

Introduction: It has generally been accepted that the Moon is depleted in volatile elements [e.g., 1]. However, the recent discovery of measurable water in lunar glasses and apatites [2, 3] suggests that volatiles are not as depleted as was once thought. And, in fact, some authors have claimed that water contents of the lunar and terrestrial mantles are similar [e.g., 2, 4].

Moderately volatile alkali elements may have a bearing on this issue. In general, bulk Moon alkalis are depleted relative to the bulk silicate Earth [1]. Although the bulk lunar chemical composition is difficult to reconstruct, good correlations of alkali elements with refractory lithophile incompatible trace elements make this conclusion robust. These observations have been taken to mean that the Moon overall is depleted in volatiles relative to the Earth (Fig 1). Since water is more volatile than any of the alkali elements, presumably this conclusion is true for water, or even more so.

Figure 1

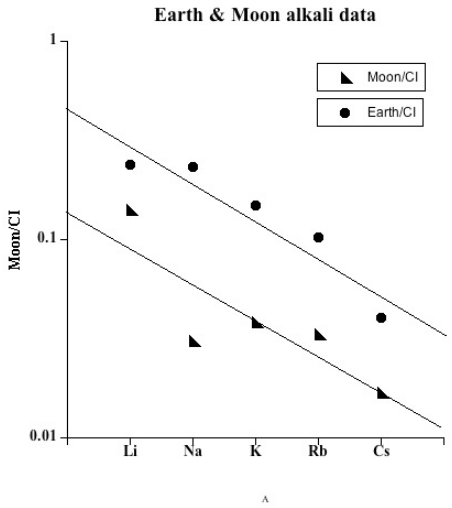

Given this conclusion, it is then of interest to explore how much water exists in the terrestrial mantle and investigate the origin of that water.

What is the water content of the terrestrial mantle? In general, the water content of the Earth's mantle is unknown. But based on (i) bulk analyses of mantle peridotite xenoliths, (ii) analyses of MORB glasses, and (iii) FTIR measurements of water in nominally anhydrous minerals, a value of a few hundred ppm water seems reasonable [5].

Origin of water in the terrestrial mantle: There are two endmember possibilities for the origin of water in the Earth's mantle: (i) it is primordial (i.e., "juvenile") or (ii) it has been emplaced over geologic time by subduction of hydrated oceanic lithosphere.

The isotopic composition of mantle water is presumably of importance in addressing that water's origin. Since oxygen in mantle water is presumably buffered by exchange with mantle silicates and oxides, we turn to H isotopes as a guide.

As a generality, "juvenile" waters have ∂D values of ~ -50-80 ‰. Perhaps coincidentally, this value is approximately that of a vertically integrated column of oceanic crust [6].

Hydrothermal cells at oceanic spreading ridges circulate deep (several kilometers) into the oceanic crust, partially altering the primary igneous minerals into hydrous phases. The nature of these hydrous phases changes with (P,T) conditions, as does the D/H fractionation between the alteration assemblage and the altering fluid. As a consequence, the ∂D of the oceanic crust is variable with depth, but its integrated value is about that of "juvenile" water.

As a consequence of this observation, it is now believed that "juvenile" water does not exist [6]. Or if it does, there is no evidence for it. Water in the Earth's mantle is most probably a secondary phenomenon, the result of subduction plate tectonics. By geochemical standards, the Earth's primordial mantle was probably dry.

Recapitulation: The water content of the terrestrial mantle is to some degree artificial. Our mantle has been highly modified by several eons of subducting hydrated slabs. Of course, this process is not very efficient. A large portion of a slab's water budget tends to be lost early in the subduction process, producing arc volcanics. That said, it is not inconceivable that an ocean of water could have been subducted over geologic time. A corollary of this view is that the water of the Earth's oceans were probably not formed *via* mantle outgassing, but by the late accretion of hydrous materials.

It is not possible to specify with certainty the primordial water content of the terrestrial mantle. Because the Earth has a metallic core, the water content of the Hadean mantle was presumably dictated by water-metal reactions. Regardless, the prediction based on alkali metals is that the Moon has less water than the early Earth.

References: [1] Taylor, S.R. (1982) *Planetary Science: A Lunar Perspective.* Lunar and Planetary Institute. pp. 481. [2] Saal A. et al. (2008) *Nature* **454**, 192-196. [3] McCubbin F.M. (2010) *Lunar Planet. Sci. 41st*, #2468. [4] Boyce J.W. (2010) *Nature* **466**, 466-469. [5] Bell D.R. and Rossman G.R. (1992) *Science* **255**,1391-1397. [6] Criss R.E. (1999) *Principles of Stable Isotope Distribution*. pp. 264.

THE NATURE OF SPACE WEATHERING EFFECTS RECORDED IN LUNAR MATERIALS. L. P. Keller[1], S. K. Noble[2], S. Zhang[1] and R. Christoffersen[3], [1]Mail Code KR, ARES, NASA/JSC, Houston, TX 77058, [2]Code 3Y55, NASA/HQ, Washington, D.C. 20062, [3]Code JE23, Jacobs Tech., Houston, TX 77058. (Lindsay.P.Keller@nasa.gov).

Introduction: On the Moon, the exposed surfaces of lunar soil grains and lunar rocks become modified over time through complex interactions with the lunar surface environment [1]. These interactions encompass many processes including micrometeorite impacts, vapor and melt deposition, and solar wind implantation/sputtering effects that collectively are referred to as "space weathering". A key product of these combined effects is the development of nm- to μm-scale coatings on the surfaces of both exposed rocks and lunar regolith grains. Studies of space weathering effects in lunar soils and rocks aid in understanding the origin and evolution of the lunar regolith as well as the interpretation of global chemical and mineralogical datasets obtained by remote-sensing missions. The interpretation of reflectance spectra obtained by these missions is complicated because the patina coatings obscure the underlying rock mineralogy and compositions. Space weathering effects collectively result in a reddened continuum slope, lowered albedo, and attenuated absorption features in reflectance spectra of lunar soils as compared to finely comminuted rocks from the same Apollo sites [2]. Understanding space weathering effects in fine-grained (<50 μm) fractions of lunar soils is important because they constitute the bulk of the surface area of lunar soils and reflectance spectra from this size fraction most closely approximates the spectra of the bulk soils.

Results and Discussion: The majority of space weathering effects are directly linked to the production of nanophase Fe metal in lunar materials [3]. Nanophase metal is produced in situ by the direct irradiation of Fe-bearing minerals, by condensation of impact-generated vapors, and within melt glass (agglutinitic glass). Size is important when it comes to nanophase Fe metal. The Fe grains observed in soil grain rims tend to be small (~3 nm) and are the major contributor to the reddening effect in soils whereas larger Fe grains tend to darken [4]. These effects were demonstrated quantitatively through a series of experiments utilizing silicas with known distributions and sizes on nanophase Fe metal [5] and feed directly into models to deconvolve space weathering effects from lunar reflectance data [6].

Surface alteration of lunar soil grains has been recognized since shortly after the return of the Apollo samples. Using analytical electron microscopy, Keller and McKay [7, 8] showed that amorphous rims on lunar soil grains are highly complex and span the range between erosional surfaces modified by solar wind irradiation to depositional surfaces modified by the condensation of sputtered ions and impact-generated vapors. Bulk measurements of certain rim elemental compositions allow the simple end member processes to be identified: irradiated rims are cation depleted due to preferential sputtering and show excess oxygen in chemical analyses due to the inferred presence of OH. Irradiated rims retain a chemical memory of their host grain. The vapor deposited rims contain species in reduced oxidation states (e.g. Fe, Si), are oxygen deficient, and are compositionally distinct from their substrates [8]. Subsequent work has confirmed the earlier results but has also identified complexities and additional important processes that are involved in space weathering on the Moon, especially melt addition to grain surfaces as a component of space weathering [e.g. 9-10] and post-depositional thermal processes [11].

Lunar soil grains have a typical lifetime of 10^4-10^5 years until they are destroyed, usually by impact processes, and this lifetime constrains the time-window for the accumulation of space weathering effects on individual grains. Studies of rock patinas extend this window of opportunity to longer exposure times. Recent studies have shown that rock patinas are much thicker than those on soil grains and display a complex stratigraphy that includes irradiated layers, vapor deposited layers, melt glass layers and entrained grains [9]. The thickness of rock patinas is dominated by melt layers that have accreted on the rock surfaces. The patina melts are compositionally heterogeneous and contain abundant nanophase Fe metal particles.

The processes involved in space weathering on the Moon are reasonably well understood but major unresolved questions exist regarding the rate at which these effects accumulate in the lunar regolith and the efficiency of nanophase Fe metal production by irradiation effects compared to condensation of impact generated vapors. Using solar flare track densities as a proxy for exposure time, [12] showed that the thickness of irradiated rims is positively correlated with exposure, whereas vapor-depositional effects are episodic and do not reflect a gradual accumulation of material with time. Efforts are focusing on quantifying irradiation effects through laboratory experimentation to determine the chemical effects due to sputtering and sputter deposition [13].

References: [1] Hapke, B. (2001) *JGR* **106**, E5, 10039. [2] Pieters, C. M. *et al*. (2000) *MAPS*, **35**, 1101. [3] Taylor, L. A. *et al*. (2001) *JGR*, **106**, E11, 27985. [4] Keller, L. P. *et al*. (1998) *LPSC* **29**, #1762. [5] Noble, S. K. *et al*. (2007) *Icarus*, **192**, 629. [6] Lucey, P. G. and Noble, S. K. (2008) *Icarus*, **197**, 348. [7] Keller, L. P. and McKay, D. S. (1993) *Science*, **261**, 1305. [8] Keller, L. P. and McKay, D. S. (1997) *GCA*, **61**, 2331. [9] Noble, S. K. *et al*. (2007) *LPSC* **38**, #1338. [10] Wentworth, S. *et al.* (1999) *MAPS*, **34**, 593. [11] Zhang, S. and Keller, L. P. (2010) *LPSC* **41**, 1533. [12] Zhang, S. and Keller, L. P. (2011) *LPSC* **42**, #1947. [13] Christofferesen, R. *et al*. (2010) *MAPS*, **45**, #5379.

PROGRESS TOWARDS DETERMINING THE TEMPERATURE OF LUNAR GLASS BEADS

P. L. King[1], W. A. McCutcheon[1], C. K. Shearer[1], C. M. D. Schofield[2], R. J. Lee[3], and M. S. Ramsey[3], Inst. Meteoritics, Univ. New Mexico, Albuquerque NM 87131 USA (penking@unm.edu), [2]Dept. Earth Sciences, Univ. Western Ontario, London ON N6A5B7 Canada, [3]Dept. Geol. & Planet. Sci., Univ. Pittsburgh, Pittsburgh PA 15260 USA.

Introduction: Lunar glass beads, thought to have formed during pyroclastic fountaining events, have been used to constrain lunar heat flow, magma temperatures, volcanic processes and also volatile diffusion processes [1-4]. Orange glass beads from the Apollo 17 site include largely crystal-free beads that are inferred to have erupted above their liquidus temperature (≥1400 °C [4]), and crystal-bearing beads that may have formed under unusual thermal conditions in the lunar eruption column (e.g. with gases or heat-radiating particles [4]). The conditions during eruption, degassing and quench are important for constraining volatile diffusion processes because diffusion coefficients depend on temperature [5]. In this contribution, we evaluate the usefulness of micro-reflectance thermal IR (TIR) spectroscopy for determining the temperature of lunar orange glass beads.

Basis for using TIR: Our previous work [summarized in 6] shows that, in general, the SiO_2 content of glasses is related to the wavenumber position of the major band in TIR spectra (Fig. 1), although Na_2O+K_2O may also play a role. The shift in band position is ~+4cm^{-1} per 1 wt% SiO_2 for glasses with similar Na_2O+K_2O contents.

TIR is sensitive to the overall glass composition and structure because the major band position (~10 μm or ~1000 cm^{-1}) is related to asymmetric stretching of Si-O-Si. However, TIR spectra are strongly influenced by temperature also [7]. Glasses that are cooled rapidly commonly retain a structural configuration representative of the glass transition temperature (T_g) and this is reflected in the position of the TIR major band. However, if glasses are annealed at temperatures ≤T_g long enough to rearrange the glass structure, and then the glass structure, and subsequently the TIR band position, reflects a lower temperature, known as the fictive temperature, T_f [e.g., 8].

Methods: Johnson Space Center provided lunar "orange glass" beads (Apollo 74220). Glasses were analyzed with the electron probe and the same locations were analyzed using micro-FTIR specular reflectance spectroscopy (μR-FTIR) on a Nicolet Nexus 670 FTIR and a Continuμm microscope with a Globar source, XT-KBr beamsplitter and an MCT-A detector over 30x30 to 100x100μm areas.

Results. Glass beads were group into those that were entirely glassy in cross-section, those with low amounts of crystals (<10 modal%), and those with a moderate amount of crystals (~20-60 modal%). The major element chemistry of each group is within error of the other groups, indicating that any changes in IR spectra should not be due to the glass chemistry. The beads with no or few crystals had TIR band positions and shapes within error. Glass beads with moderate crystals had TIR band positions ~+5-10cm^{-1} relative to those with no or few crystals, suggesting they formed at lower temperatures. We plan to calibrate the TIR shift using glasses heated over a range of temperatures.

Conclusions. The μR-FTIR band position may be used to probe the thermal history of glasses; creating an opportunity to better understand lunar volcanic processes.

References: [1] Delano, J. W. (1986) *LPS XVI, J. Geophys. Res., 91, Suppl.*, D201. [2] Saal, A. E. et al. (2008) *Nature, 454,* 192. [3] Fogel, R. A. & Rutherford, M. A. (1995) *Geochim. Cosmochim. Acta, 59,* 201. [4] Arndt, J. & von Engelhardt, W. (1987) *LPS XVII, J. Geophys. Res., 92, Suppl.*, E372. [5] Zhang, Y. & Stolper, E.M. (1991) *Nature* 851, 306-309. [6] King, P.L. et al. (2011) *Lunar Planet. Sci. Conf.* 42nd, #2069. [7] King, P. L. et al. (2004) in: King, P. L. et al. (eds.) *Infrared Spectroscopy in Geochemistry, Exploration Geochemistry and Remote Sensing.* Mineral. Assoc. Canada, Short Course 33, 93. [8] Stebbins, J. F. et al. eds. (1995*) Rev. in Mineral., 32.* Mineral. Soc. Am.

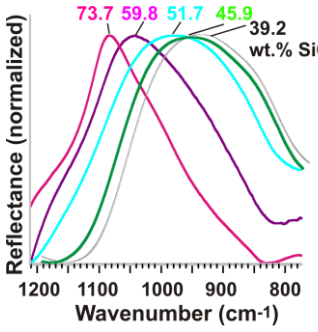

Figure 1. μR-FTIR reflectance versus wavenumber for representative glasses: rhyolite (green), andesite (purple), basalt (cyan) and lunar "orange" glass (red). The SiO_2 contents are given in wt. %.

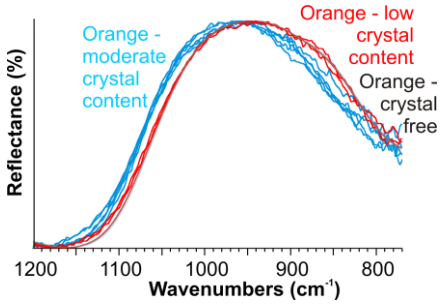

Figure 2. μR-FTIR reflectance versus wavenumber for orange glasses (Apollo 74220. From left to right - Blue: glasses with moderate crystal content. Red: glasses with low crystal content. Grey: glasses with no crystals in the two-dimensional cross-section.

A MOON ORIGIN SCENARIO JUSTIFYING THE PERCEPTIBLE PRESENCE OF VOLATILES IN ITS BODY AND MOON'S RELIEF RANGE. G. G. Kochemasov, IGEM of the Russian Academy of Sciences, 35 Staromonetny, 119017 Moscow, Russia, kochem.36@mail.ru.

The comparative wave planetology [1-3 & others] demonstrates graphically its main conceptual point: orbits make structures. The structures are produced by a warping action of stationary waves induced in bodies by non-circular orbits with periodically changing bodies' accelerations. A geometric model of tectonic granulation of planets is a schematic row of even circles adorned with granules radii of which increases in direction from Sun to the outer planets. It was shown that the granule radii are inversely proportional to the orbital frequencies of planets. Thus, there is a following row of these radii: Mercury πR/16, Venus πR/6, Earth πR/4, Mars πR/2, asteroids πR/1. It was also shown that these radii well correlate with planetary surface "ruggedness" (Fig.). This observation led to a conception of the "relief-forming potential of planets"[2]. So, this potential is rather weak in Mercury and Venus, rather high in Mars and intermediate in Earth. Certainly, orbital eccentricities were even higher at the earlier stages of planetary formation, in debris zones of their accretion causing scattering debris material. This scattering was small at Mercury' and Venus' zones, large at the Mars' zone and intermediate at the Earth's zone. Consequently, gravity kept debris in the first zones, allowed them escape in the martian zone, and allowed to separate an outer sub zone in the vicinity of the Earth's zone or around not fully consolidated (accreted) Earth.

Rejecting the giant impact hypotheses of Moon formation as contradicting the fact of the universal wave induced tectonic dichotomy of celestial bodies (Theorem 1 [3]) we consider a formation hypotheses from primordial debris in a near-Earth heliocentric orbit or in a circumterrestrial orbit. Wave scattering of primordial material from an accretion zone is a normal process traces of which we observe now as satellites around all planets except Venus and Mercury (both with smallest granules). So, Venus during its formation was not able to throw away enough solids to form a satellite. Earth with the larger amplitude of its granule forming waves produced enough solids to make a satellite. Mars with still larger granule forming waves threw away a lot of material but its small gravity keeps now only two tiny satellites. And what is important in this wave debris scattering process, the outer zones become inreached in less dense and volatile satiated material.

The martian body itself warped by huge waves lost a lot of its mass and is semi-destructed. In the asteroid belt still larger wave (granule size πR/1, and in the 1:1 resonance with the fundamental wave!) scattered away almost all primary material and there was no chance to accrete any decent planetary body. In the outer Solar system large planets with important gravities keep "exuberant" satellite systems and debris rings. The comparative wave planetology, thus, introducing the conception of structurizing warping waves, is not surprised by the Moon appearance. What is needed, just to recognize a special position of Earth in the planetary sequence determining its orbital frequency and thus a size of its tectonic granulation.

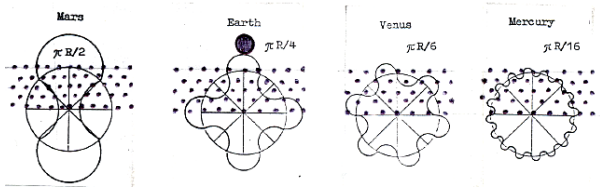

Lunar relief range is about 16 km. It is less than the terrestrial one - 20 km. In the row of terrestrial planets there is a rather well correlation between radii of tectonic granules and surface relief ranges [2]. The relief ranges also increase with solar distances of planets. They are: Mercury ~1-4 km, Venus 14, Earth 20, Mars ~30 km. But the Moon being a satellite has two orbits: around Sun and Earth. Two orbits, thus, influence its relief-forming potential. Induced by the terrestrial orbit (1/1 year frequency) 20 km range has to be diminished (smoothed) by the fast 1/1month fr. photosphere orbit producing rather negligible relief range. A more substantial smoothing, however, can be done by one of two modulated fr-s. Moon has 2 main fr-s (around Earth and Sun) and 2 modulated side fr-s (division and multiplication of the higher fr. by the lower one). It appears that the lunar crater size-frequency curve has anomalously high numbers of craters exactly at ranges calculated by the wave approach, namely, at 80-140 and more than 600 km in diameter (corresponding to the main orbital fr-s) and 10-30 and 300-400 km in diameter (corresponding to the modulated side fr-s). The main fr-s produce granule (crater) sizes πR/4 and πR/60; side fr-s give sizes πR/240 and πR/15. The radii of the πR/60 and πR/240 granules produce very weak surface roughness to significantly smooth the 20 km πR/4 relief. But tied to the πR/15 granule (almost similar to the πR/16 Mercury granule) relief has rather important roughness (relief range) diminishing 20 km to sought for about 16 km (20-4=16).

References: [1] Kochemasov, G.G. (1992) 16th Rus Am. Microsymp. on Planetology, Abstr., Moscow, Vernadsky Inst., 36-37. [2] Kochemasov G.G. (2009) New Concepts in Global Tectonics Newsletter, #51, 58-61. [3] Kochemasov G.G. (1999) Geophys. Res. Abstr., V.1, #3, 700.

Hydrogen on the Moon: A Summary of Lunar Prospector Neutron Measurements of Lunar Hydrogen Concentrations. David J. Lawrence[1], [1]Johns Hopkins University Applied Physics Laboratory (11100 Johns Hopkins Drive, Laurel, MD 20723; David.J.Lawrence@jhuapl.edu).

Introduction: Planetary neutrons are created from nuclear spallation reactions when high-energy galactic cosmic rays (GCR) hit planetary surfaces. These high-energy (E_n=MeV) neutrons undergo scattering and absorption reactions through which the concentrations of various elements (H, Fe, Ti, Gd, Sm) can be inferred [1,2,3,4,5]. In the presence of hydrogen (H), which has the same mass as neutrons, neutrons lose their energy very efficiently because of the large scattering cross section of H and their closely equal mass. While epithermal neutrons ($0.4<E_n<500$keV) are somewhat sensitive to neutron absorbing elements (Fe, Ti, Gd, Sm)[6,7] they are most dominantly sensitive to H concentrations [7].

The Lunar Prospector Neutron Spectrometer (LP-NS) was the first successful use of planetary neutron spectroscopy. Global measurements were carried out over 18 months in two mission phases [6]. The first phase lasted 12 months and collected data from a 100 km altitude polar orbit; the second phase lasted six months and collected data from a 30 km altitude polar orbit. Because the LP-NS is an omni-directional detector, the spatial resolution of the measurements is ~1 – 1.5 times the mean altitude above the surface [6].

Initial LP Measurements: In the studies of Feldman et al. [1,2,3], clear evidence was given for enhanced H at the lunar poles based on decreases of epithermal neutrons in the vicinity of permanent shaded craters. When averaged over the entire LP-NS field of view, the measured H was found to be 100 – 150 ppm H, compared to ~50 ppm H observed at more equatorial latitudes due to solar wind implanted H. If it is assumed that the H signal only comes from permanently shaded regions (PSR), it was inferred that the average H concentration within PSRs is 1.5±0.8 wt.% water equivalent hydrogen (WEH). Due to the broad spatial resolution, it is not possible to isolate H signals from any PSR.

Follow On Studies Using LP-NS Data: More recent studies of LP data have focused on various aspects of lunar H concentrations that can be inferred from LP neutron data. Lawrence et al. [7] carried out detailed neutron transport modeling to conclude that H is the most likely cause of the polar epithermal neutron decreases as opposed to other elements such as Si or Ca, as was suggested by Hodges [8]. [7] also used combined thermal and epithermal neutron data to conclude that the polar H enhancements were likely covered by 10s of centimeters of dry lunar soil.

A series of studies have been completed that utilize spatial deconvolution techniques as constrained by other measurables (e.g., shade, temperature) to improve our spatial distribution knowledge of polar H concentrations [9,10,11]. These studies conclude that LP data require most of the H to be concentrated in PSRs at up to 1 wt.% WEH. Higher H concentrations in small locations (<few km^2) are also consistent with these analyses. These abundances are greater than the highest solar wind H abundance in returned lunar samples, and may indicate ice between regolith grains. Finally, as prompted by recent detections of surficial lunar volatiles in non-polar regions (e.g., Goldschmidt crater)[12], it has been determined that spatially coincident detections of surficial H with LP-NS data cannot yet be ruled out [13]. New neutron models and analyses are needed to better understand the surficial form of water that may be detectable with LP data.

Future Directions for LP-NS Studies: Even 10+ years after acquisition, the LP-NS dataset remains a valuable and unique resource of information due to its high statistical precision, good spatial resolution, and analysis maturity [6]. A variety of future studies can be carried out with LP-NS data. First, new spatial deconvolution studies using updated lighting and temperature constraints from the Kaguya and LRO missions are already in progress [14]. Second, further modeling and correlation studies with M3 spectral data need to be carried out to understand the extent to which LP-NS data can constrain surficial H concentrations. Finally, non-polar H concentrations are not fully understood with current analyses of LP epithermal neutron data [15]. New data from LRO (Diviner and LEND) should be combined with LP epithermal neutron data to better understand global H concentrations.

References: [1] Feldman et al., *Science*, 281, 1496, 1998; [2] Feldman et al., *JGR*, 105, 4175, 2000; [3] Feldman et al., *JGR*, 106, 23231, 2001; [4] Elphic et al., *JGR*, 105, 20333, 2000; [5] Feldman et al., *JGR*, 105, 20347, 2000; [6] Maurice et al., *JGR*, 109, 10.1029/2003JE002208, 2004; [7] Lawrence et al., *JGR*, 111, 10.1029/2001JE001530, 2006; [8] Hodges, *JGR*, 107, 10.1029/ 2000JE001483, 2002; [9] Elphic et al., *GRL*, 32, 10. 1029/2007GL029954, 2007; [10] Eke et al., *Icarus*, 200, 12, 2008; [11] Teodoro et al., *GRL*, 37, 10.1029/ 2010GL042889, 2010; [12] Pieters et al., *Science* 326, 568, 2009; [13] Lawrence et al., *JGR*, 10.1029/ 2010JE003678, 2010; [14] Elphic et al., *42nd LPSC*, #2751, 2011; [15] Johnson et al., *JGR*, 107, 10.1029/ 2000JE001430.

PROPERTIES OF MOON PSRs from LEND/LRO DATA. M.L. Litvak[1], I. G. Mitrofanov [1], A. B. Sanin [1] ,W. V. Boynton [2], G. Chin [3], J. B. Garvin [3], D. Golovin [1], L. G. Evans [4], K. Harshman [2], A. S. Kozyrev [1], A. Malakhov [1], T. McClanahan [3], G. Milikh [5], M. Mokrousov [1], G. Nandikotkur [5], I. Nuzhdin[1], R. Sagdeev [5], V. Shevchenko [7], V. Shvetsov [8], D. E. Smith [9], R. Starr [6], V. I. Tretyakov [1], J. Trombka[5], A. Varennikov [1], A. Vostrukhin [1] and M. T. Zuber [9], [1]**Space Research Institute, RAS, Moscow, 117997, Russia, litvak@mx.iki.rssi.ru,** [2]University of Arizona, Tucson, AZ USA **,** [3]NASA Goddard Space Flight Center, Greenbelt, MD USA, [4]Computer Science Corporation, Greenbelt, MD USA, [5]University of Maryland, College Park, MD USA, [6]Catholic University, Washington DC, USA, [7]Sternberg Astronomical Institute of Moscow State University, Moscow, Russia, [8]Joint Institute of Nuclear Energy, Dubna, Russia, [9]Massachusetts Institute of Technology, Cambridge, MA USA

Introduction: Radar and neutron spectroscopy measurements onboard Clementine and Lunar Prospector spacecrafts revealed indications that deposits of pure water ice might exist in permanently shadowed regions (PSRs) near the lunar south pole [1]. In particular Lunar Prospector Neutron Spectrometer (LPNS) discovered a significant suppression of epithermal neutrons around the both lunar poles above 70° latitude. This effect was interpreted as a possible signature of hydrogen enhancement or even presence of water ice distributed within PSRs areas [2-4].

In our analysis we plan to use Lunar Exploration Neutron Detector (LEND) data to look at distribution of neutron flux at Moon poles with much better spatial resolution then was achieved at previous space missions. LEND is a collimated neutron spectrometer onboard LRO spacecraft which is capable to distinguish footprint with radius ~ 5 km [5-6]. It is comparable with large PSRs and provides unique possibility to test hypothesis if all major PSRs are reservoirs of Hydrogen or even water ice.

Data Analysis: In our analysis we plan to process LEND data gathered in collimated detectors of epithermal neutrons from July, 2 2009 up to June, 1 2011. Using these data we would like to accomplish statistical comparison between distribution of neutron flux inside and outside PSRs. It includes:

1) Collective estimation approach to test all known large PSRs in order to estimate significance of average local variations of neutron flux inside and outside PSR area.
2) Sampling approach to test average neutron suppression for different sets of PSRs selected by various criteria such as area, exposure time, location and etc.
3) Individual approach to test properties of particular PSRs with well visible effect of neutron suppression.

Discussion: First LEND results already shows that variations of neutron flux at moon poles are not so evident as was expected and predicted earlier from previous experiments and theoretical models [7]. In this study we will present further development of these results.

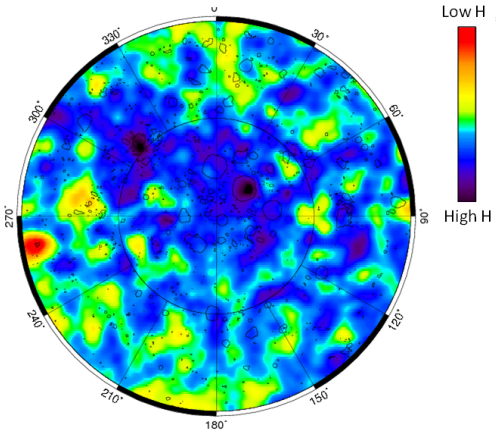

Figure 1. Lunar south pole variations of neutron flux as signature of Hydrogen enhancement measured by LEND instrument onboard LRO spacecraft.

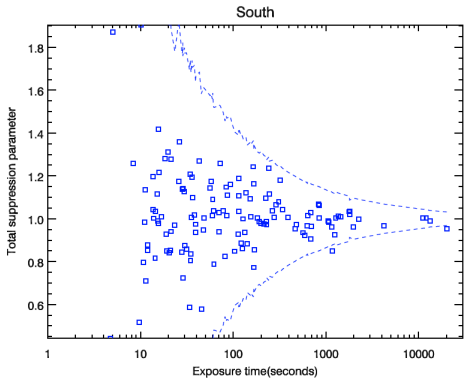

Figure 2. Distribution of southern PSRs by neutron suppression parameter as a function of exposure time. Dash line shows 3 sigma limits of significance.

References: [1] P. D. Spudis et al., Sol. Syst. Res. 32, 17 (1998). [2] W. C. Feldman et al., Science 281, 1496 (1998). [3] D. J. Lawrence et al., J. Geophys. Res. 111, E08001 (2006). [4] R. C. Elphic et al., Geophys. Res. Lett. 34, L13204 (2007). [5] I. G. Mitrofanov et al., Astrobiol. 8, 793 (2008). [6] I. G. Mitrofanov et al., Space Sci. Rev. 150, 183 (2010). [7] I.G. Mitrofanov et al., Science, 330, 483,2010.

Water and Cl in Lunar Basalts: Solubility and Degassing of OH-Cl in Basaltic Magma. Yang Liu and Lawrence A. Taylor, Planetary Geosciences Institute, Department of Earth and Planetary Sciences, University of Tennessee, Knoxville, TN 37996 (yangl@utk.edu).

Introduction: Recent studies of water in the Moon have produced conflicting implications. Analysis of Apollo samples have shown that volcanic glass beads retained up to 46 ppm OH [1]. Based on diffusive-loss models, these values have been interpreted to indicate the initial OH in the melts that formed the beads of up to 745 ppm [1]. Analyses of lunar apatite grains observed significant amounts of OH, up to 7000 ppm H_2O [2-4]. These recent findings imply that *the inteorior of the Moon contains more water than previously thought*. However, Cl-isotope compositions of lunar rocks, breccias, and apatite show large positive values, much larger than the range of variation observed in terrestrial rocks, martian meteorites, and chondrites [5]. On the basis of these observation, Sharp et al. [5] suggested that the degassing phase is metal chlorides and *molar H:Cl ratios in lunar rocks are much less than 1*. Sharp et al. [5] further inferred that the interior of the Moon is bone-dry.

Because different lunar rocks were used in the apatite studies[2-5], these oppositing views of the hydrous-status of the inteorior of the Moon could be explained by highly heterogeneous distribution of water in the Moon. However, an underlying question about volatiles in lunar basalts is the solubility and degassing behaviors of H_2O and Cl at reduced conditions of the Moon (~IW-1, [6-7]). Here, we present synthesis of literature data on this subject for terrestrial basalts.

Literature data of H_2O-Cl in basalts: To date, all experiments were conducted for terrestrial composition with >1.9 wt% Na_2O+K_2O under oxidized conditions [8-13]. All experiments were conducted at oxidized conditions (NNO to NNO+2). In H_2O-rich system, silicate melt equilibrates with vapor rich in water (Fig. 1). With increasing Cl contents, a hydro-saline (brine) equilibrates with the silicate melt. The transition occurs at molar H:Cl ratio of ~5.

Degassing of H_2O-Cl fluids: Experimental data of H_2O-Cl fluids in terrestrial basalts show that the degassing of HCl occurs at low P, when Cl reaches saturation and after extensive degassing of H_2O [9-14]. Figure 2 shows that the calculated HCl/NaCl ratio increases with decreasing P and H_2O, modeled by Shinohara [15].

Summary: The literature data on terrestrial basalts sugeest that H_2O facilitate the degassing of Cl in vapor or in aqueous fluids. Howevr, no experiments have been conducted for lunar basalt with <0.5 wt% Na_2O + K_2O, and under reduced conditions, prohibiting an accurate prediction of the degassing behaviors of H_2O-Cl in lunar samples. Presence of other volatiles (H_2, CO, CO_2, and S) need also be considered as they may also complicate the degassing behaviors of H_2O-Cl [13-15].

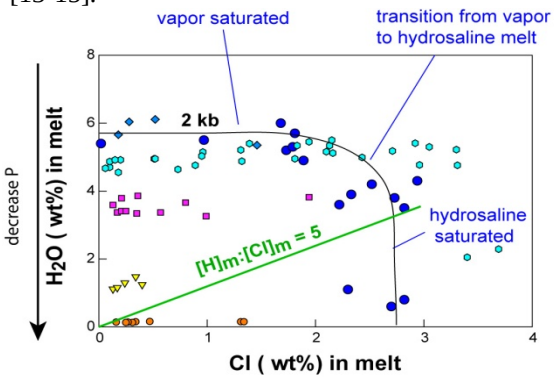

Fig. 1. Solubility of H_2O-Cl fluid in basalt. Data are from [10-12]. The black curve is from [10].

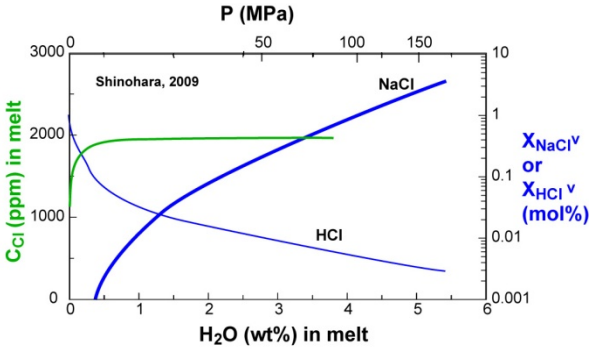

Fig. 2. Variation of Cl in vapor and melt under decompression conditions [14]. The vapor is rich in NaCl at higher P and in HCl at lower P.

References: [1] Saal A. E. *et al.* (2008) *Nature*, 454, 192-196. [2] Boyce J. W. *et al.* (2010) *Nature*, 466, 466-469. [3] McCubbin F. M. *et al.* (2010) *PNAS*, 107, 11223-11228. [4] Greenwood J. P. *et al.* (2011) *Nature Geosci*, 4, 79-82. [5] Sharp Z. D. *et al.* (2010) *Science*, 329, 1050-1053. [6] Sato M. (1976) *Proc. 7th Lunar Sci. Conf.*, 1323-1344. [7] Sato M. *et al.* (1973) *Proc. 4th Lunar Sci. Conf.*, 1061-1079. [8] Kilinc I. A., Burnham C. W. (1972) *Economic Geol.*, 67, 231-235. [9] Webster J. D. *et al.* (1999) *Geochim. Cosmochim. Acta*, 63, 729-738. [10] Webster J.D. and De Vivo B. (2002) *Am. Min.*, 87, 1046-1061. [11] Stelling J. *et al.* (2008) *Chem. Geol.*, 256, 102-110. [12] Alletti M. *et al.* (2009) *Chem. Geol.*, 263, 37-50. [13] Webster J.D. et al. (2009) *Chem. Geol.*, 263, 19-36. [14] Shinohara H. (2009) *Chem. Geol.*, 263, 51-59. [15] Zhang Y. (2011) *42nd LPSC*, 1957.

SPECIAL, UNOPENED LUNAR SAMPLES: ANOTHER WAY TO STUDY LUNAR VOLATILES. G. E. Lofgren, Code KT, NASA-JSC, Houston, TX 77058, gary.e.lofgren@nasa.gov.

Introduction: During the last three Apollo missions several samples were collected and immediately placed in vacuum tight-containers. Three of these samples have never been opened and, together with 2 samples not placed in vacuum, are the only lunar samples that have not been examined, Table 1. There were, however, samples collected immediately adjacent to some of these samples that have been studied. Because there was nothing notable about these samples, there was no compelling reason to open them, and it was decided that they be preserved for future studies. With the increased interest in volatiles on the moon, perhaps that time has come.

Sample Description: The vacuum samples were collected in stainless steel containers that have an indium/silver alloy seal (Fig.1). A stainless steel knife edge is pressed into

Table 1: Unopened vacuum containers and core tubes [2]

Sample Number	Container	Close by sample*	Amt. of sample
15014	SESC	15030	333 g
69001	CVSC	69940	558 g
73001	CVSC	none	809 g
73002	Drive tube	none	429 g
70012	Drive tube	none	434 g

Indium alloy to create the seal [1]. The 5 containers collected are listed in Table 1. The drive tube samples are stored in Teflon bags. The SESC (Special Environmental Sample Container) vacuum container, 15014 has no additional vacuum container and is sealed in Teflon bags. The SESC containers that were opened immediately upon return of the

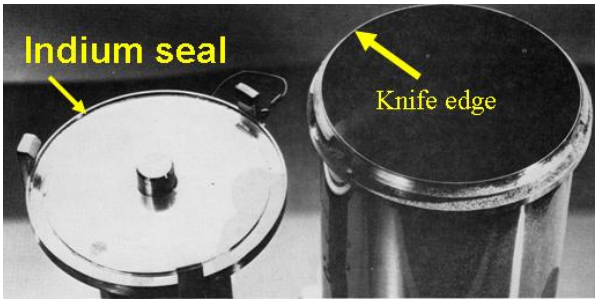

Figure 1. The seal for the SESC vacuum containers used on to contain samples in vacuum. An indium/silver alloy is embedded in the lid. The knife edge of the stainless steel container is forced into the seal material as the lid is tightened onto the container.

samples from the Moon appeared to seal with the exception of the SESC on Apollo 16 where a SS wire that connects the lid to the can was inadvertently caught up in the seal. The CVSC (Core Vacuum Special Container) container is an extended SESC that holds a standard drive core tube section. A section of a drive tube was placed in the container on the lunar surface by the Astronauts. A-16 and 17 Sample Return Containers containing 69003 and 73001 had a pressures of 89 and 28 microns Hg respectively prior to opening in the nitrogen processing cabinets [2,3]. 69001 is a single drive tube that sampled to a depth of 27.5 cm while 73001 is the upper section of a double drive tube that sampled to a depth of 77 cm, depth of 73001 is approximately 27 cm [4]..

The CVSC containers 73001 and 69001 appeared to be sealed based on their outward appearance and were placed in additional vacuum containers immediately upon return to the Lunar Receiving Laboratory. These containers have a standard, high quality vacuum seal to help maintain the vacuum and prevent contamination. It is not anticipated that the CVSC containers still retain the level of vacuum that exists on the Moon. Analyses of the atmosphere in the SRC's before opening showed no evidence of terrestrial atmosphere (Bogard, personnel communication). We will not know for sure the status of the seals until the containers are opened.

The "close by" column (Table 1) gives the number of sample collected immediately adjacent to the samples sealed in the SESC or CVSC containers. The "close by" samples can be considered as nearly identical to the samples sealed in vacuum.

Discussion: There are 2 important questions. Can these samples contribute to our understanding of volatiles on the moon and, if so, how do we open these containers and extract the samples so as to preserve any information they contain about volatiles.

It is important to note the nature of the sample collection process. The SESC sample was scooped from the regolith and poured into the SESC container. In the video of the sample collection, is it evident that the finest fraction was winnowed away as the sample was poured from the scoop into the SESC container. In contrast the drive tube samples have the best chance of having preserved volatiles because the sample was forced into the tube with a minimum disturbance.

Assuming the core tubes are the most pristine lunar samples that remain in the Apollo Collection and have the best chance of containing indigenous volatiles, how do we open the containers and extract the samples in a manner to best preserve them.

Curation currently does not have a vacuum facility that would allow us to open the samples in a vacuum. If it is a requirement that the samples be opened in a vacuum there are two options. Curation will need to acquire a vacuum facility or it will need to gain access to such a facility for a limited time for this purpose. If processing in our nitrogen cabinets is deemed appropriate, we can proceed with sample allocation. Whatever atmosphere is used, the next task would be to devise a technique to sample the material in the core in a manner to best preserve the volatiles for study.

References: [1] Allton J. A. (1989) JSC 23454, NASA Johnson Space Center, Houston, TX 77058. [2] Apollo 16 Lunar Sample Information Catalog (1972) MSC 03210 [3] Apollo 17 Lunar Sample Information Catalog (1973) MSC 03211 [4] Heiken G. H. et al. (1991) Lunar Sourcebook, Cambridge University Press, New York, p 328.

ILLUMINATION CONDITIONS OF THE LUNAR POLES FROM LUNAR ORBITER LASER ALTIMETER DATA. E. Mazarico[1,2], G.A. Neumann[2], D.E. Smith[1,2], M.T. Zuber[1] and M.H. Torrence[1,3]. [1]Massachusetts Institute of Technology, Cambridge MA, [2]NASA Goddard Space Flight Center, Greenbelt MD, [3]SGT Inc., Greenbelt MD.

Introduction: Although diurnal temperature variations over most of the Moon's surface can be extreme, the lunar polar regions have the potential to trap volatiles in permanently shadowed regions (PSRs). Because the Moon's spin axis is nearly perpendicular to the ecliptic plane, the Sun is always low on the horizon in the polar regions, and topographic relief such as impact craters can be sufficient to provide permanent shadow. Although the Moon obliquity has been larger in the past, many PSR regions have likely been stable over tens to hundreds of millions of years. This was recognized before good topographic knowledge of the polar regions existed **[1]**, and was confirmed by more recent studies using ground-based radar **[2]** or spacecraft data **[3,4,5,6]**.

Data: We use data collected by the Lunar Orbiter Laser Altimeter (LOLA) instrument **[7]** onboard the Lunar Reconnaissance Orbiter (LRO) **[8]**. With more than 3.4 billion LOLA altimetric measurements (as of January 31, 2011), and the polar orbit of the LRO spacecraft, the data coverage of the poles is excellent. We construct topographic maps of the lunar polar regions, from ~75° to the pole, at a resolution of 240 meters per pixel. The map filling ratios are 68.8% and 67.6% in the north and south, respectively, and will continue to improve as the LRO mission progresses.

Method: The horizon method was described in detail in **[6]**. Horizon (angular) elevation maps are constructed for the region of interest (~80°-90°) for 720 azimuthal directions ($\delta\theta$=0.5°). The illumination conditions at any epoch can then be obtained by comparing the Sun elevation to that of the horizon (in the Sun direction).

Results: We conduct simulations with the LOLA topography to survey the extent of PSRs in both polar regions, and to characterize the solar illumination conditions (average and maximum incident flux). We find consistently larger total PSR areas than previous studies **[2,4,5]** (e.g., 1769 and 3660km^2 polewards of 87.5° , compared to 844 and 2751km^2 for **[4]**, in the north and south poles respectively), likely because smaller PSR areas (<10km^2) are now resolved thanks to the higher LOLA altimetric data density. We also describe the influence of the Moon obliquity on the total PSR area.

Updated results will be presented, based on more recent and accurate LOLA maps constructed from improved LRO orbit knowledge **[9]** and crossover adjustment techniques **[10]**.

References: [1] Watson K.B. et al. (1961) *JGR*, *66*, 3033. [2] Margot et al. (1999) *Science*, *284*, 1658. [3] Cook et al. (2000), *JGR*, *105*, 12023. [4] Noda et al. (2008), *GRL*, *35*, L24203. [5] Bussey et al. (2010), *Icarus*, *208*, 558. [6] Mazarico et al. (2011), *Icarus*, *211*, 1066. [7] Smith et al. (2010), *GRL*, *37*, L18204. [8] Chin et al. (2007), *Sp. Sci. Rev.*, *129*, 4. [9] Mazarico et al. (2011), J. Geod., submitted. [10] Mazarico et al. (2010), Lunar Science Forum, 215.

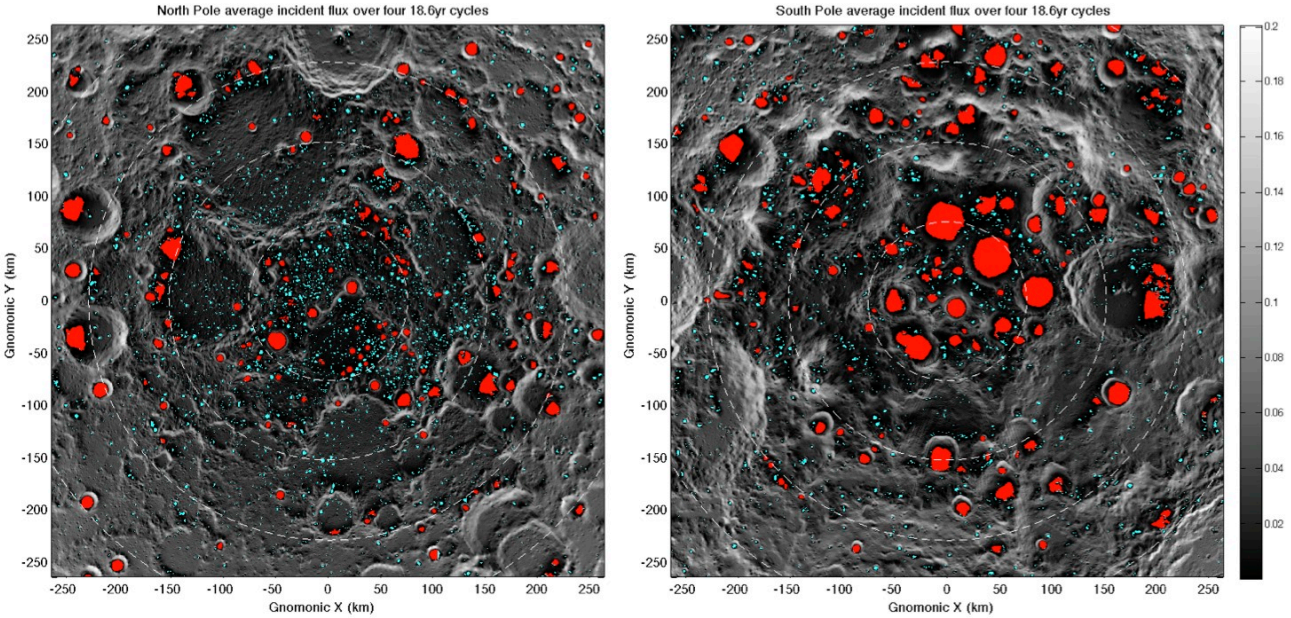

Figure 1. Permanently Shadowed Regions shown over a grayscale map of the average incident flux, for the northern (left) and southern (right) polar regions. The simulation duration was four 18.6yr cycles. For each pole, the 150 largest PSRs are in red, and the smaller ones in cyan. The dashed circles indicate latitude, in 2.5° steps from the pole. From [6].

INSOLATION EFFECTS ON LUNAR HYDROGEN: OBSERVATIONS FROM THE LRO LEND AND LOLA INSTRUMENTS. T.P. McClanahan[1] , I.G. Mitrofanov[2], W.V. Boynton[3], G. Chin[1], G. Droege[3], L.G. Evans[1,6], J. Garvin[1], K. Harshman[3], M.L. Litvak[2], A. Malakhov[2], G.M. Milikh[4], M. Namkung[1], G. Nandikotkur[5], G. Neumann[1], D. Smith[1,7], R. Sagdeev[6], A. G. Sanin[2], R.D. Starr[1,4], J.I. Trombka[1,5], M.T. Zuber[1,7], [1]Space Exploration Division, NASA Goddard Space Flight Center, Greenbelt, MD, USA., [2]Inst. for Space Research, Moscow, Russia, [3]Lunar and Planetary Laboratory, University of Arizona, Tucson, AZ, USA, [4]Catholic Univ., Washington , DC, USA. [5]Space Physics Dept., Univ. of Maryland, College Park, MD, [6]Computer Sciences Corp., Glenn Dale, MD, USA, [7]Dept. of Earth, Atmos., and Planet. Sci., MIT, Cambridge, MA, USA.

Introduction: The Moon's polar permanent shadow regions (PSR) have long been considered the unique repository for volatile Hydrogen (H) [1,2]. Largely, this was due to the extreme and persistently cold environment that has been maintained over eons of lunar history. However, recent discoveries indicate that the H picture may be more complex than the PSR hypothesis suggests. Observations by the Lunar Exploration Neutron Detect (LEND) onboard the Lunar Reconnaissance Orbiter (LRO) indicate some H concentrations lie outside PSR [3]. Similarly, observations from Chandraayan-1's M^3 and Deep Impact's EPOXI near infra-red observations indicate diurnal cycling of volatile H in lower latitudes [4,5]. These results suggest other geophysical phenomena may also play a role in the Lunar Hydrogen budget.

Clearly epithermal neutron evidence from [2,7] indicates correlated suppression of epithermal neutron rates and higher inferred H concentrations at the poles. Both instrument systems also indicate higher equatorial epithermal rates and lower H concentrations at the equator. These bulk observations are consistent with an insolation effects process where the effective solar irradiance and near surface thermal environment is highest at the equator and decreases as a cosine function of increasing latitude.

However, insolation contrast can also be evaluated locally, in the context of pole vs equator facing slopes. In terrestrial polar environments this effect is readily observed both above and below the surface as the lower insolation poleward slopes maintain lower thermal conditions and stay wetter longer than commensurate equator facing slopes establishing the concept of a **local insolation contrast**. This effect similarly extends into the sub-surface as the thickness of insulating layers above permafrost are similarly dependent on local insolation conditions. We isolate localized insolation contrast and correlate this process with LEND epitheral mapping data and evaluate the potential for thermally induced loss / redistribution processes influencing the Moon's near-surface < 1m volatile H budget.

To implement this physical process we correlate mapping data sets collected from the ongoing, 1.5 year long mapping mission of the Lunar Reconnaissance Orbiter (LRO) [6]. Epithermal neutron mapping data from the Lunar Exploration Neutron Detector (LEND) is registered and analyzed in the context of slope derivations from Lunar digital elvation models maps produced by the Lunar Observing Laser Altimeter (LOLA) [7][8]. Slope derivations provide a continuum of slope orientation between pole facing and equator facing slopes, range 0 to 180°. Insolation effects seen on the topography increase as a function of orientation. LEND map pixels are aggregated and averaged from sparsely distributed map pixels in the context of the defined insolation continuum.

High latitude results >+/-60° reported in [9] indicated that both North and South Polar cases epithermal rates were consistently lower (wetter) in pole facing slopes vs equivalent equator facing (dryer) slopes ~0.01 to 0.02 cps. Results suggested epithermal rates were positively correlated with insolation effects and Further, insolation is a factor influencing H spatial distributions on the Moon.

In this presentation we review the techniques and results from the recent high latitude analysis and apply similar techniques to equatorial regions. Results from our low latitude analysis will be reported. We discuss interpretations and implications for Lunar Hydrogen studies

References: [1] Arnold (1979) *JGR*, #84, 5659-5668 [2] Feldman et al.,(2001) *JGR*, 106-E10, 23231-23251 [3] Mitrofanov et al.(2010) *Science*, 330-6003, 483-486 [4] Pieters et al.(2009) *Science*, 326(5952), 568-572 [5] Sunshine et al., (2009), *Science*, 326(5952) [6] Chin et al. (2007) *Sp. Sci. Rev.,* 150(1-4), 125-160 [7] Mitrofanov et al.(2010) *Sp. Sci. Rev., 150(1-4),* 183-207. [8] Smith et al.(2010) *Sp. Sci. Rev., 150(1-4)*. [9] McClanahan et al., (2011), *Lunar and Plan. Sci Conf. , #1970*

MAGMATIC VOLATILES IN LUNAR APATITE: A HEXAGONAL PRISM OF TRUTH OR A HOUSE OF CARDS? F. M. McCubbin[1], C. K. Shearer[1], S. M. Elardo[1], Z. D. Sharp[2]. [1]Institute of Meteoritics, University of New Mexico, Albuquerque, NM 87131. [2]Department of Earth and Planetary Sciences, University of New Mexico, Albuquerque, NM 87131 (fmccubbi@unm.edu)

Introduction: Significant progress has recently been made in determining the nature of lunar indigenous hydrogen because recent SIMS analyses of lunar apatites have revealed that hydroxyl is structurally bound within apatite from a number of different lithologic types [1-4]. These studies, along with previous SIMS analyses of lunar fire fountain glasses [5], confirm that there is at least some hydrogen in the lunar interior. Although the absolute concentrations of hydroxyl that have been measured in lunar apatite are consistent among the various studies, there is some disagreement regarding what the analyses imply about hydrogen contents in the lunar interior, and there are also important questions regarding the sources and reservoirs of this H. The purpose of the present study is to review the required information, as well as the potential pitfalls, for using apatite to estimate the H content of a magmatic source region. Furthermore, we demonstrate that although the new findings of H in the lunar interior are potentially very exciting, there is considerable work ahead that is needed before we can fully understand the importance of lunar H with respect to the thermal and magmatic evolution of the Moon.

Is apatite a reliable tool for probing the interior volatile contents of the Moon? The absolute volatile abundances of a parental liquid (and hence the magmatic source region) are difficult to constrain from apatite volatile data alone. Even if one can discount the possibility of post- and pre-crystallization processes having disturbed either the parental magmatic volatile abundances or the volatile abundances in the apatites themselves, there are no apatite-melt partition coefficients for F, Cl, and OH for lunar compositions, and it is difficult to constrain the amount of crystallization that occurred before the start of apatite crystallization in each of the samples investigated. Both of these parameters must be known before any tight constraints can be placed on the H content of a lunar source region.

Given the very loose constraints that are currently available for the parameters discussed above, estimates of H in the lunar interior span several orders of magnitude from approximately 7 ppb to 1 ppm H [1,5,6], indicating the Moon is likely depleted in H relative to the interiors of Earth and Mars.

Volatiles in the lunar interior: It gets more complicated/Fun. The magmatic volatile abundances of apatite from several lunar lithologic types have been determined, and there are some striking differences in the volatile abundances that correlate to lithologic type. Specifically, rocks from the highlands magnesian-suite, alkali-suite, and KREEP-rich impact melts, all of which are KREEP-rich lithologies, plot together in an OH-poor, relatively Cl-rich portion of the F-OH-Cl ternary. Furthermore, apatite from the various mare basalt compositions plot over a range of OH-rich to F-rich compositions that are consistently Cl-poor. Apatite from the single KREEP basalt sample that has been analyzed thus far, 15386, plot between the mare basalt and KREEP-rich highlands rocks portion of the ternary, although significantly more data is needed to confirm this observation (Figure 1). The difference between the Cl contents of the mare apatites versus the KREEP-rich lithologies' apatites indicate that there are significant compositional differences at the time of apatite crystallization in mare basalts versus KREEP-rich rocks that cannot be reconciled by post- or pre-crystallization secondary processes [7]. In fact, the compositional differences indicate there is a heterogeneous distribution of magmatic volatiles, including H, in the lunar interior. Therefore, all lunar lithologic types must be investigated before we can determine anything regarding the abundances of magmatic volatiles in the bulk Moon.

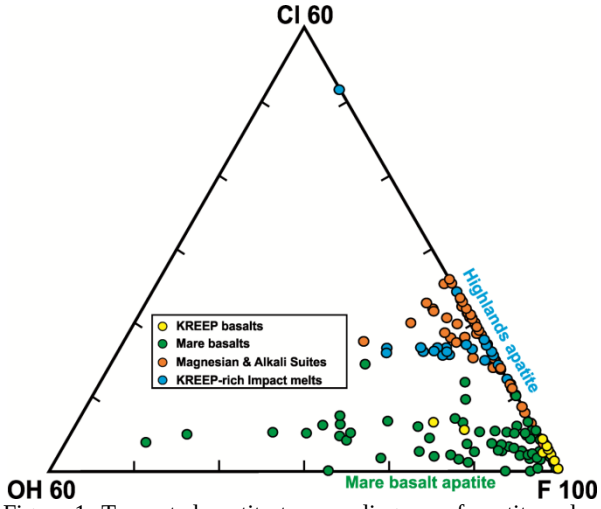

Figure 1. Truncated apatite ternary diagram of apatite volatile contents (F and Cl measured by EPMA, OH calculated by difference and has been generally confirmed by SIMS[1-4]) from several different lithologic types from the Moon.

References: [1] McCubbin et al. (2010) *Proc. Natl. Acad. Sci.* 27, 11223-11228. [2] McCubbin et al. (2010) *Am Min.* 95 1141-1150. [3] Boyce et al. (2010) *Nature* 466, 466-469. [4] Greenwood et al. (2011) *Nature Geoscience* 4, 79-82. [5] A. E. Saal et al., Nature 454, 192-195 (2008). [6] Sharp et al. (2010) Science 329, 1050-1053. [7] McCubbin et al. (Submitted) *GCA.*

DESORPTION OF ADSORBED WATER ON THE MOON BY PHOTONS AND IONS. Emily H. Mitchell, Micah J. Schaible, Daniele Fulvio, Catherine A. Dukes, and Raúl A. Baragiola, University of Virginia, Laboratory for Atomic and Surface Physics, Thornton Hall, Charlottesville, VA 22904. Emails: emma.mitchell@virginia.edu, ms5vf@virginia.edu, df6vz@virginia.edu, cdukes@virginia.edu, raul@virginia.edu

Introduction: Sunshine et al. [1] have observed a diurnal variation in the hydration of the lunar surface through the OH infrared absorption band, using the infrared spectrometer on board the Deep Impact spacecraft.

We postulate that the decrease in the surficial OH/water during the lunar day is due to photodesorption from solar photons and sputtering by the solar wind. In this study we examine, in the laboratory, the removal of monolayers of water adsorbed on minerals and lunar highland soil by 121.6 nm, 193 nm, and 253.7 nm ultraviolet photons, as well as by 1 keV/amu protons and He^{++} ions.

Experimental: Samples of terrestrial olivine and anorthite, as well as lunar highland soil, are mounted at the center of an ultra-high vacuum chamber at a base pressure of 10^{-10} Torr. The samples are initially cleaned by a low-energy plasma [2], and then exposed to gaseous water from a capillary-array gas doser at room temperature to form a single water monolayer on the surfaces.

A Thermo-Nicolet FTIR spectrometer is used in reflectance to characterize the surface of the samples *in situ*, both before and after water dosing. Reflectance spectra are taken over the range 0.8 - 12 μm and we center our attention at the 3-μm OH stretch band to quantify the concentration of adsorbed water. The area of this absorption band gives the relative measure of water on the surface, after baseline subtraction. Long measurement times require subtraction of absorption by water condensed on the LN2-cooled infrared detector [3].

Irradiations: The adsorbed water is exposed to 121.6 nm (Lyman-α) photons from a microwave hydrogen lamp at normal incidence. The lamp consists of a quartz tube coupled to a microwave power supply (Opthos MPG 4M) and connected to a gas manifold. It is filled with a gas mixture of 10% H_2 and 90% Ar to a pressure of 1.0 Torr. Photons enter the vacuum chamber through an MgF_2 window. An aluminum cylindrical mirror serves to collimate the light and align it directly toward the sample [4].

The photon flux is measured via an in-line photodetector, which is a thin Al wire mounted at the end of the collimating cylinder, calibrated against a photodiode standard traceable to NIST.

The hydrogen lamp is run at fluxes between 5 x 10^{13} and 10^{15} photons cm^{-2} s^{-1} until the desired fluence is reached, while the water remaining on the surface is analyzed using reflectance FTIR as a function of irradiation fluence. The decreases in the ratio of the OH absorption band area after irradiation to before irradiation give a quantitative indication of the amount of water desorbed. By monitoring the sample at a variety of fluences with subsequent FTIR measurements, we can calculate the photodesorption yield in terms of desorbed molecules per incident photon, or the cross section by dividing by the surface density of the water monolayer.

In addition, we measure the photodesorption yield of water from olivine and anorthite for 253.7 nm photons from a Hg light source. Furthermore, the desorption yield of water adsorbed onto a C substrate mounted on a quartz crystal microbalance with a sub-monolayer sensitivity is measured as a function of irradiation fluence of 193 nm photons from an ArF excimer laser.

Sputtering of adsorbed water will be studied using the methods described for measuring the sputtering yield of adsorbed Na from mineral surfaces [5]. In these studies, we quantify the surface concentration of adsorbed water relative to silicon from the mineral lattice by X-ray photoelectron spectroscopy (XPS). These measurements are taken as a function of hydrogen and helium fluence to obtain a depletion cross section, which can be converted into coverage-dependent sputtering yields. In addition, ions ejected from the sample are detected with a secondary ion mass spectrometer (SIMS). These measurements are used in conjunction with XPS data to ascertain the physical processes involved in sputtering.

Results will be presented and discussed at the meeting. This research is supported by NSF Astronomy.

References: [1] Sunshine, J.M. et al (2009) *Science* 326, 565. [2] Dukes, C.A., Baragiola, R.A. (2009) *Surf. Interf. Anal.* 42, 40. [3] Burke, D.J. et al (2011) *Icarus* 211, 1082. [4] Westley, M.S. et al (1995) *Nature* 373, 405. [5] Dukes, C.D. et al. (2011) *Icarus*, in press.

LRO LEND OBSERVATIONS OF NEUTRONS AS EVIDENCE FOR POLAR HYDROGEN. I. G. Mitrofanov[1], M. L. Litvak[1], A. B. Sanin[1], D. V. Golovin[1], W. V. Boynton[2], G. Chin[3], J. B. Garvin[3], L. G. Evans[4], K. Harshman[2], A. S. Kozyrev[1], T. McClanahan[3], R. Sagdeev[5], V. Shevchenko[7], V. Shvetsov[8], D. Smith[9], R. Starr[6], J. Trombka[5] and M.Zuber[9]. [1]Institute for Space Research, 117997 Moscow, Russia imitrofa@space.ru, [2]University of Arizona, Tucson, AZ USA, [3]NASA Goddard Space Flight Center, Greenbelt, MD USA, [4]Computer Science Corporation, Greenbelt, MD USA, [5]University of Maryland, Collage Park, MD USA, [6]Catholic University, Washington DC, USA, [7]Sternberg Astronomical Institute, Moscow, Russia, [8]Joint Institute of Nuclear Research, Dubna, Russia, [9]Massachusets Institute of Technology, Cambridge, USA.

Introduction: The first suggested detection of water ice in polar craters was claimed by the bistatic radar team of the *Clementine* mission [1], but this result was not supported by subsequent high-resolution Earth-based radar measurements [2]. Indirect evidence for the presence of water ice in polar regolith was provided by the *Lunar Prospector Neutron Spectrometer* (LPNS), in the form of extended suppression of neutron emissions around both lunar poles [3]. The first direct detection of H_2O and/or OH in the top layer of the lunar polar regolith was performed by means of the M^3 hyperspectral IR mapping spectrometer onboard the ISRO *Chandrayaan-1* mission [4]; however such IR data characterizes only the uppermost few micrometers of the regolith. The final proof for the presence of localized areas with a relatively high content of water and another volatiles at the lunar poles has been recently provided by the remote sensing measurements of NASA's LRO and LCROSS missions [5 – 7].

Observations: studying local Neutron Suppression Regions (NSRs), as potential locations of polar Hydrogen. Currently available LEND neutron data has allowed us to identify several local areas around both lunar poles which most plausibly display rather high content of Hydrogen with about several % of WEH (Water-Equivalent Hydrogen) within a ~1 meter thick layer of the regolith. They are detected as localized *Neutron Suppression Regions*, or NSRs. Among all of them, the strongest suppression effect of epithermal neutrons is found associated with the NSR of *Cabeus* [5]. The NSR of *Cabeus* has a total area of about 700 km^2. The average enhancement of Hydrogen in this NSR is about 360 ppm in comparison with the local vicinity. The northern part of this NSR, with an area of about 300 km^2 , lies in the permanently shadowed region (PSR) of *Cabeus*; the surface of this part is never illuminated by direct sunlight, and its temperature is constantly below 100 K [8]. The southern part of the *Cabeus* NSR , with an area of about 400 km^2 , is illuminated during the lunar polar day, when surface temperatures increase well above 100 K, suggesting that water ice should intensively sublime from the regolith.

Another well-observed NSR with an area about 1500 km^2 was detected within another polar crater known as *Shoemaker*. Its boundary coincides very well with the outer contour of PSR in the bottom of this crater. The average enhancement of Hydrogen in the NSR is about 190 ppm. Figure compares a profile of the surface topography of the crater (from LOLA) along 50° longitude together with the profile of neutron suppression from LEND. The two profiles are surprisingly similar at the northern edge (a clear illustration of LEND "imaging" capability at a scale of ~10 km), but at the poleward edge, the local topography is clearly changing at a much higher rate than neutron suppression. The surface of the NSR in *Shoemaker* is permanently cold, and there exist nearly ideal conditions for permanent storage of frozen water in the regolith. On the other hand, there are many another craters at both the south and north poles, which also have associated PSRs, but do not manifest any detectable signature of neutron suppression.

The third example of a well-defined NSR is located at the northern polar crater *Rozhdestvesnky*. The LEND-based NSR (with a total area of about 240 km^2) is also coincident with the PSR within this crater. The average enhancement of Hydrogen in this PSR is about 330 ppm.

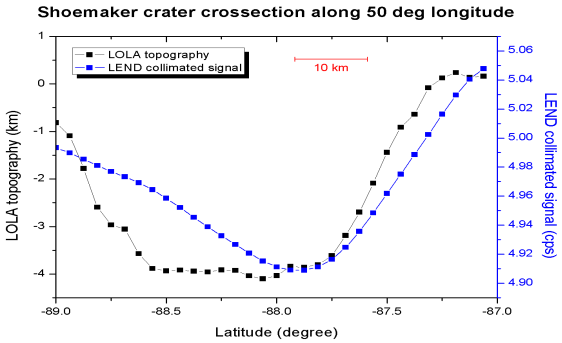

Figure: *Shoemaker* crater cross-section along 50° longitude for LOLA topography (*black*) and LEND neutron counting rate (*blue*).

References: [1] Nozette S. et al. (1996) *Science, 274*, 1495. [2] Campbell D. et al. (2006) *Nature, 443,* 835. [3] Feldman W. et al. (1999) *Science, 281*, 1496. [4] Pieters C. et al. (2009) *Science. 326*, 568. [5] Mitrofanov I. et al. (2010) *Science, 330*, 483. [6] Colaprete A. et al. (2010) *Science, 339*, 463 [7] Gladstone R. et al. (2010) *Science, 330*, 472.

THE LANTHANIDE TETRAD EFFECT IN LUNAR GRANITES: EVIDENCE FOR THE OCCURRENCE OF WATER ON THE MOON? T. Monecke[1], J. C. Andrews-Hanna[2], R. W. Hinton[3], P. H. Warren[4], U. Kempe[5], and J. Götze[5], [1]Department of Geology and Geological Engineering, Colorado School of Mines, Golden, CO, tmonecke@mines.edu, [2]Department of Geophysics, Colorado School of Mines, jcahanna@mines.edu; [3]Grant Institute of Geology, University of Edinburgh, Scotland; [4]Institute of Geophysics, UCLA, Los Angeles, CA; [5]Institute of Mineralogy, TU Berg-akademie Freiberg, Germany.

Early analyses of lunar samples suggested that the lunar interior was anhydrous. More recent studies found evidence for the presence of trace (several to several 100's of ppm) water during the formation of some lunar glass beads [1] and apatites [2]. Here, we present preliminary evidence for the aqueous alteration of a lunar granite clast during or shortly after its formation. We note that the REE pattern of an accessory mineral within a granite clast shows convex tetrads, resembling those observed for evolved granites on Earth that either formed in the presence of or were subsequently altered by an aqueous and/or fluorine-rich phase.

Previous studies [3, 4] revealed that Apollo 14 alkali-feldspar granite clast 14321,1024 shows a granophyric texture consisting of 60% potassium feldspar and 40% quartz (Fig. 1). Whole-rock chemical analysis demonstrated that the granite is chemically pristine [3]. Dating of zircons in grain mount 14321,1613 by the $^{207}Pb/^{206}Pb$ method yielded an age of 3,956±21 Ma [5]. The lunar granite clast contains rare accessory minerals, including oxycalciobetafite (previously described as yttrobetafite) found in intergrowth with potassium feldspar [4]. The normalized REE pattern of the oxycalciobetafite shows a split into four consecutive curved segments that are referred to as tetrads (Fig. 2; first tetrad: La-Ce-Pr-Nd; second tetrad: (Pm)-Sm-Eu-Gd; third tetrad: Gd-Tb-Dy-Ho; fourth tetrad: Er-Tm-Yb-Lu). The convex curvatures of the three quantifiable tetrads are found to be significant from an analytical point of view [6].

The oxycalciobetafite represents the first extraterrestrial material that shows unequivocal evidence for the occurrence of the tetrad effect. On Earth, tetrad occurrences in natural geologic materials are restricted to samples that interacted with water during their formation or alteration. Terrestrial rock and mineral samples from evolved granites and associated hydrothermal ore deposits show the most pronounced convex tetrads, which are comparable to those observed in the oxycalciobetafite [7-8]. However, experimental studies have shown that tetrads can also arise from silicate-liquid immiscibility involving a fluorine-rich phase [9].

The observation of tetrads in a lunar granite clast suggests the involvement of a H_2O- or F-rich fluid phase during its formation and/or alteration. The role of water may be limited by the lack of identified hydrous minerals and the presence of anhydrous mafic grains [3]. Water commonly plays an important role in the formation of terrestrial granites, though silicate liquid immiscibility may be primarily responsible for some lunar granites [10]. While granites make up a small fraction of the lunar sample collection, they may be related to areas of silicic highland volcanism such as the Gruithuisen Domes [11]. If water or fluorine played a role in the formation or alteration of other lunar granites as well, then the existence of distinct granitic provinces may support the possibility of a heterogeneous distribution of volatiles in the early lunar interior.

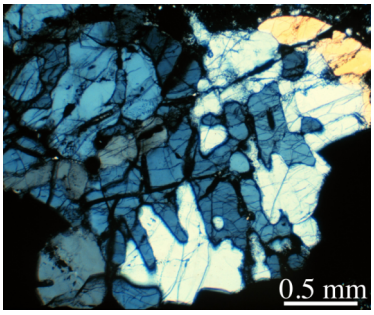

Fig. 1: Granophyric intergrowth texture of quartz (bluish grey and yellowish) and K-feldspar (white and light-grey) in thin section 14321,1047.

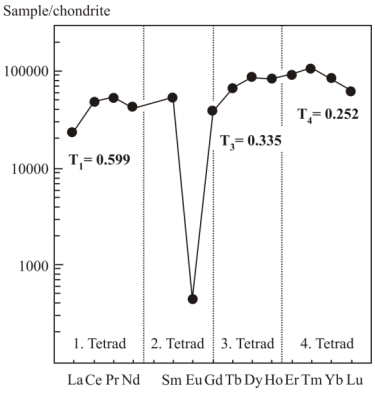

Fig. 2: REE pattern of oxycalciobetafite in lunar granite 14321,1027.

References: [1] Saal A. E. et al. (2008) *Nature*, 454, 192-195. [2] McCubbin F. M. et al. (2010) *PNAS*, 107, 11,223-11,228. [3] Warren P. et al. (1983) *EPSL*, 64, 175-185. [4] Hinton R. W. and Meyer C. (1991) *LPSC*, 22, 575-576. [5] Meyer C. et al. (1989) *LPSC*, 20, 691-692. [6] Monecke T. et al. (2002) *GCA*, 66, 1185-1196. [7] Irber W. (1999) *GSA*, 63, 489-508. [8] Monecke T. et al. (2011) *Geology*, 39, 295-298. [9] Veksler I. V. et al. (2005) *GCA*, 69, 2847-2860. [10] Jolliff B. L. et al. (1999) *Am. Min.*, 84, 821-837. [11] Glotch T. D. et al. (2010) *Science*, 329, 1510-1513.

NEW CONSTRAINTS ON THE RELATIVE ABUNDANCES OF WATER, F, AND CL IN PARENTAL MAGMAS OF KREEP-BEARING LITHOLOGIES – TAKING DEGASSING INTO ACCOUNT. H. Nekvasil[1] [1]Department of Geosciences, Stony Brook University, Stony Brook, NY 11794-2100 Hanna.Nekvasil@sunysb.edu

Introduction: Two basic questions have arisen from the recent discovery of significant OH in lunar apatites [1-3]: How much water does this imply for lunar magmatic source regions, and, what is the abundance of water relative to that of other major volatiles with significant melt solubility, such as F, Cl, and S? As a first step towards answering these questions, [1] converted the volatile contents measured in apatite from three KREEP-bearing lithologies to the volatile contents of the instantaneous co-existing melts and, assuming an incompatible increase in water, Cl, and F during crystallization of volatile-free minerals, approximated both the parental magma and source region volatile contents. However, if magma degassing took place during apatite growth and the composition of the fluid lost differed in relative abundance of volatiles from that of the magma, the absolute abundance of volatiles can be greatly underestimated and the relative abundances of volatiles changed drastically from that calculated in this manner.

In order to assess the possibility that the apatites themselves preserved information on degassing, [4], [5] conducted a mass balance analysis of the apatite analyzed by [1]. They concluded that the apatites from all three lithologies showed evidence of a degassing history that involved first loss of a water- and Cl-rich bulk fluid (Fluid I in Fig 1) followed by a more water-poor, Cl-rich bulk fluid (Fluid II in Fig 1). Using partition coefficients for F, Cl and OH between melt and apatite of [1],[6],[7] they computed the compositions of the instantaneous melts coexisting with each apatite analysis (colored hexagons in Fig. 1) and mapped out melt evolution paths during degassing (heavy colored solid arrows in Fig. 1). Their results indicated that both the absolute and relative abundances of these volatiles in the melts changed during degassing.

Such analysis was continued to determine if information regarding the relative abundance of water, F, and Cl in fluid and melt *prior to open system degassing* could be extracted in order to provide first insights into the relative volatile abundances of parental magmas of KREEP-bearing lunar lithologies.

Fluid evolution: Computed fluid compositions for the two-stage degassing process recorded in the analysis of apatites from 14053,16 and 15404,51 (open colored circles) form two linear arrays that emerge from the calculated bulk fluid composition of NWA 2977 (thin colored arrows, Fig. 1) at a molar ratio of 86:7:7 (H_2O:F:Cl). It is proposed that this common ratio represents the composition of fluid just before open-system processes commence and loss of fluid causes divergence of residual magma compositions.

Melt evolution: The calculated melt compositions show a path in H_2O-F-Cl space that reflects the two-stage degassing process recorded in the apatites. Although the path for each lithology is unique, the melt paths emerge from a common point - the initial melt volatile ratio computed for NWA 2977 (as shown by the heavy dashed colored lines of Fig. 1). This suggests that these different lithologies and melt evolutionary paths shared the same initial water:F:Cl ratio. It is proposed that the emergence point at the molar ratio of 82:10:8 (H_2O:F:Cl) represents the point at which simple incompatible increase due to crystallization ended and fluid exsolution and open-system degassing began. Thus, this ratio would be that of the parental magma of these KREEP-bearing lithologies since the ratio does not change upon crystallization of volatile-free minerals (or only changes to a small extent upon crystallization of minor amounts of apatite).

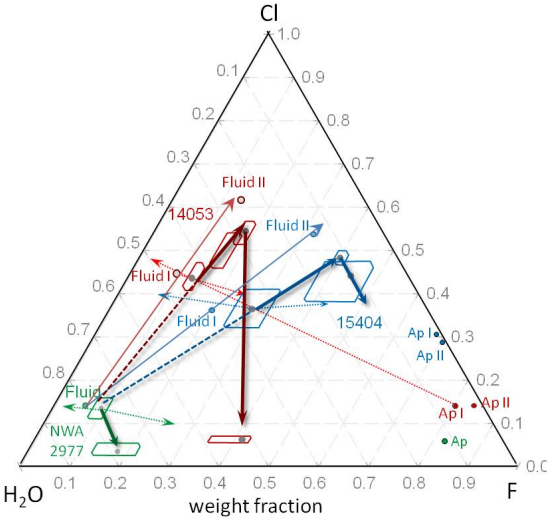

Figure 1. Melt and fluid evolution paths in F-Cl-H_2O space based on apatite analysis of [1] for 14053, 16 (red), 15404, 51(blue), NWA 2977(green). Arrows and symbols as described in text.

References: [1] McCubbin F.M. et al. (2010) *PNAS* 107, 11223. [2] Boyce J.W. et al. (2010) *Nature, 466,* 466-469. [3] Greenwood J.P. et al. (2011) *Nature Geoscience, 4*, 79-82. [4] Nekvasil H. et al. (2010) Fall *AGU*, P41A05. [5] Nekvasil H. et al. (2011) *LPSC XLII, 2240*. [6] Boyce J.W. and Hervig R. L. (2009) *Contr. Mineral. Petrol 157*, 135-145. [7] Mathez, E.A. and Webster, J.D. (2005) *GCA 69*, 1275-1286.

DIVINER LUNAR RADIOMETER OBSERVATIONS OF THE NORTH AND SOUTH POLAR REGIONS OF THE MOON. D. A. Paige[1], M. A. Siegler[1] and J. P. Williams[1], [1]Dept. of Earth and Space Sciences, UCLA, Los Angeles, CA 90095, dap@moon.ucla.edu.

Introduction: The Diviner Lunar Radiometer Experiment aboard the Lunar Reconnaissance Orbiter (LRO) has been mapping the moon nearly continuously since July, 2009. The instrument has acquired thermal emission and solar reflectance data in nine spectral channels spanning a wavelength range from 0.3 to 400 microns, at spatial resolutions ranging from 0.2 to 1.3 km [1]. Diviner's unprecedented and growing dataset is revealing the extreme nature of the lunar thermal environment and its diurnal and seasonal variability.

Polar Mapping: In the lunar polar regions, Diviner's swath provides two spatially continuous thermal images at latitudes greater than 84 degrees twice per month at a spatial resolution of less than 240 meters. At these highest latitudes, Diviner has obtained sufficient spatial and temporal coverage to determine annual minimum, maximum, and average surface temperatures at both poles. The results show that the coldest regions on the Moon achieve annual average temperatures of less than 38K, and that surface temperature excursions below 23K are briefly observed.

Large areas of the lunar polar regions are currently cold enough to cold-trap water ice as well as a range of both more volatile and less volatile species [2]. The cold trap regions include surface cold-traps in permanent shadow as well as more extensive subsurface cold traps that experience brief periods of direct sunlight. A range of volatile species predicted by Diviner temperature maps were observed in the impact plume of LCROSS in Cabeus Crater in October, 2009 [3,4], suggesting that impacts from primitive bodies from the outer solar system have contributed volatiles to the moon's polar cold traps over time. However, the physical properties of the lunar regolith in the cold traps, and the horizontal and vertical distribution of volatiles within the cold traps is highly uncertain.

References: [1] Paige D. A. et al. (2009) *Space Science Reviews*, DOI: 10.1007/s11214-009-9529-2. [2] Paige D. A. et al. (2010) *Science* 330, 479. [3] Colaprete A. et al. (2010) *Science* 330, 463. [4] Gladstone G. R. et al. (2010) *Science* 330 472.

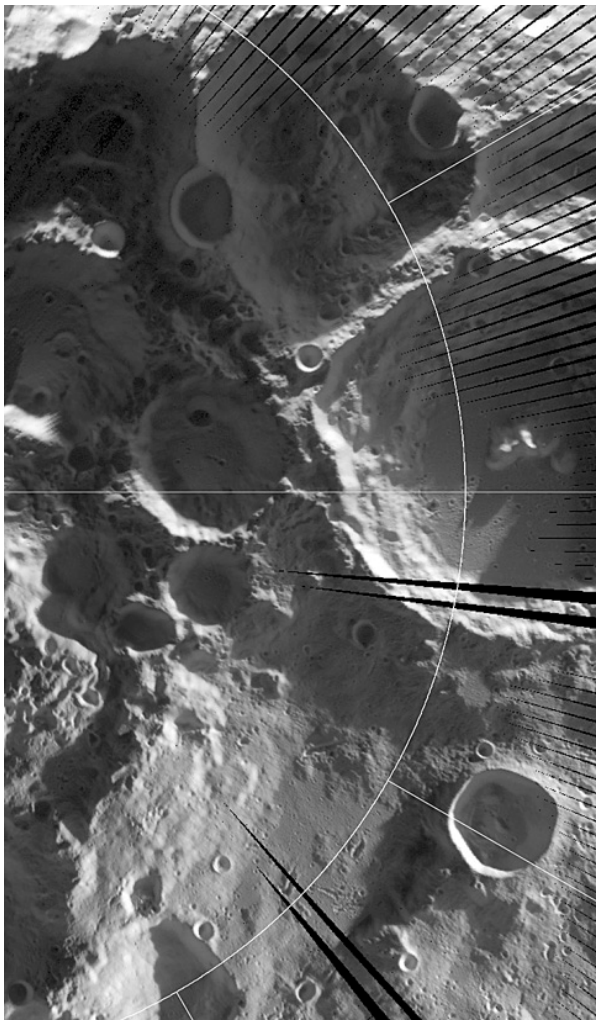

Figure 1. Dviner daytime thermal image of the south polar region of the Moon acquired in August, 2009.

LUNAR ROBOTIC EXLORATION OBJECTIVES IN THE NEXT DECADE. J. B. Plescia[1], [1]The Johns Hopkins University, Applied Physics Laboratory, Laurel, MD USA (Jeffrey.plescia@jhuapl.edu).

Introduction: Robotic missions to the Moon can provide a wealth of data for both scientific and exploration objectives. Some objectives require large complex systems, but others can be addressed by simple, short-lived stationary systems. The current fiscal climate suggests that NASA will be constrained to relatively small (Discovery and New Frontiers class) mission for the foreseeable future. While such missions may not be capable of sample return or discovering that water has existed on Mars, they can provide important steps in understanding the Moon.

Scientific Goals: Several reports (e.g., LEAG Roadmap; NRC Scientific Context for Exploration of the Moon; Vision and Voyages for Planetary Science in the Decade 2013-2022) have outlined key lunar science questions and the results of recent lunar missions (e.g., LRO, Chandrayaan, Kaguya, Selene) have provided data that have answered some questions and opened up many more.

Volatiles: Perhaps the most intriguing of the questions that has received recent attention is lunar water - its form, source and distribution. The Apollo view was that the Moon was largely devoid of water; however Lunar Prospector neutron data suggested that significant hydrogen was present in the polar regions, interpreted to be water. Data from the LRO neutron spectrometer suggest that the distribution might be quite complex. Spectral data from the Chandrayaan M^3 instrument indicate that H_2O or OH occurs on the surface across the polar regions. Chandrayaan and LRO radar data have been interpreted to indicate that several shadowed craters hold significant water ice. Analysis of lunar samples has also suggested that water was/is present in the mantle.

Exploration Approach: While the neutron, spectral and radar data can be interpreted to indicate the presence of H and H_2O at the lunar poles (inside and outside of permanent shadow) its form, origin, and distribution are unknown. The most direct way to assess this is to explore a permanently shadowed area having an appropriate neutron and radar signature. Such missions were studied as part of the RLEP and LPRP programs.

Rovers: A rover outfitted with sample acquisition and analysis instrumentation and powered by nuclear (RTG/ASRG), fuel cells or even primary batteries would have the capability to explore a permanently shadowed area to determine the nature of the H-bearing species. Using a neutron spectrometer, an appropriate site could be located and sampled using a drill to obtain subsurface samples. The recovered samples would be analyzed to determine the nature of the H-bearing species. Further traverses would mapping the spatial distribution. Assuming that the complete volatile inventory could be examined and its isotopic composition measured, the origin of the volatiles could be determined as well.

Landers: A static lander placed in an illuminated area of high H (as indicated by orbital neutron data) could address the distribution of H, although in a less direct manner. The assumption has been that most of the H is cold-trapped in permanent shadow. A lander in a non-permanently shadowed region would measure the regolith H abundance. If the H concentration were high (100s ppm) it would suggest that the H was broadly distributed across the poles; if the content was low, then the case that the "missing" H was sequestered in permanent shadow would be stronger. Such a mission could also measure the surface H_2O/OH (indicated by spectral data) and assess the amount and any temporal variation.

Cratering and Volcanism Chronology: The objectives of the lunar cratering chronology and mare volcanism could also be addressed with a simple lander. Crater counts suggest that some mare areas may be as young as 1 Ga. A mission to such a young area could acquire a basalt sample and determine an absolute age *in situ* using the K/Ar or Rb/Sr methodology. While not as precise as a laboratory measurement, it would indicate whether such surfaces are really only 1 Ga. Such a measurement would provide important <3 Ga constraints on the absolute cratering chronology and it will have important implications for models of the lunar thermal history.

Discussion: These examples serve only to illustrate how robotic missions can address important scientific questions. While some objectives (e.g., sample return) require large complex (i.e., expensive) systems, other objectives can be addressed with smaller low-cost systems. In some cases the precision may not be what is ultimately desired, but an actual good measurement maybe be more useful than great measurement that is never obtained.

Mobility is always an important aspect of a mission. While a small mission might only have mobility of the order 100s of meters, such mobility allows collection and analysis of multiple samples to avoid a single unrepresentative measurement.

THE COMPARISON CONTENT OF HYDROGEN IN THE REGION OF THE NORTH POLE AND SOUTH POLE OF THE MOON. S.G. Pugacheva, V.V. Shevchenko, Sternberg State Astronomical Institute, Moscow University, 13 Universitetskiy pr., 119992 Moscow, Russia, pugach@sai.msu.ru

Introduction: The article is devoted to studying the hydrogen content in the lunar craters of the South and North Poles. The surface of the craters that are situated in the area South Pole and North Pole is not exposed to the direct sun light and has extremely low temperature (below 90 K) that remains for billions of years. The estimated values of photometric parameters in visible and infrared spectral ranges show that conditions of the solar radiation of the pole areas create prerequisites for formation of considerable water ice fields [3, 4].

Craters with the high contents of hydrogen: Measurements made by KA Lunar Prospector (LP) and Lunar Reconnaissance Orbiter (LRO) proves high content of hydrogen in the Moon's soil [1, 2]. We have compared the hydrogen presence in the soil of the five craters near the South Pole and six craters near the North Pole. The craters located near the South Pole: Cabeus (85.28°S, -41.81°W, D=100.58 km), Shackleton (89.63°S, 132.32°E, D=21 km), Faustini (81.18°S, 85.02°E, D=42.48 km), Shoemaker (88.03°S, 39.85°E, D=48.33 km), Haworth (87.2°S, -7.49°W, D=51.42 km). Craters located near the North Pole: Peary (88.57°N, 25.73°E, D=85.15 km); Rozhdestvenskiy (85.49°N, -158.44W, D=180 km); Whipple (89.14°N, 119.92°E, D=14.53 km); Hermite (87.08°N, -91.31°W, D=104.64 km), Byrd (85.38°N, 12.05°E, D=91.92 km); Lenard (85.17°N, -109.32°W, D=45.24). The histogram in Figure 1 shows the distribution content of the hydrogen in the craters near the South Pole. According to figure 1 the general distribution of hydrogen in Cabers crater is of polymodal nature and can be divided into two marginal distributions that have form close to normal distribution. In this case, the first mode means 127 ppm, and the second mode of the hydrogen distribution is 172 ppm. The second mode of the hydrogen distribution matches with the northern shadowed border of Cabeus formation (83.78°S, 338.96°E). LCROSS has discovered out presence of water at this area of the crater Cabeus [4]. The histogram in Figure 2 shows the distribution of the hydrogen in the craters near the North Pole. The distribution of the hydrogen in the craters of the North Pole had form of the normal distribution. A maximum content of the hydrogen was found in the crater Peary (152 ppm) which significantly less the content of the hydrogen of the crater Cabeus (172 ppm). The content of the hydrogen in the regions of the North Pole varies in the interval values from 140 ppm to 170 ppm.

Conclusions: The analysis of the results obtained confirms that the macrostructure surface polar areas of the Moon are homogenous. The contents of hydrogen are positively correlation with solar insolation of slopes of the pole craters. The changes in basalts are contributed with the meteoroid- and comet impacts that cause the substance melting and formation of various breccias [5]. Probably, the regolith in the area of craters Cabeus and Peary has higher porosity and irregular macrostructure that can create conditions to accumulation of H_2O in the subsurface.

References: [1] Lawrence, D. J. et al., (2002) *J. Geophys. Res., Ser. E*, vol. 107, no. 12, p. 5130. [2] Lawrence, D. J. et al., (1998) *Science*, vol. 281, 1484–1489. [3] Pugacheva S. G., Shevchenko V. V. (2003) *LPS XXXI*, Abstract #1112. [4] Ivatury V., McClanahan T.P. (2009) *LPS XXXX*, Abstract #1134. [5] Pugacheva S. G., Shevchenko V. V. (2009) *LPS XXXXI*, Abstract #1297.

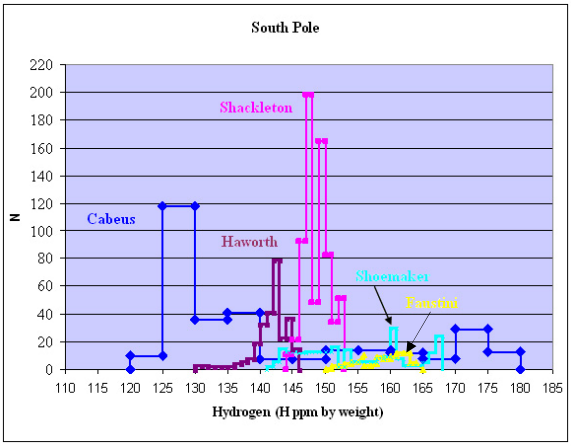

Fig. 1. The hydrogen distributions in the surface layer at the lunar craters located near the South Pole.

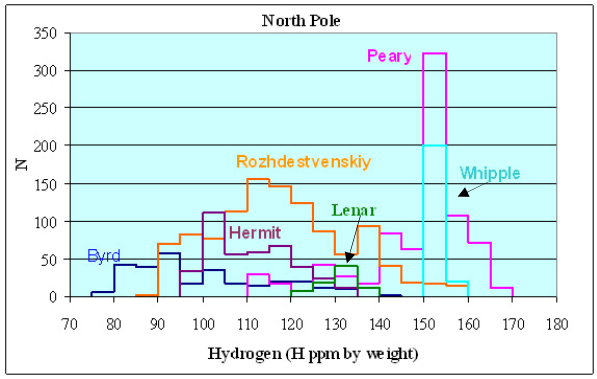

Fig. 2. The hydrogen distributions in the surface layer at the lunar craters located near the North Pole.

RESOLVE-A Payload to Groundtruth the Presence of Volatiles on the Moon. J.W.Quinn (NE-S, Kennedy Space Center, FL 32899, Jacqueline.W.Quinn@nasa.gov) , W.E. Larson (NE-I, Kennedy Space Center, FL 32899, William.Larson@nasa.gov) G. B. Sanders (JSC-EP111, Johnson Space Center, Houston, TX77058, Gerald.Sanders@nasa.gov), R. S. Baird (JSC-EP111, Johnson Space Center, Houston, TX 77058, R.S. Baird@nasa.gov), A. Colaprete (SST, Ames Research Center, Moffitt Field, CA 94035, Anthony.Colaprete-1@nasa.gov), Martin Picard (Candian Space Center, 6767, route de l'Aéroport, Saint-Hubert (Québec) J3Y 8Y9, Martin.Picard@asc-csa.gc.ca)

Introduction: Data from remote sensing missions to the Moon such as the Clementine (1994), Lunar Prospector(1998) and the Lunar Reconnisance Orbiter (2009) the later, indicated the presence of potentially significant quantities of hydrogen bearing molecules in permanently shadowed craters near the lunar poles. The LCROSS mission in 2009 provided our first look at the compounds found in the craters. These hydrogen bearing volatiles along with any other possibly co-located volatiles would be extremely useful resources whatever their form. The extraction and processing of space resources (whether from Lunar, near earth asteroid, comet, or Mars sources) into useful products is known as In-Situ Resource Utilization (ISRU) and can have a substantial impact on individual missions and mission architecture concepts. In particular, the ability to make propellants, life support consumables, and fuel cell reagents can significantly 1) reduce mission cost by reducing launch mass, providing affordable pre-positioning of consumables, and enabling hardware reusability; 2) reduce risk by providing backup life support consumables and reduced dependence on Earth; and 3) enable extended surface operations by providing an energy rich environment and affordable access to multiple surface targets.

Knowing that useful resources, such as hydrogen and water ice, are available on the lunar surface and other locations around the solar system is important; however, questions remain to be answered before ISRU development of these resources is practical. What are the constituents and distribution of the hydrogen rich volatiles located by the previous probes/missions? What other volatiles are also available? What are the environments and physical properties of the source materials that could drive ISRU extraction and processing hardware design?

In cooperation with the Canadian Space Agency, NASA has undertaken the development of the payload Regolith and Environment Science & Oxygen and Lunar Volatiles Extraction (RESOLVE) which will be designed to answer these questions as the next logical step toward human exploration and expansion out into the solar system.

Science Goal: The overall long-term objectives of the RESOLVE Project are to verify the presence of water ice and other volatiles on the lunar surface, determine resource distribution and extraction characteristics, and serve as a precursor for future prospecting missions to a variety of locations around the solar system including Mars, asteroids, and comets by direct, ground truth measurements of the materials at those locations. For the purpose of the initial demonstration and development phases of the RESOLVE Project, work shall focus on analyzing lunar regolith in and around permanently shadowed Polar Regions. These focused objectives have been defined by the Exploration Technology Development and Demonstration (ETDD) and ISRU Domain customers to include:

- Determination of the form, concentration, and spatial distribution of hydrogen and other volatiles inside and outside of shadowed lunar Polar Regions to a depth of at least 1 m.
- Determination of bulk properties of lunar material inside and outside of shadowed lunar Polar Regions.
- Demonstration of regolith prospecting, extraction, and processing operations in the lunar environment.
- Demonstration of oxygen (water) extraction from regolith via hydrogen reduction in the lunar environment.

Presentation Focus: This presentation will review the overall system architecture from software to onboard instrumentation planned for RESOLVE. It will also highlight previous RESOLVE field demonstrations and how the current architecture will morph to meet the new challenges of working with the volatiles now known to exist on the lunar poles. The presentation will also highlight three mission scenarios for RESOLVE and the impact to technology and operations based upon those architectures:
- All operations occur in sunlight near permanently shawdowed regions.
- Dash and grab with short duration excursions into shadowed areas and processing in the sunlight.
- Full permanently shadowed crater mission.

ORIGIN AND COMPOSITION OF LUNAR VOLCANIC GAS: THE PICRITIC GLASS MODEL. M.J. Rutherford[1], D. Wetzel[1], E.H. Hauri[2], and A.E. Saal[1]. [1]Dept. of Geological Sciences, Brown University, Providence RI 02912 (malcolm_rutherford@brown.edu@brown.edu), [2]DTM Carnegie Institute of Washington, DC 20015 (hauri@DTM.ciw.edu).

Abstact: The composition and origin of the initial gas phase produced in the picritic lunar glass magma has been determined from analyses of the natural galsses and experiments. Partitioning of S, Cl and F into the CH_4-bearing CO-rich gas has also been determined for a range of pressures up to 1000 MPa.

Introduction: The existence of a gas phase in lunar basaltic magmas is demonstrated by the ubiquitous presence of vesicles in returned samples (1). Additionally, the fine-grained glass bead deposits formed during eruption of the lunar picritic glasses (2,3) required a large (>90 v%) gas-bubble volume at the time of eruption (4). Theoretical studies (5) of the lunar picritic glasses suggest that in the absence of water, the only way to generate a gas phase at depth in the Moon is by the oxidation of reduced C, and the result would be a CO-rich gas containing anion species (S, Cl and F) and metals depending on the melt-gas partition coefficients. This theory has been confirmed by the analyses of the condensed coatings (Cu,Zn,Ga,Pb,S,Cl,B,F) on beads of the lunar orange and green picritic glass deposits (6). The process of generating a gas in ascending lunar, hydrogen-depleted, magmas depends fundamentally on the intrinsic oxygen fugacity (fO_2) of the magma and the presence of carbon either dissolved in the magma, or as excess graphite in the magma. Because of the strong pressure dependence of the graphite C-O equilibrium (7), carbon (graphite) in ascending magma is oxidized to form a CO-rich gas at a pressure that depends on the intrinsic oxygen fugacity. For most lunar magmas, this oxygen fugacity is close to the Fe-FeO (IW) equilibrium. FeNi-metal grains in the picritic glasses, and trapped in olivine phenocrysts in the orange glass beads are interpreted as forming by C reduction (8). Experiments on the orange and green glass compositions (9,10) demonstrate that the Fe-rich metal is generated at a pressure of 40 MPa when the fO_2 was at IW-1.0 log units. Trace amounts of Ni, S, F, Cl and F in the magma do not affect the 40 MPa pressure at which the CO-rich gas is formed (10).

Water in the lunar picritic magmas: Recently, (12,13) used SIMS to determine that water (H) is present in lunar glass beads; abundances of H_2O ranging up to 100 ppm were identified at the center of beads, and diffusion loss profiles were determined in core to rim NANOSIMS profiles. Importantly, the H abundance is positively correlated with S, Cl, F and C abundances indicating that the volatiles including H (H_2O) were dissolved in the melt at higher concentrations at the time the beads formed. Using available diffusion rate data, (12) estimated that the original H concentrations in some beads were as high as 700 ppm. Graphite-saturated experiments on the A15 green glass composition indicate how this water would affect the origin and composition of the gas phase in the green glass magma (10). The results show that there is a strong positive correlation between the concentration of dissolved C and dissolved H (water) in the glasses for water concentrations up to 1500 ppm. The abundances of dissolved C and H also increase with increasing pressure, and many of the < 200 MPa experiments did contain an excess gas phase. We interpret these data as outlining the gas-saturated surface for C and H in the melt at graphite saturation for the lunar IW oxidation state. The correlation of C and H abundance with increasing pressure indicates the C is dissolved primarily as CH species at these reduced conditions, an observation constant with recent high-pressure results at the same oxidation state (13,14) where the C and H abundance was sufficiently high that CH species signatures were observed in Raman and IR spectra. Our experiments confirm this and yield data on the partitioning of S, Cl and F between the GG melt and the CH-CO vapor.

Conclusions: We conclude that ascending picritic lunar magmas containing H at 500 to 1500 ppm H_2O concentration levels and graphite will produce small amounts of gas prior to reaching the graphite oxidation pressure where FeO is reduced to Fe-metal. The initial gas production is caused by the reduced CH-species solubility with decreases in pressure; in magmas without H, all of the gas phase would be produced in association with graphite oxidation at ~40 MPa or about 8.5 km depth in the moon. Cl and S partition modestly into the early forming CH-CO gas. This process of gas formation and FeO-reduction should have also operated during convection in the LMO that carried C and melt above ~8 km depth in the moon.

References: **(1)** Heiken G.H., et al., 1974, GCA 38, 1703-1718. (2) McKay et al.,1992, LPI Tech Rept 92-09, LPI. (3) Delano, J.W., 1986, PLPSC 6Th, D201-213. (4) Rutherford M. and Papale, P., 2009, Geology, 37, 219-22. (5) Sato, M., 1976, PLPSC 7th, 1323-35. (6) Meyer, C., et al., 1975, PLPSC, 6th, 1673-1699. (7) French, B. and Eugster, H.P., 1965, JGR, 70, 1329-39. (8) Fogel R.A., and Rutherford, M.J., 1995, GCA, 59, 201-215. (9) Nicholis, M. and Rutherford, M.J., 2009) GCA, 73, 5905-17. (10) Wetzel., D et al., 2010, LPSC abst #1827. (11) Saal, A.E., et al., 2008, Nature, 454, 192-195. (12) Saal, A., et al., 2009, LPSC 40th, (13) Ardia, P and Hirschmann, M.M., 2010, LPSC abst 1347. (14) Mysen B.O., et al., 2010, AGU fall metg abst V33F-02.

THE VOLATILE CONTENT AND D/H RATIOS OF THE LUNAR PICRITIC GLASSES. A. E. Saal[1], E. H. Hauri[2], M. J. Rutherford[1,] J. Van Orman[3]. [1]Department of Geological Sciences, Brown University, 324 Brook St., Box 1846, Providence, RI, 02912. [2]Department of Terrestrial Magnetism, Carnegie Institution of Washington, 5241 Broad Branch Road, NW Washington, DC 20015.[3]Department of Geological Sciences Case Western Reserve University, Cleveland, OH 44106.

Introduction: The general consensus is that the Moon formed and evolved through a single or series of catastrophic heating events in which most of the highly volatile elements, especially hydrogen, were evaporated away. That notion has changed with the new reports showing evidence of indigenous water in lunar volcanic glasses [1] and in lunar apatites from mare basalts [2, 3, 4]. These results represent the best evidence for the presence of a deep source within the Moon relatively rich in volatiles. We compiled new and old volatile data (C, H_2O, F, S, Cl) for more than 360 individual Apollo 14, 15 and 17 lunar glasses with composition ranging from very-low to high-Ti contents, and present δD ratios of over 200 single volcanic beads.

Samples and Analytical Techniques: The glassy volcanic spherules range in size from ~100 μm to ~ 1 mm. The abundances of volatiles dissolved in the interior of the lunar picritic glasses were measured by SIMS using a Cameca IMS 6F and NanoSIMS at DTM, CIW, employing methods recently developed for the microanalysis of trace amounts of H, C, F, S, Cl in glasses and nominally anhydrous minerals [5]. Our new SIMS detection limits (~0.13 ppm C; ~0.4 ppm H_2O, ~0.05 ppm F, ~0.21 ppm S, ~ 0.04 ppm Cl by weight determined by the repeated analysis of synthetic forsterite located on each sample mount), represent at least 2 orders of magnitude improvement over previous analytical techniques.

Results: After background correction the volatile contents of the lunar volcanic glasses have the following maximum contents: C ~ 20 ppm; H_2O ~ 160 ppm; F ~80 ppm; S ~ 800 ppm; Cl ~ 10 ppm with A14 glasses ranging to the highest volatile contents. Our data support the hypothesis that there were significant differences in the initial volatile content, and/or the mechanism of degassing and eruption among these glasses was different. Interestingly, a general correlation was found between the volatile enrichment and the incompatible trace elements. This suggests that degassing did not completely erase the initial difference in volatile contents between the distinct compositional groups of volcanic glasses. δD measured in the lunar glasses range from +179‰ to +5420‰, and thus, are undisputably fractionated from terrestrial values. However, the δD is inversely correlated with water contents; some of the D enrichment results from in-situ spallation during interactions with solar and galactic cosmic rays. The cosmic ray exposure ages of individual lunar volcanic glasses from the same samples examined in this study range from 130 to 300 million years, with a well-defined average of 283±51 Myr [6]. A notable feature of the highest-H_2O lunar glasses after spallation correction is that they exhibit a much smaller range in δD values than the overall data. The average δD of the five highest-H_2O glasses is +340‰ (+180‰/-240‰). It is very likely that the original pre-eruptive δD value of these lunar magmas was significantly lower, and that kinetic D/H fractionation has resulted in preferential loss of H during magmatic degassing. A simple kinetic degassing calculation, starting with pre-eruptive magma compositions with H_2O of 250 ppm and 745 ppm [1], and δD identical to the terrestrial mantle (-80‰), defines kinetic degassing trends that reproduce most of our observations within error when hydrogen ions are the diffusing species.

Conclusions: We reported volatile contents (C, H_2O, F, S, Cl) for the lunar picritic glasses, which by virtue of SIMS analysis provide improved detection limits by one to two orders of magnitude. Our results suggest not only a much wetter Moon's interior than previously thought [1], but also suggest that the KREEP component, either through shallow assimilation by the melt or deep hybridization of the LMO cumulate, may influence the volatile composition of the erupted glasses. The δD of the highest-H_2O glasses after corrections for spallation and kinetic degassing suggest a similar isotope ratios to that of the terrestrial MORB.

References: [1] Saal, A. E. et al. (2008) *Nature 454, 192*.[2]. [2] McCubbin, F.M. et al. (2010) *PNAS, 107 (25), 11223*. [3] Boyce, J. W. et al. (2010) *Nature 466, 466.* [4] Greenwood, J. P. et al. (2010) *Proc. 41th LPSC* Abs 2439. [5] Hauri, E. H. et al. (2006) *EPSL 248,* 715. [6] Spangler, R. et al. (1984), *J. Geophys. Res. 89, 487*. *Proc. 40th LPSC* Abs 2374.

FINE SCALE SPATIAL VARIATIONS OF HYDROGEN PRESENCE FROM NEUTRON COUNTING OVER LUNAR NSR'S. R. Sagdeev[1], I.G. Mitrofanov[2], W.V. Boynton[3], G. Chin[4], G. Droege[3], L.G. Evans[4,6], J. Garvin[4], K. Harshman[3], M.L. Litvak[2], A. Malakhov[2], T.P. McClanahan[4], G.M. Milikh[1], M. Namkung[1], G. Nandikotkur[1], G. Neumann[1], A. G. Sanin[2], R.D. Starr[4,5], J.I. Trombka[1,4], [1]Space Physics Department, University of Maryland, College Park, MD, USA, [2]Inst. for Space Research, Moscow, Russia, [3]Lunar and Planetary Laboratory, University of Arizona, Tucson, AZ, USA, [4]Space Exploration Division, NASA Goddard Space Flight Center, Greenbelt, MD, USA, [5]Catholic Univ., Washington, DC, USA, [6]Computer Sciences Corp., Glenn Dale, MD, USA.

The regions of a highest suppression in neutron counting around the poles (Cabeus, Shoemaker) provide sufficient statistical data to look for a fine scale spatial variations. Here we demonstrate the results obtained with the use of LEND's [1] collimated sensors as applied to few selected target areas with spatial resolution within 10 km for Hydrogen presence in Lunar soil. Important distinction is brought by the dependence on the altitude of actual measurements. At the same time the focusing at such target spots serves to validate the calibration of LEND's collimation capability. These results are compared with the collimation model, based on several factors including: 1) geometry of the LEND collimated detector system, 2) the lunar neutron production due to the current epoch of GCR flux. As a reference set of GCR parameters (and of resulting neutron flux), we use the Apollo 17 neutron experiment (December, 1972) and [2]. The recent LEND measurements were taken at a historic low for solar activity subsequent increased lunar neutron flux than in the reference case. We quantify the increase neutron production rate due to higher GCR flux.

References: [1] I.G. Mitrofanov at al., Science, Vol. 330, Issue 603, pg. 483, doi:10.1126/scince.1185696, 2010; [2] G.W. McKinney, D.J. Lawrence et al., J. Geophys. Res., 2005, Vol. 111, EO6004, doi:10.1029/2005JE002551, 2006.

THE IMPACT OF LUNAR POLAR VOLATILES ON IN-SITU RESOURCE UTILIZATION. G. B. Sanders[1] and W. E. Larson[2], [1]NASA Johnson Space Center, 2101 NASA Parkway, Mail Code EP, Houston, TX 77058, Gerald.b.sanders@nasa.gov, [2]NASA/KSC, Code NEI20, Kennedy Space Center, FL, 32899, william.e.larson@nasa.gov.

Introduction: The ability to extract and utilize resources at the site of exploration, known as In-Situ Resource Utilization or ISRU, can significantly reduce the launch mass and cost of robotic and human exploration missions while also reducing risk if properly considered early in the mission development phase. Based on resource data from the Apollo missions, NASA has focused to date on the extraction of oxygen, metals, and solar wind volatiles. Oxygen can be utilized for propulsion and life support, metals can be used for fabrication of spare parts, and solar wind implanted volatiles can supplement propellant and life support consumable production activities. The Lunar Prospector and Clementine missions of the '90's brought to light the existence of higher concentrations of hydrogen-bearing materials (possibly water/ice) at the lunar poles. However, these resources have not been readily considered in human exploration plans due to the uncertainty in the form and distribution of these resources as well as the terrain and environment in which these resources would be found. Recent findings from the Chandrayaan-1, Lunar Reconnaissance Orbiter (LRO), and Lunar Crater Observation and Sensing Satellite (LCROSS) missions have provided greater understanding of the resources, environment, and terrain at the polar regions of the Moon to the extent that new possibilities on harnessing and utilizing these resources can be pursued.

Recent Lunar Resource Findings [1]: The Moon Mineralogy Mapper (M3) instrument on Chandrayaan found that hydroxyls/water at concentrations up to 1% are possible on the surface of the Moon in the polar region, but that this is transitory. The neutron spectrometer, radiometer, and laser altimeter on the LRO satellite has provided information on hydrogen concentrations, surface temperatures, and surface topography such that locations that have high concentrations of hydrogen, have long periods of cold temperature near sunlit regions, and have reasonable terrain for roving and direct communication to Earth are possible. The mini-SAR on LRO has identified areas of potential ice sheets in permanently shadowed craters. Lastly and most importantly, the LCROSS mission identified large amounts of volatiles in the regolith in Cabeus crater (up to 20% by mass) with large concentrations of carbon monoxide, water, and hydrogen, and lower concentrations of ammonia, hydrogen sulfide, carbon dioxide, and other hydrocarbons such as methane, ethane, and methanol.

Impact on Recent Findings on ISRU: The volatiles found at the lunar poles opens up resource extraction and production possibilities that had not previously been considered in defining lunar exploration architectures. The ability to readily acquire water/hydrogen on the Moon can significantly impact transportation and life support system development and deployment by enabling reusable landers/hoppers and cis-lunar transportation systems, reducing the complexity of life support systems, providing radiation shielding, and enabling large scale food production. However, the other volatiles found by LCROSS are equally important. Ammonia can be used as a coolant for thermal control systems, as a fuel for electric propulsion and fuel cell applications, and the production of fertilizers. Carbon monoxide/dioxide and hydrocarbon volatiles can provide a ready source of carbon for fuel, plastic, and food precursor production.

The first step in incorporating these newly identified polar volatiles into future human missions is to perform surface prospecting to not only identify the form, concentration, and distribution of these volatiles, but also to determine the amount of energy to excavate and extract the volatiles and better understand the environment in which future ISRU systems must operation. A joint exploration/science mission to 'ground truth' the volatiles at the lunar poles while providing the engineering data to design subsequent mission hardware is highly recommended. While work proceeds on developing a resource prospecting experiment, further work on excavation, regolith heating, and volatile collection and separation must be pursued. To date, work on these technologies has assumed operation in sunlit areas for oxygen extraction from regolith, so design and material considerations for colder conditions and potentially harder/bound regolith must be considered. The large fraction of water/ice in the regolith opens up possibilities of utilizing microwave heating devices, and while power beaming is much less efficient than other forms of power generation and storage, it may make long-term operation in shadowed regions practical in comparison to other power system options.

References: [1] Information obtained directly from Dr Rick Elphic, Dr. Larry Taylor, Dr. Tony Colprete, and Dr. Paul Spudis.

DEFINITION OF THE LEND-DERIVED CONTOURS OF NEUTRON SUPPRESSED REGION IN CABEUS CRATER. A. Sanin[1], I. Mitrofanov[1], W. Boynton[3], D. Golovin[1], L. Evans[4], K. Harshman[3], A. Kozyrev[1], M. Litvak[1], A. Malakhov[1], T. McClanahan[8], G. Milikh[2], M. Mokrousov[1], R. Sagdeev[2], V. Shevchenko[5], V. Schvetsov[6], R. Starr[7], J. Trombka[8], A. Vostrukhin[1], [1]Space Research Institute, RAS, Moscow, 117997, Russia, sanin@mx.iki.rssi.ru ; [2]University of Maryland, Collage Park, USA; [3]University of Arizona, Tucson, AZ 85721, USA; [4]Computer Science Corporation, Washington, USA; [5]Sternberg Astronomical Institute, Moscow, Russia; [6]Joint Institute of Nuclear Research, Dubna, Russia; [7]Catholic University, Washington, DC 20064, USA; [8]Goddard Space Flight Center, Greenbelt, USA

Introduction: The Lunar Exploration Neutron Detector (LEND) instrument is designed to perform orbital mapping of Moon neutron flux in wide energy range [1]. The primary goal of the LEND experiment is to search of enhanced content of hydrogen in circumpolar regions of Moon. Here we are describing a search for contours of Neutron Suppressed Region (NSR) in Cabeus crater. The NSR is a region with deficiency of epithermal neutron flux from regolith which associated with high Hydrogen abundance in subsurface.

Scientific background: High energy protons and nuclei of cosmic rays collide with nuclei in regolith within a depth of first meters and produce secondary neutrons with high energies. Neutrons diffuse in the subsurface colliding with soil nuclei until they leak from the surface, or are absorbed due to capture reaction, or decay due to finite life time. The energy spectrum of leaking neutrons depends on the soil composition and, mostly, on the content of hydrogen, because H nuclei are the best neutron moderators.

The LEND onboard the NASA LRO mission have spatial resolution up to 10 km from 50 km orbit. To find water-rich region at lunar circumpolar regions one may suggest at least two methods of LEND neutron data analysis: 1) analysis based on PSR contours known from lunar topography data and 2) analysis based on neutron only data. Here we will presenting the second method.

The boundaries of LEND-defined NSRs are determined from the neutron measurement data only, because there is no *a priori* information to facilitate its definition. Contours for iso-neutron-suppression are determined from the smoothed map (Figure 1) in order to remove the small-scale noise due to local statistical fluctuations. The counting rate statistic for the area inside each of the contours is determined from the raw instrument counts, i.e. *without smoothing*. The difference between the neutron counting rate for the areas inside the contours and the reference belt at the same latitude is shown in Figure 2. Two types of contours may be selected: 1) a contour with most significant epithermal neutron suppression in comparison with the reference belt (the primary boundary of NSR) and 2) a contour represented the deepest part of the NSR, i.e. strongest suppression in neutron counts associated with the area inside.

This method of NSR searching may be used with neutron map with different smoothing parameters to be able to find a most confident area and an area with most suppressed epithermal neutron flux.

References: [1] Mitrofanov I.G. et al. (2008) *Astrobiology*, 8, 4, 793–804. [2] M. T. Zuber et al., *Space Sci. Rev*. 150, 63 (2010).

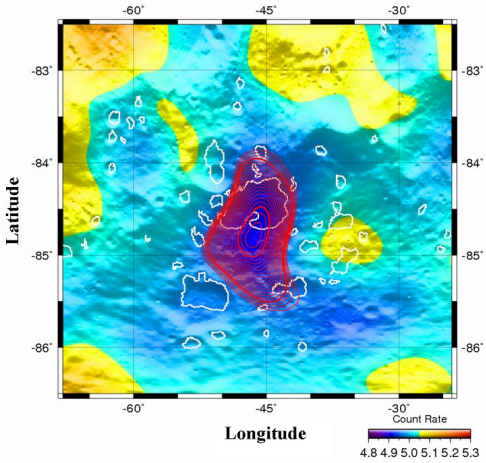

Figire 1. Iso-neutron-suppression contours for NSR within *Cabeus*. Bold lines correspond to contours with highest H concentration and most significant epithermal neutron suppression. White contours for PSRs determined from the LOLA topography data [2].

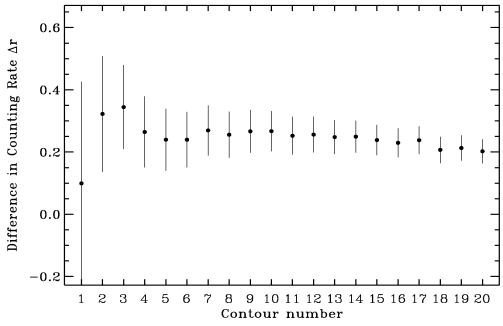

Figure 2. Suppression of epithermal neutron flux at the NSR within *Cabeus* is shown as the difference in counting rate Δr at the area of reference latitude belt and area inside the successive contours.

Formation of OH/H_2O by 1 keV Proton Irradiation of Apollo 16 Lunar Highland Soil. M.J. Schaible, C.A. Dukes, E. H. Mitchell, and R.A. Baragiola, Laboratory for Atomic and Space Physics, University of Virginia, Charlottesville, VA 22904. E-mails: ms5vf@virginia.edu, cdukes@virginia.edu, emma.mitchell@virginia.edu, raul@virginia.edu

Introduction: The question of whether water exists on or within the Moon has long been debated. Though early measurements of returned lunar soil suggested a virtually anhydrous planetary surface [1], near-infrared spectroscopy measurements by three separate spacecraft showed a broad absorption band near 3 μm, attributable to the OH stretch absorption of water, at or near the lunar surface [2-4]. The absorption is present across the entire lunar surface and is stronger toward the lunar poles. Water or ice in the polar regions is substantiated by observation of a water vapor plume during the LCROSS mission [5].

The apparent ubiquitous nature of OH/H_2O is surprising since there are many mechanisms (sputtering and impact vaporization) that can remove surficial water, but few clear mechanisms for replenishment. One formation mechanism, indicated by the relatively global spatial distribution of the OH signal, follows the interaction of the solar wind protons with oxides in the lunar soil. Low energy protons impact the surface penetrating up to ~50 nm, breaking bonds and implanting hydrogen which subsequently may be combined with nearby oxygen atoms to form hydroxyl or water.

Previous experiments investgating the formation of water products by 1 keV hydrogen irradiation on terrestrial ilmenite and anorthite gave null results for OH/H2O [6]. We continue these studies, and report here findings for H^+ irradiation of lunar highland soils.

Experiment: To test the solar wind hypothesis, experiments are performed in an ultrahigh vacuum chamber pumped to a base pressure of $< 5x10^{-9}$ Torr. Lunar highland soil samples of varying maturity (65901, 61241) are mounted onto a copper platen, outgassed by heating,. The samples are first analysed with X-ray photoelectron spectrsocopy (XPS) to determine their surface composition and chemistry, then characterized with vis-NIR diffuse reflectance. The samples are then irradiated using rastered 1 keV hydrogen ions to fluences in the range: 10^{14} - 10^{19} H^+ cm^{-2}. During irradiation, the sputtered ion flux is monitored with a secondary ion mass spectrometer (SIMS).

The lunar soil is again characterized with XPS after irradiation to monitor changes to the O 1s peak. *In situ* diffuse reflectance of the soil measures changes in the 2.8 - 3.0 μm region, indicating the production of hydrous species. After a final irradiation at 10^{19} H^+ cm^{-2}, we observe the OH/H_2O content of the surface layers of the soil through the ion penetration depth by sputtering the altered layers and monitoring ions via SIMS. This technique will allow us to identify the composition of outermost surface of the lunar grains and to measure the sputter removal of OH/H_2O as a function of depth with near monolayer resolution.

A second chamber is being used to analyze lunar thin sections in vis-NIR transmittance. For these experiments we will use 30-μm sections of lunar highland rocks. In situ diffuse reflectance measurements can then be correlated to the transmission spectra for the 0.7 - 8 micron range to ascertain that the IR sampling depth exceeds the maximum H^+ penetration depth (~50 nm). Ions ejected from the lunar material during and after H^+ bombardment are monitored with SIMS.

Discussion: Previous experiments with terrestrial anorthosite and ilmenite provide an upper limit of 0.1% band depth in the OH spectral region after saturation fluences [6]. These results are consistent with the EPOXI observations by Sunshine et al. that show OH/H_2O water depletion during the lunar day, as the solar wind sputter removes adsorbed water that redeposits during lunar evening/night [4], and supported by laboratory measurements by Gruen et al. [7] for 15 keV protons on sapphire. However, studies have found significant (~60%) differences in the rate of surface change in the irradiation of powders and thin sections [8]. In fact, recent data on lunar soil powders have shown positive results for the production of OH/H_2O after hydrogen ion irradiation [9] but such measurements need to be repeated in ultrahigh vacuum and with mass analyzed ions. In any case, we expect measurements on lunar powder to enhance sputter redeposition and reduce the rate of oxygen loss. A comparision of O-H band depth change after proton bombardment will be compared with the 3-14% enhancement observed by spacecraft measurements.

This work was supported by NASA Cosmochemistry and a NASA NESSF fellowship to MJS.

References: [1] Taylor, L.A. et al (1995) *LPSC* XXVI, 1399. [2] Clark R.N. (2009) *Science*, 326, 562. [3] Pieters C.M. et al. (2009) *Science*, 326, 568. [4] Sunshine J.M. et al. (2009) *Science*, 326, 565. [5] Colapetre, A. et al. (2010) *Science* 220, 463. [6] Burke, D. et al. (2011) *Icarus*, 211, 1082. [7] Gruen, D.M. et al. (1976) *J. Chem. Phys.* 65**,** 363. [8] Loeffler, M.J. et al. (2009) JGR, **114,** E03003. [9] Ichimura, S. et al. (2011) LPSC 41, 2724.

DELAYED RELEASE AND DELIVERY OF VOLATILES TO POLAR RESERVOIRS. P.H. Schultz, Brown University, Geological Sciences, 324 Brook St., Box 1846, Providence RI, 02912-1846 (peter_schultz@brown.edu)

Introduction: Recent missions demonstrate that volatiles (OH, H_2O) cling to the lunar regolith grains [1,2,3], especially near the poles [4,5,6] along with other mobilized species such as CO, CO_2, Cl, N, and S [7,8]. Mechanisms for delivering these volatiles include: solar wind implantation or replacement [9,10]; collisions by volatile-rich asteroids and comets [e.g., 10,11]; and trapping within the impact glasses [12].

Background: The LCROSS impact also excavated a wide variety of elements stored at South Pole, including Na [7,13] as well as Hg, Au, Mn, Si, P, Zn, Fe [8], and Ag [7]. Consequently, highly volatile elements and compounds are not the only components trapped near the poles. These additional components could have come from trapped "old" components that date from the last stages of lunar volcanism or from recent degassing events [e.g., 14]. Or they represent impact-released migrants. Here we explore one mechanism that could temporarily store and release volatile elements/compounds at small scales (by impact-injection into the regolith) and at large scales (by release from gases trapped in impact melts).

Laboratory Experiments: At the NASA Ames Vertical Gun Range, quarter-space experiments allow looking inside a hypervelocity impact crater. High-speed spectrometers probe emission lines created by impact-generated vapor while high-speed cameras capture the evolving phenomenology. Quartz fibers from four separate telescopes (2.5cm field of view) are connected to one of two 0.35m spectrometer. Dolomite targets provide a surrogate target in order to interpret processes created by much higher speed impacts into silicate targets.

During the first 50µs, disassociation products (Ca, C_2, and Mg) dominate the spectral emissions (**Fig. 1**). Disassociation products (CaO and CO) represent minor constituents at early times (first 5µs) but dominate the signal later. The greatest intensities occur above, while vapor within the crater cavity ("below") fills the growing cavity.

The relative intensities of calcium lines change depending on time and location, reflecting contrasting temperatures in a non-uniform vapor plume. Above the surface, the 615.6nm Ca emission line corresponds to a low-T component directed uprange. This low-T component also means a low thermal expansion speed

Discussion: Impact-generated vapor exhibits a wide range of conditions depending on location. Below, low-temperature vapor fills the transient cavity, indicating that a component will be injected between (or condensed on) regolith grains. Above, free expansion of high-T vapor exceeds escape speeds.

Consequently, small impacts into in the regolith could temporarily retain traces of both high-T and low-T byproducts trapped below the crater floor or wall. This process also occurs for impactor components. For example, even high-angle impacts (60°) by glass spheres (0.635cm) into solid copper and basalt targets leave behind intact fragments as large as 200µm (some retaining the surface projectile surface). The much higher impact speeds on the Moon will generate higher temperature vapor; nevertheless, the process of injecting, depositing, and retaining low-T products still applies. Consequently, volatiles should be temporarily stored beneath small (<1m) craters in the regolith. Thermal cycles (as well as impact gardening) later release these components gradually with a much lower kinetic temperature, enabling trapping at the poles.

Implications: Release of regolith-stored volatiles from small impacts (and from cooling melts within large, recent craters) represents reservoirs that gradually supply volatiles to polar cold traps. Such a process would offset losses such as impact gardening.

References: [1] Sunshine, J. M. *et al.* (2009), *Science*, **326**, 565-568; [2] Pieters *et al.* (2009), *Science*, **326**, 568-572; [3] Clark, R. N. (2009), *Science*, **326**, 562-564; [4] Spudis, P.D. *et al.* (2010) *GRL*, **37**, L06204, doi: 10.1029/2009GL042259. [5] Bussey, D. B. J. *et al.*, *LPSC 42*, no. 2086; [6] A. Colaprete *et al.* (2010), *Science*, **330**, 463-468; [7] Schultz, P. H. *et al.* (2010), *Science,* **330**, 468-472; [8] Gladstone, R. *et al.* (2010)*, Science*, **330**, 472-476; [9] Stern, A. (1999), *Revs. of Geophys.*, **37**, 453-491; [10] Potter, A. E., Morgan, T. H. (1988), *Science*, **241**, 675-680; [11] Ong, E. *et al.* (2009), *Icarus*, **207**, 578; [12] Harris *et al.*, R. S. (2007), *LPI Contrib. No. 1360*, abstract # 8051; [13] Killen *et al.*, GRL, 37, L23201; [14] P. H. Schultz *et al.* (2006), *Nature,* **444**,184-186.

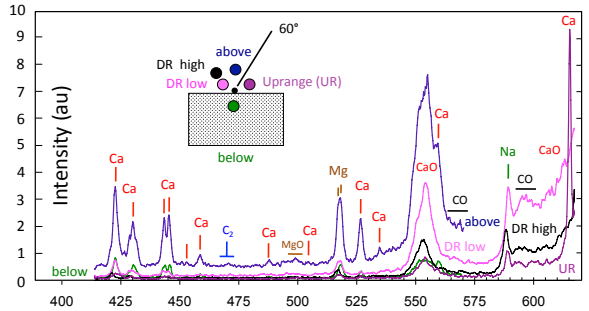

Figure 1: Emission lines created by excited species during the first 50µs within the vapor plume (1/4" Pyrex at 5.72km/s). Different colors correspond to different fields of view (~2.5cm). Note the "cool" (Ca, 615.6nm) line that dominates the uprange vapor component. Intensities are in arbitrary units.

A Consortium to Study "Special" Lunar Samples. Exploring Volatile Reservoirs on the Moon Now and Preparing for Future Lunar Exploration. C.K. Shearer[1] and C.R. Neal[2], [1]Institute of Meteoritics and Department of Earth and Planetary Sciences, University of New Mexico, Albuquerque, New Mexico 87131 (cshearer@unm.edu. [2]University of Notre Dame, Notre Dame, Indiana. 46556.

Introduction: The results from a variety of recent lunar missions carried out by NASA and other national space agencies and numerous terrestrial laboratory studies have demonstrated that a high priority for future lunar exploration will be the collection of lunar samples that potentially contain a record of volatile reservoirs on the Moon. These volatile reservoirs could be a high value resource for future human exploration and eventual colonization and reduce the launch mass from the Earth to the lunar surface. The preservation of this volatile record during collection, transport, and curation is a high science and engineering priority for lunar surface activities [i.e. 1-4]. Numerous lessons learned from the Apollo Program and extracted from Apollo samples may be directly applicable to the future return of lunar samples. Samples were returned to Earth in several different sample containers. A catalog of Apollo lunar surface geological sampling tools and containers has been prepared [5]. The different sample containers were designed for specific purposes although their success was variable. The Apollo Lunar Sample Return Container (ALSRC or rock box) was an aluminum box with a triple seal. Two ALSRCs were used on each Apollo mission. Two 4-cm drive tube core samples were sealed in a Core Sample Vacuum Container (CSVC) on the Apollo 16 and Apollo 17 missions. Special Environmental Sample Container (SESC) was designed to ensure that samples were not exposed to terrestrial atmosphere or spacecraft cabin gases. They were used on all of the Apollo missions. The Gas Analysis Sample Container (GASC) was designed to hold a small amount of lunar soil within a large volume. The GASC was used only on the Apollo 11 and 12 missions. Most samples were stored under conditions selected to limit contamination and best preserve their integrity [6]. As noted earlier, the volatile element record in these samples were disturbed to varying degrees. However, a subset of samples was stored under significantly different conditions for over 38 years (i.e. freezer samples, stored in vacuum or He) and these samples may provide insights for future sample collection. A detailed discussion of these special samples is provided by Lofgren [7]. These uniquely collected, stored, and curated lunar samples are very relevant to both current missions and future sampling of lunar volatiles as they potentially preserve lunar characteristics no longer present in most of the Apollo Program collection and illustrate alternative approaches to sampling lunar materials. The purpose of this abstract is to (1) identify potential science and engineering studies that could be conducted in a consortium framework, (2) illustrate pathways for studying these valuable samples and (3) engage the community's interest in participating in such a consortium study.

Consortium studies:

Science goals. The first goal is to evaluate the nature of the samples to see if they are (relatively) uncompromised. If they are, a large number of measurements may be made that will provide a better understanding of volatiles on the lunar surface. For example: (1) gas composition in the container head space (that could be a mixture of both captured exosphere and released from sample); (2) solar wind volatile species that are weakly bound to mineral surfaces; (3) volatile species in the lunar regolith that have limited terrestrial contamination; (4) other environmentally sensitive or fragile surface coatings on mineral and glass surfaces.

Engineering goals. These goals are to gain an understanding of what types of sample containers will preserve environmentally sensitive lunar samples. Establishing sampling protocol and designing sample containers feeds forward to exploring other planetary bodies (NEOs, Mars). We envisage that such understanding will also aid in the development of cryogenic sample collection and storage. If these Apollo sample containers are compromised, several of science goals and all of the engineering goals may still be accomplished.

Access to samples for consortium studies: Any consortium assembled to study these special samples will be required to provide a well-defined science and engineering rationale for the study of these rare and valuable samples. A consortium study must define sample handling-processing protocols that will not compromise samples and define a logical sequence for conducting analyses-experiments. For example, analyses of gas from the containers and curation and documentation of container contents must occur before the allocation and analysis of solid samples.

References: [1] Jolliff et al. (2007) LEAG Workshop on Enabling Exploration. Abst.# 3056. [2] Neal et al., (2007) LEAG Workshop on Enabling Exploration. Abst.# 2109. [3] Committee on the Scientific Context for Exploration of the Moon, National Research Council (2008) 97pp [4] OSEWG (2009) Unpublished NASA whitepaper NP-2009-00-00-HQ, 58pp. [5] Alton (1989) JSC-23454 97pp. [6] Heiken et al., (1991)) Lunar Source Book. Cambridge Press, New York, 736pp. [7] Lofgren (2011) abstracts for this meeting.

Chlorine isotope composition of "rusty rock" 66095 and Apollo 16 soil. Implications for volatile element behavior on the Moon. C.K. Shearer[1,2], and Z.D. Sharp[2] . [1] Institute of Meteoritics, Department of Earth and Planetary Sciences, University of New Mexico. Albuquerque, New Mexico 87131 (cshearer@unm.edu), [2] Department of Earth and Planetary Sciences, University of New Mexico. Albuquerque, New Mexico 87131.

Introduction: "Rusty Rock" 66095 has yielded significant confusion concerning its origin, yet it has and will continue to reveal significant insights into the behavior of volatiles on the Moon. Most of 66095 is composed of a fine-grained, subophitic to ophitic impact melt-rock, which also contains a wide variety of lithic clasts [1,2]. Alteration is found in the interior as well as on the surface of 66095. A brownish alteration extends from margins of metallic iron grains into the adjacent silicates and consists of a variety of relatively low-temperature minerals [1-6]. The origin of this alteration and hydrogen and oxygen isotopic signatures have been attributed to alteration on the Moon [7,8] to "terrestrial" alteration during or following transport to Earth [4,9]. Recent observation by Moon Mineralogy Mapper (M^3) on the Chandrayaan-1 spacecraft indicating the existence of H species on the lunar surface [10] could be interpreted as indicating the alteration is lunar in origin. Another interesting aspect of 66095 is its enrichment in ^{204}Pb, Cd, Bi, Br, I, Ge, Sb, Tl, Zn, and Cl indicating that portions of this sample contain substantial sublimates [e.g.11-15]. The origins of these enrichments have been attributed to fumarolic-hydrothermal [15], magmatic, or impact processes [12,13]. Here, we examine the Cl isotope composition of 66095 and selected regolith at the Apollo 16 site to gain additional insights into the transport of volatiles in the lunar crust and on the lunar surface.

Cl isotopes and the Moon: Sharp et al [16] observed that unlike the Earth and most other materials in the solar system, samples from the Moon exhibited an extremely wide range of δ^{37}S (Where δ^{37}Cl = (R_{sample}/$R_{standard}$ - 1)1000 and R = ^{37}Cl/^{35}Cl. All data are reported relative to SMOC (Standard Mean Ocean Chloride) with a δ^{37}Cl value of 0‰). They concluded that the bulk Moon had a δ^{37}S that was similar to Earth (~ 0 ‰) and that the wide variation of δ^{37}Cl (-0.7 to 24.5‰) was produced by volatilization of metal halides during the eruption of low H basalts.

Cl isotope composition of 66095 and A16 soils: In addition to mare and KREEP basalts, Sharp et al [16] also analyzed sample 66095 and select A16 soils. The A16 soils that were analyzed included mature soil 64501,232 (maturity index I_s/FeO=61) and immature soil 61220,39 (maturity index I_s/FeO=9.2). In these samples, there is a substantial correlation between Cl and Zn, Cd. In 66095, the leachate had a Cl isotope composition of +14.0‰, whereas the non-leachable Cl has a composition of +15.6‰. The leachate from mature soil (64501) had a Cl isotope composition of +5.6‰ and a non-leachable Cl composition of +15.7‰. The immature soil has a similar Cl isotope composition with the leachate with a Cl isotope composition of +6.1‰ and the non-leachable Cl composition of +14.3‰. Like all the other lunar lithologies analyzed by Sharp et al. [16], the leachates have a lower δ^{37}Cl than the non-leachable Cl. There is no apparent correlation between δ^{37}Cl and other stable isotopic measurements (e.g. δ^{34}S, δ^{13}C).

Discussion: Although coming from different lunar environments, samples that exhibit mobility of elements in the shallow lunar crust (sulfide replacement of magmatic silicates) or at the lunar surface (pyroclastic deposits, rusty rock) have common attributes in that they exhibit similar enrichments of Cl and calcophile elements (e.g. Zn, Cu, Se, Sb) and fractionation of both Cl and S isotopes from bulk Moon. All of these processes have a common link: the vapor phases that are responsible for elemental mobility and isotopic fractionation are relatively low in water. In the case of rusty rock 66095, these enrichments and fractionations may be a product of fumarolic activity. The few Apollo 16 soil samples analyzed by Sharp et al [16] may have a Cl component derived from "rusty rock" lithologies. The Cl isotopic fractionation observed in these soils is not a product of different degrees of soil maturity.

References: [1] Garrison and Taylor (1980) In Proc. Conf. Lunar Highland Crust (ed. Papike and Merrill). 395-417. GCA Supp. 12, Lunar Planetary Institute, Houston. [2] Hunter and Taylor (1981) *Proc. 12th Lunar Planet. Sci. Conf.* 253-259. [3] Hunter and Taylor (1981) *Proc. 12th Lunar Planet. Sci. Conf.* 261-280. [4] Taylor et al. (1974) *Geology* **2**, 429-432. [5] El Goresy et al. (1973) *Proc. 4th Lunar Sci. Conf.* 733-750. [6] Taylor et al. (1973) *Proc. 4th Lunar Sci. Conf.* 829-839. [7] Freidman et al. (1974) *Science* **185,** 346-349. [8] Lunar Sample Compendium. http://curator.jsc.nasa.gov/ lunar/lsc/66095.pdf. [9] Epstein and Taylor (1974) *Proc. 5th Lunar Sci. Conf.* 1839-1854. [10] Pieters et al. (2009) Science 326, 568-572. [11] Nunes and Tatsumoto (1973) Science 182, 916-920. [12] Allen et al. (1973) *Proc. 6th Lunar Sci. Conf*. 2271-2279. [13] Hughes et al. (1973) Lunar Sci. IV 400-402. [14] Jovanovic and Reed (1981) P*roc. 12th Lunar and Planet. Sci. Conf*. 2271-2279. [15] Krahenbuhl et al. (1973) *Proc. 4th Lunar Sci. Conf.* 1325-1348. [16] Sharp et al. (2010) Science 329, 1050-1053.

Volatile element transport in the lunar crust. C.K. Shearer[1], P.V. Burger[1], Y. Guan[2], J.J. Papike[1], and S.R. Sutton [3], [1]Institute of Meteoritics and Department of Earth and Planetary Sciences, University of New Mexico, Albuquerque, New Mexico 87131 (cshearer@unm.edu), [2]Division of Geological and Planetary Sciences, California Institute of Technology, Pasadena, California 91125, [3] Department of Geophysical Science and Center for Advanced Radiation Sources, University of Chicago, Chicago, Illinois 60637.

Introduction: The existence of troilite fracture-fillings, veins and intergrowths with low-Ca pyroxene in plutonic rock clasts from a variety of lunar breccias implies that elements have been mobilized in the lunar crust [1-4]. Numerous studies have speculated on the composition and source of these fluids, their capability for the transport of vapor-mobilized elements, and the scale and environment under which these types of process occurred [3,5-8]. These models all assumed a Moon with a very dry mantle, crust, and surface. However recently this assumption has been questioned and the role of H_2O in lunar processes has been investigated. Combining more traditional petrologic analytical approaches (optical microscopy, electron microprobe) with relatively newer instrumental approaches (Nano SIMS, Synchrotron X-ray Microprobe Analysis), we have reexamined these troilite veins and replacement textures in lunar samples to (1) differentiate among transport models proposed by previous studies [3,5-8], (2) examine the potential for the involvement of indigenous (magmatic) or exogenous (solar wind, cometary) H (or OH, H_2O) in these types of models, (3) identify potential sources for the S and heat responsible for driving elemental migration, and (4) identify the potential scale of these processes and the environment under which they occurred. These inquires may provide a clearer understanding of volatile element transport in the lunar crust, and the composition of such volatiles.

Results: Lunar samples 67016,294, 67915,150, and 67016,297 represent clasts of Mg-suite and ferroan anorthosite lithologies that have interacted with a S-rich vapor. The olivine in these lithologies is partially to totally replaced by troilite and low-Ca pyroxene. The troilite makes up 30 to 54 volume % of the troilite + low-Ca pyroxene pseudomorphs after olivine. Other silicates in the assemblages have experienced post-magmatic, pre-sulfurization reequilibration (pyroxene exsolution, recrystallization) and were not affected by the introduction of S. The troilite also occurs in veins cross-cutting individual phases and metamorphic textures. The sulfide veining and replacement features are restricted to individual clasts and do not cut across the matrix surrounding the clasts, and thus predates the breccia-forming event. The proportion of troilite to low-Ca pyroxene and silicate chemistries indicate that simple reactions (such as olivine + $S_2 \leftrightarrow$ low-Ca pyroxene + troilite + O_2) do not adequately represent the replacement process. The sulfides exhibit some compositional variation and exhibit limited exsolution features. The sulfides have compositions that are similar to those found in mare basalts [9]. In particular, the sulfides generally are enriched in Co relative to Ni. The sulfur isotopic composition of the vein and replacement troilite ranges from approximately δS^{34}= -4.0 to -8.0 ‰. Spinels in all clasts exhibit "exsolution" of ilmenite suggestive of post-crystallization reduction that appears to be contemporaneous with the sulfurization event.

Discussion: Based on our observations, it appears that the model suggested by Norman et al. [3] is the most appropriate for the origin of the troilite veining and troilite-pyroxene pseudomorphs after olivine. Our data and interpretations add significant definition to this proposed model. Interpretation of pyroxene exsolution indicates this process occurs in the relatively shallow lunar crust on a scale that involves vapor interaction with multiple plutonic lithologies of various ages and compositions. These reactions occur at distinct conditions of f_{S2}, f_{O2}, and temperature. The reacting vapor is S-rich, and low in H. The reduction of the oxides in the clasts was not a product of H-streaming as has been suggested for similar textures in lunar rocks, but more likely related to "S-streaming". These vapors had the capability to transport other elements such as Fe and minor chalcophile-siderophile elements. The heat source driving the transport of elements is closely tied to the emplacement of magmas into the shallow lunar crust. The fluids were most likely derived from indigenous sources (magmatic) and do not appear to have exogenous components. The process that drove the derivation of the S-rich volatiles from these intrusions was also instrumental in fractionating the isotopic composition of S from 0‰ in the magmas to -5‰ in the vapor phase. This fractionation was not controlled by the proportions of SO_2^{-2} to H_2S, but more likely COS, S_2 and CS_2 species.

References: [1] Roedder and Weiblen (1974) Proc. of the 5th LSC, 303-318. [2] Norman et al. (1981) Proc. 12th LPSC, 235-252. [3] Norman et al. (1995) GCA 59, 831-847. [4] Lindstrom and Salpas (1983) JGR 88 (Suppl.), A671-A683. [5] El Goresy et al. (1973) EPSL 18, 411-419. [6] Haskin and Warren (1991) Lunar Chemistry. Lunar Source Book (eds. Heiken, Vaniman, and French) 357-474. [7] Colson (1992) Proc. 22nd LPSC, 427-436. [8] Haskin et al. (1993) In Resources of Near-Earth Space (ed. J.S. Lewis, M.S. Matthews and M. L. Guerrieri) Univ. of Arizona Press, Tucson, AZ, pp. 17-50. [9] Papike et al. (2011) Am. Min. In press.

LUNAR POLAR ICE AND THE OBLIQUITY HISTORY OF THE MOON. M.A.. Siegler[1] B.G. Bills[2] D.A. Paige[1], [1]UCLA Dept. of Earth and Planetary Sciences, Los Angeles, CA, 90095 (siegler@ucla.edu), [2]NASA Jet Propulsion Laboratory, Pasadena, CA, 91109

Abstract: Water ice is currently stable in shadowed environments near the lunar poles. This however has not always been true. Roughly halfway through its outward migration (due to tidal interaction with the Earth) the Moon was tilted (currently 1.5^o) up to 83^o with respect to the ecliptic. During this time, illuminated polar craters would have been far to warm (up to 380K) to preserve water ice [1].

This extreme change in insolation is a result of a spin-orbit configuration, within which the Moon currently resides, known as a Cassini state. A Cassini state results from dissipation within the satellite and drives the spin axis of the satellite to precess at the same angular rate as its orbit. As spin precession is controlled by the satellite moments of inertia and orbit precession by its semimajor axis, the satellite is driven into an obliquity that will cause their angular rates to sychonize [2].

According to theory, when the lunar semimajor axis measured roughly 30 Earth radii (currently 60.2) it transitioned between two stable Cassini states, reaching very high obliquities (~77^o) [1,3]. Since that time (roughly 2.5-3.5 Bya) the obliquity has slowly decrease (to the current 6.7^o), causing each currently shadowed crater to go through a period of partial illumination.

During these periods, water molecules reaching such regions of the lunar surface may have been in the right temperature range to be considered stable, but mobile. This is important as lack of current surface ice deposits in polar craters imply that some mechanism of burial is required to preserve ice before it is lost to surface processes. When in the right temperature range, ice may be stable in the near subsurface, but mobile enough to be driven downward by diffusion along thermal gradients at a faster rate than it is lost.

When a given environment was in this "icetrap" temperature regime, generally between 95 and 150K (depending on supply rates and temperature amplitudes), ice had a better chance to be preserved by burial via thermal diffusion processes than any time before or since. Once a shaded environment cools below roughly 90K, thermal diffusion processes can be considered negligible and only burial by impact gardening [4, 5] has been proposed as a viable mode of ice preservation.

We examine the thermal environments resulting from the slow orbital evolution since the Cassini State transition. With new topographic thermal models produced in association with the Diviner Lunar Radiometer [6], we can examine how changing insolation impacted temperatures at specific locations near the lunar poles. These models have been shown to accurately reproduce current surface temperatures and can be extracted to depth based on past subsurface temperature measurements [7].

Given an assumed supply and loss rate, one can then model how specific locations would have gained or lost subsurface ice by vapor diffusion [8,9]. Such modeling has proven to accurately reproduce ground ice distribution on Mars [10] and differs here only in that past supply rate of water molecules to the surface is unknown. However, given the reasonable assumption that the supply rate of volitiles was higher in the past [11] and the fact that more of icetrap regions existed at higher obliquties this appears to be a viable mode to deliver ice in the quantities observed on the Moon today [12, 13].

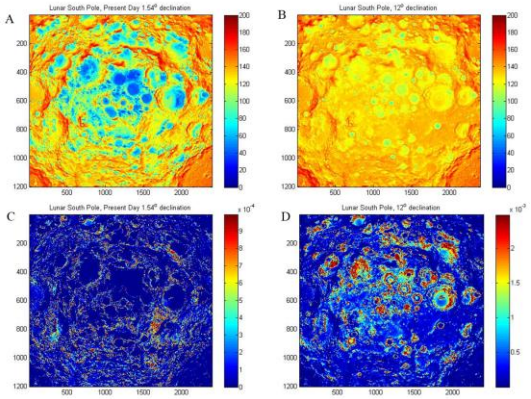

Figure 1: (A) Mean annual temperature in the current (1.54^o tilt) lunar south polar region (stretched 0-200K), (B) Mean annual temperatures at 12^o tilt, (C) Modeled ice mass (kg m^{-2} yr^{-1}) gained at 1.54^o assuming simple model [8], (D) Modeled ice mass (kg m^{-2} yr^{-1}) gained at 12^o.

References:

[1] Siegler, M.A., Bills, B.G., Paige, D.A.(2011) JGR in Press, April. [2] Peale S.J.(1969) Astronomical Journal 74, 483-489. [3] Ward ,W.R. (1975) Science 189, 377-379.[4] Crider,D.H. and Vondrak R.R (2003a) JGR,108(E7).[5] Crider,D.H.and Vondrak R.R (2003b) JGR 108(E7). [6] Paige,D.A.et al. (2010) Science, 330 (6003), 479-482.[7] Langseth,M.G., Keihm,S.J.,Peters,K.(1976) 7th LPSC, 3143-3171.[8] Schorghofer, N. and Taylor,G.J. (2007)JGR 112, E02010.[9] Schorghofer,N. (2010) Icarus 208, 598-607.[10] Schorghofer, N., Aharonson, O., (2005) JGR 110 (E5), E05003.[11] Chyba,C.F. (1990)Nature, 837 343, 129-133.[12] FeldmanW.C. et al. (2001) JGR 106(E10), 23231-23251.[13] Coleprete, A (2010) Science, 330 (6003), 463-468.

MICROCOMETS AS A POSSIBLE SOURCE OF ORIGIN OF THE SURFACE WATER AND HYDROXYL LAYER ON THE MOON. M. P. Sinitsyn[1] [1] Moscow State University, Sternberg Astronomical Institute ,13 Universitetsky prospect,Moscow 119992,Russia (msinitsyn.sai@gmail.com).

Introduction: Currently achieved very significant preliminary results in the investigation of the origin and evolution of lunar hydrosphere. The first results of the LRO spacecraft and space experiment LCROSS, released recently in Science [1,2], provide ample material for research and analysis. Taking into account the results of previous programs [3,4,5] becomes clear very intriguing and contradictory situation. One of the striking contradictions is the different nature of the ice deposits in the northern and southern polar regions [1].

The fact that the radar onboard Chandrayan-1 is not found at the bottom of the crater Cabeus responses related to surface fragmented ice, but it found two dozen mid-sized craters in the northern polar region, with clear signs of a fresh surface of ice.

Discussion: As established by the spectrometer LEND[2], the location of high concentrations of hydrogen (a significant suppression of the flux of epithermal neutrons) beyond the area of the cold traps associated with the crater Cabeus. Similar differences between areas of high hydrogen content with the location of the cold trap is found in other craters of the southern polar region. From this it was concluded that ice lies under a layer of regolith thickness of several centimeters. Thus, in the south polar region were detected subsurface ice, lying at the depth expected in a few centimeters. At the same time, in the northern polar region revealed a fresh surface ice.

How is this possible?

It is obvious that if the reason for the formation of surface water and hydroxyl are considered the reaction of solar wind protons with the surface, then through of the process of migration [6], its distribution will occur equally to all poles. This character of the process will take place in connection with a fairly uniform formation of OH / H_2O almost everywhere across the surface of the moon. Thus, to explain the situation with a significant difference in the accumulation of water on the opposite poles rather search a source that consistently (right now) acts on the surface of the Moon. In addition, the effect of this source should be substantially anisotropic, for asymmetries in the accumulation of ice.

As pointed out Klumov and Berezhnoi[7], the collision of comets and asteroids with the Moon's surface creates temporary atmosphere, resulting in the capture probability of volatile elements cold traps is the same as in north and south polar regions. But if we assume that the size of the comet is quite small (about 10 meters), the differences in the accumulation of volatiles at different poles are possible.Therefore, in the case of pre-emptive fall microcomets in areas close to the North Pole, the formation of water ice will prevail in the northern polar region.

Unfortunately, at present, issues related to microcomets[8] poorly understood and very existence of such comets is somewhat controversial, but according to some estimates, about 100 events microcomets collision with the Earth occur annually. If we take into account the possibility of such a large collision frequency, then we can fully explain the constant replenishment of the surface layer of lunar water and hydroxyl groups. It is possible that these comets are to the same and galactic origin [9].

For a more complete confirmation of the differences in the accumulation of ice in the southern and northern polar regions is very interesting to examine the results of the neutron flux measurement device LAND also for the northern polar regions.

Acknowledgment:
The author thank A. Berezhnoi for useful comments and discussion.

References:

[1] Kerr R.A. (2010) *Science,* 330, 434.
[2] Mitrofanov I.G. et al. (2010) *Science* 330,483
[3] Pieters C.M. et al. (2009) *Science,* 326,568.
[4] Clark R.N. (2009) *Science*, 326,562.
[5] Jessica M. Sunshine et al. (2009) *Science*,326,565.
[6] Crider D.H. and Vondrak R.R. (2008) *NLSI Lunar Science Conference,* Abstract #2055.
[7] Klumov B.A., Berezhnoi A.A. (2002) , *Adv. Space Res.*,30,8, 1875-1881.
[8] Frank L.A. and Sigwarth J.B. (1993) Reviews of Geophysics (ISSN 8755-1209),31,1,1-28
[9] Crozaz G., et al.(1977), *Phil. Trans. R. Soc. Lond. A* 285, 587-592.

ANALYSIS OF HIGHLY ILLUMINATED ZONES NEAR THE LUNAR POLES. E. J. Speyerer[1] and M. S. Robinson[1], [1]School of Earth and Space Exploration, Arizona State University, Tempe, AZ (espeyerer@ser.asu.edu).

Introduction: The spin axis of the Moon is tilted by only 1.5° (compared with the Earth's 23.5°), leaving some areas near the poles in permanent shadow, while other nearby regions remain sunlit for the majority of the year. Previous studies have delimited these regions using theoretical models, Clementine images, and topography from Kaguya and LRO [1-5]. Theory, radar data, neutron measurements, and Lunar CRater Observation and Sensing Satellite (LCROSS) observations suggest that volatiles may be present in cold traps in permanently shadowed regions [6-10]. Thus, areas of near permanent illumination are prime locations for future lunar outposts due to their benign thermal conditions and near constant access to solar power [11-12].

One of the primary scientific objectives of the Lunar Reconnaissance Orbiter Camera (LROC) is to unambiguously identify regions of permanent shadow and near permanent illumination using its two imaging systems that provide medium and high-resolution views of the poles [13]. Since the start of the nominal mission, LROC has acquired over 11,000 Wide Angle Camera (WAC) images and over 6,500 Narrow Angle Camera (NAC) image pairs within 2° of the poles. We reduced a subset of these images (illumination maps, movie sequences, and high resolution maps) to delimit lighting conditions over one year. Analysis of these products reveal a region near the south pole that remain illuminated for a majority of the year (92% of the year, a 10% increase over some previous studies [1,4]).

Wide Angle Camera Products: LRO's 50-km polar orbit enables images of each pole to be acquired every ~2 hours during normal spacecraft and instrument operations (average time between WAC observations is 2.3 hours including spacecraft and instrument disturbances). This repeat coverage enables the creation of illumination movies and multi-temporal illumination maps that can be used to delimit permanently shadowed regions and permanently (or near permanently) illuminated regions [14].

Narrow Angle Camera Products: The two NACs provide high-resolution (0.7 to 1.5 m/pixel) images of select regions around the each pole. Due to the NAC's 2.85° field of view (5.7° combined) broad scale multi-temporal mapping is limited. However, during summertime months, when shadows are at a minimum, the NACs acquire 100s of images that are used to create meter scale maps of the illuminated terrain at the south pole. During the winter months, a majority of the region is in shadow, so NAC imaging is focused on previously identified illuminated peaks that stay illuminated for a majority of the year [1, 3-4]

Due to its high resolution, the NAC images can be used to validate previous illumination studies that used lower-resolution topographic models (200-500 m/pixel). NAC images revealed several cases where small regions of the surface were illuminated when previous models predicted they would be in shadow. Similarly, NAC images have also shown some regions in shadow at times in which models showed them illuminated.

South Pole Illumination Analysis: Previous studies have identified peaks around the south pole that remain illuminated for a majority of the year, including a massif (Point B) located ~10 km off the edge of Shackleton crater that is estimated to be illuminated for 82% of the year [4]. Due to the much higher resolution dataset provided by the WAC and the NAC, we can investigate in greater details these highly illuminated regions.

Currently we have not found a point near either pole that is illuminated all the time, however, we have located a 2.25 km^2 region (centered at 89.4° S, 223° E) that remains illuminated for 92% of the year, which is 10% higher than the value previous reported in studies that examined only single points in only topographic models [4]. A recent work by Mazaeico et al. [5] identifies a 240m x 240m region centered at the same location to have an average solar visibility of 92.66%. This difference maybe due to our conservative threshold values and that our accuracy will be improved with a dynamic threshold that accounts for residual scattered light in the instrument as well as scattered light off of nearby illuminated surfaces.

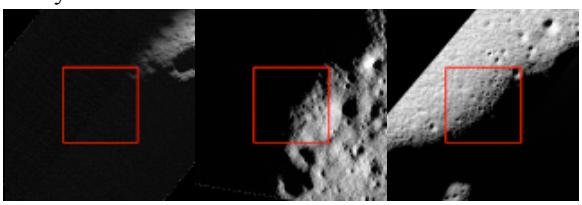

Figure 1- Detailed look at the illumination conditions of the same 2.25 km^2 region (red box centered at 89.4° S 223° E) throughout the mission using NAC images. Left to Right: M108578776, M121951177, and M112490681.

Conclusions: The Moon's slightly tilted axis provides a unique opportunity for regions near the vicinity of the pole to be permanently shadowed while other nearby regions can have extended periods of sunlight. Illumination in these regions has been previously studied with Clementine UVVIS data and topographic models from laser altimeters. LROC compliments this analysis with higher resolution data (up to meter scale) that can unambiguously identify these regions. Together, the NAC and the WAC can enhance our knowledge of the lighting conditions at the pole and provide a new dataset planning future science and exploration missions to these unique regions.

References: [1] Bussey et al. (1999) *GRL*, 26, 1187-1190. [2] Bussey et al. (2003) *GRL*, 30, 1278. [3] Noda et al. (2008) *GRL*, 35, L24203. [4] Bussey et al. (2010) *Icarus*, 208, 558-564. [5] Mazarico et al. (2010) *Icarus*, In press. [6] Watson et al. (1961) JGR, 66, 1596-1600 [7] Ingersoll et al. (1992) *Icarus* 100, 40-47. [8] Feldman et al. (2000) *JGR*, 105, 4175-4195. [9] Nozette et al. (2001) *JGR*, 106, 23253-23266. [10] Colaprete et al. (2010) *Science*, 330, 463-468. [11] Goddard (1920) *The Papers of Robert H. Goddard*. McGraw-Hill, New York. [12] Heiken et al. (1991) *Lunar Sourcebook*, Cambridge University Press, Cambridge. [13] Robinson et al. (2010) *Space Sci. Rev*., 150, -124. [14] Speyerer et al. (2010) abstract #2540, 44th Lunar and Planetary Science Conference.

MINI-RF EVIDENCE FOR WATER ICE AT THE POLES OF THE MOON P. D. Spudis[1], D.B.J. Bussey[2] and the Mini-RF Team 1. Lunar and Planetary Institute, Houston TX 77058 (spudis@lpi.usra.edu) 2. Applied Physics Laboratory, Laurel MD 20723

The existence of ice in the polar cold traps of the Moon has been debated for many years [1, 2]. Lunar Prospector found enhanced hydrogen levels in the polar regions [3]. The question was whether this hydrogen is present in the form of water ice [2]. Mini-RF is a synthetic aperture radar that flew on both the Indian Space Research Organization's Chandrayaan-1 mission to the Moon and on NASA's Lunar Reconnaissance Orbiter spacecraft [1]. Mini-RF is designed to map the permanently dark areas of the lunar poles and characterize the nature of the deposits there.

Mini-RF uses an unusual analytical approach to look for ice [4]. Traditionally, the key parameter used to determine if ice is present is the circular polarization ratio (CPR). This quantity is defined to be the magnitude of the same sense (i.e., the left or right sense of the transmitted circular polarization) divided by the opposite sense polarization signals that are received. Volumetric water-ice reflections are known to have CPR greater than unity, while surface scattering from dry regolith has CPR less than unity [2]. Mini-RF transmits a left-circular polarized signal and receives coherently the linear Horizontal and Vertical polarizations. This hybrid architecture preserves all of the information conveyed by the reflected signals [4]. From these data, all four Stokes parameters of the backscattered field are fully recoverable. These characterizations are critical to determine if the returned signal is caused by an ice-regolith mixture, or simply rocks on the lunar surface.

Mini-RF obtains data in S-band (2380 MHz, 12.6 cm) or X-band (7140 MHz, 4.5 cm) has an illumination incidence angle of 48°, and image strips have spatial resolution of 30 or 150 meters. Because the instrument looks off-nadir, there is a gap in SAR coverage within a couple of degrees of latitude around both poles. Portions of these gaps in coverage were partly filled by high-incidence angle SAR obtained by rolling the spacecraft slightly. Our data products include complete maps of both polar regions of the Moon at 15 and 75 m/pixel in both wavelengths. These images consists of Stokes parameters and derived maps of CPR and other Stokes "daughter" products, including degree of linear polarization [4].

Both poles have been well covered by Mini-RF data. The polar regions display backscatter properties typical for the Moon, with circular polarization ratio (CPR) values in the range of 0.1- 0.3, increasing to > 1.0 for young primary impact craters. These high CPR values likely reflect a high degree of surface roughness associated with these fresh features [5]. We have identified a group of craters in the north polar region that show elevated CPR (between 0.6 and 1.7) in their interiors, but no enhanced CPR in deposits exterior to their rims ([5], typical CPR values ~0.2 to 0.4; Fig. 1). Almost all of these features are in permanent sun shadow and correlate with proposed locations of polar ice modeled on the basis of Lunar Prospector neutron data [6]. The high interior and low exterior CPR are seen in data taken at both wavelengths and from opposite look directions, so it is a property of the Moon, not an observational artifact. These relations are consistent with deposits of water ice in these craters [5]. The south polar region shows similar relations, except that it has more extensive low CPR terrain and fewer anomalous high-CPR interior craters. Small areas of high CPR are found in some south pole craters, notably Shoemaker and Faustini; these areas might be deposits of water ice. Additionally, recent studies of the interior of Shackleton suggest patchy ice deposits may occur within this crater [7]. Modeling the response of mixtures of lunar regolith with varying degrees of ice and comparison with Mini-RF data for these anomalous craters supports the interpretation that the craters contain variable amounts of water ice [8]. Work continues to more fully understand the properties of these anomalous craters and ice at the poles.

References [1] Spudis P.D. *et al*. (2009) *Current Science* (India) **96**, 533; Nozette S. *et al*. (2010) *Space Science Reviews* **150**, 285-302 [2] Spudis P.D. (2006) *The Space Review* http://tinyurl.com/5g8kf4 [3] Feldman W. *et al*. (2001) *JGR* **106**, 23231 [4] Raney R. K. *et al*. (2010) *Proc. IEEE* **99**, 1-6, 10.1109/ JPROC. 20102084970 [5] Spudis, P. D. *et al*. (2010) *Geophys. Res. Lett*. **37**, L06204, doi:10.1029/2009GL042259 [6] Eke V.R. *et al*. (2009) *Icarus* **200**, 12-18 [7] Thomson B.J. *et al*. (2011) *Lunar Planet. Sci.* **XLII**, 1626 [8] Thompson, T. W. *et al*. (2011) *JGR* **116**, E01006, doi:10.1029/2009JE003368

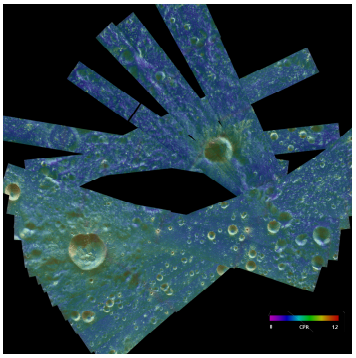

Fig. 1 CPR map of the lunar north pole. Small craters with high interior CPR and low exterior CPR probably contain deposits of water ice [5].

DEPTH OF 3-μm LUNAR ABSORPTION BANDS: THE EFFECT OF SURFACE BRIGHTNESS

L. V. Starukhina, Astronomical Institute of Kharkov National University, Sumskaya 35, Kharkov, 61022, Ukraine, starukhina@astron.kharkov.ua

Introduction: IR spectroscopy near 3 μm is one of instruments for search of water on the lunar surface. However, 3 μm absorption can be due to OH-groups formed in chemical trapping of solar wind (SW) protons on dangling bonds of oxygen in the implanted zone damaged by ion bombardment. This hypothesis was supported by theoretical simulation [1-3] as well as by experiments [4-7] before the discovery of 3 μm absorption on the Moon [8-10]. Deeper band depths in polar regions were explained by stronger retention of the implanted SW protons with decreasing temperature [1-3]; local variations of the depth being due to variance of retention ability with surface material. Mapping of the absorption depth over the lunar surface [11] stimulate further analysis of the observed spatial variations.

Theoretical modeling of lunar 3μm absorption: *Shape and position of 3μm absorption.* The shape and depth of the SW-induced 3 μm feature for the Moon was simulated in [12] on the base of spectral model for regolith [13]. Calculations have shown that the deepest 3 μm feature observed in [9] can be obtained at reasonable values of surface concentration of OH n_s = $2 \cdot 10^{17}$ cm^{-2}.

3μm absorption is most probably due to OH, because H_2O molecules in silicates dissociate into OH and H ions [14], so the shift of the band minima from ~2.8μm to ~2.9μm observed for highland-type material [11] may be due to difference in surface mineralogy. The band shape and width were reproduced in [12] taking account of different vibration frequencies of OH (between 2.7 and 3.5 μm [5-7]) located near different cations in various positions in complex atomic structure disordered by ion bombardment. In present work, such calculations are carried out for varied reflectance of regolith and OH abundance.

Surface brightness effect on the depth of 3μm band.

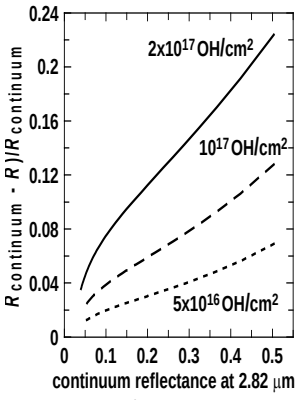

Fig. 1.

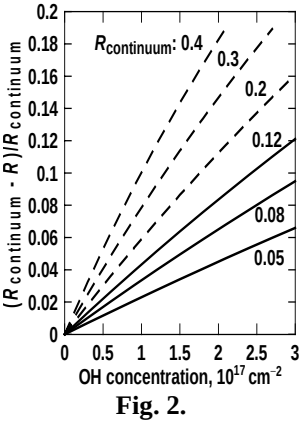

Fig. 2.

In Fig. 1, calculated 3μm depths are shown vs. reflectance of regolith at different surface concentrations n_s of OH. The range of OH abundance is from $5 \cdot 10^{16}$ cm^{-2}, typical of trapped hydrogen in lunar regolith particles from low-latitude regions [15], to $2 \cdot 10^{17}$ cm^{-2}, which is lower than $5 \cdot 10^{17}$ cm^{-2} obtained as saturation value for hydrogen implanted into olivine and enstatite in laboratory experiments [16]. In Fig. 2, OH abundance are varied and 3μm band depths are shown for different values of continuum reflectance of a powdered surface. The upper (dashed) and the lower (solid) lines present highland-like and mare material, respectively.

The calculated 3μm depth ranges are in consistence with M^3 observations [11]. The lower (dot) line in Fig. 1 covers 2.8μm depth range 0.015-0.045 observed for equatorial regions in reflectance range 0.067-0.32 and n_s = $5 \cdot 10^{16}$ cm^{-2} typical for such regions. The deepest absorption (0.1-0.2) shifted to longer wavelengths is observed in polar regions. There highest OH abundance (due to lower temperatures) and bright highland material dominate (see the top right corner of Fig. 2).

Conclusions: The observed spatial variations of the OH absorption are due not only to dependence of outgassing rates on surface temperature and composition, but to variation of regolith brightness, brighter soils showing deeper bands than the darker ones at the same OH concentration on particle surfaces. Calculated variations of 3μm absorption depth with surface brightness and OH abundance are consistent with those observed for lunar surface.

Acknowledgment: I thank Yu. G. Shkuratov and M. A. Kreslavsky for discussions, and CRDF grant UKP2-2897-KK-07 for support.

References: [1] Starukhina L. V. (1999) *LPS XXX*, Abstract #1094. [2] Starukhina L. V. (1999) *Solar System Res. 33*, 291-295. [3] Starukhina L. V. (2001) *JGR, 106*, 14701-14710. [4] Zeller E. J., et al. (1966) *JGR,. 71***,** 4855-4860. [5] Mattern P. L. et al. (1976) *J. Vac. Sci. Technol., 13*, 430 – 436. [6] Gruen D. M., et al. (1976) *J. Chem. Phys., 65*, 363 – 378. [7] Siskind B. et al. (1977) *J. Vac. Sci. Technol., 14*, 537 – 542. [8] Clark R. N. (2009) *Science, 326*, 562-564. [9] Sunshine J. M. et al. (2009) *ibid*, 565-568. [10] Pieters C. M. et al. (2009) *ibid*, 568-572. [11] McCord et al. (2011) *JGR, 116*, in press. [12] Starukhina L. V. and Shkuratov Y. G. (2010) *LPS XL1*, Abstract #1385. [13] Shkuratov Y. G. and Starukhina L. V. (1999) *Icarus 137*, 235-246. [14] Moulson J. and Roberts J. P. (1960) *Trans. Brit. Ceramic Soc. 59*, 388-394. [15] DesMarais D. J.et al. (1974) *Proc. LSC V*, 1811-1822. [16] Lord H. C. (1968) *JGR, 73*, 5271-5280.

WHAT DO ORIGIN MODELS TELL US ABOUT LUNAR VOLATILE DEPLETION? D. J. Stevenson, Caltech 150-21, Pasadena, CA 91125, djs@gps.caltech.edu.

Introduction: The giant impact model is a well established semi-quantitative description of the formation of Earth's moon. It is only partially quantitative because the full dynamical evolution of the impact generated disk has not yet been carried out (published models are deficient in one or more respects) and is not readily amenable to numerical simulation. The physics and physical chemistry are complex and the total evolution time (tens to thousands of years) is enormous compared to the orbital timescale. (By contrast, most of the immediate consequences of the giant impact are over in of order 24 hours.) Even the state of the disk immedatiely after the giant impact (the intial condition for orbital evolution) is not fully understood. In this presentation, emphasis will be placed on the uncertainties and how these translate into a range of possible "predictions", esepcially for the intial water of the moon. Unfortunately these range all the way from very dry to Earthlike (wet).

Limiting Cases: Pahlevan and Stevenson [1] proposed that the remarkable isotopic similarity of Earth and Moon (specifically for oxygen) may be explained by efficient mixing between Earth and Moon reservoirs, so that the Moon "looks like" Earth even if the projectile did not. It is not known whether this model is correct but it does have a variety of implications for isotopic relationships between Earth and Moon that are not violated by (and are perhaps even supported by) recent observations. This model is not as prescriptive (or as testable) as some workers have supposed because there is no simple connection between the turburlent diffusion of a tracer (oxygen or water) and the mechanism of angular momentum transport. In other words, diffusivity and kinematic viscosity need not be equal and are in general very non-equal. Current models for terrestrial planet formation suggest that Earth's water was delivered early rather than much later. Accordingly there is an identifiable limiting case in which the Moon would be initially as wet as Earth . This would be true *provided hydrodynamic escape has a longer characteristic timescale than diffusive re-equilibration.* In this limit, the region of lunar formation would be continuously replenished in water from the effectively infinite reservoir of Earth's magma ocean by outward transport (turbulent diffusion) in the disk. This limiting case cannot be excluded with certainty but seems unlikely since hydrodynamic escape rates are significant (cf [2], although the model they describe does not have a self-consistent density ansd temparature structure for the outflow region). The opposite limiting case is one in which the lunar forming region is effectively isolated from the terrestrial water reservoir, perhaps through rapid viscous evolution of the disk. Hydrodynamic escape from the outer periphery of the disk is favored by the lower gravitational energy requirement and this then dries out this isolated reservoir, leading to strong volatile depletion of the newly forming moon. There is not yet a detailed model that describes this but an outline of such a model will be provided in this presentation.

Challenges: The Moon is heterogeneous and even if the modeling strategy outlined above can be carried through, the connection to the observables requires a good understanding of the later evolution (the magma ocean phase of early lunar evolution.)

References:

[1] Pahlevan, K and Stevenson, D. EPSL, 262, 438 (2007). [2] Desch, S ad Taylor, G. J. LPSC 42 (2011).

WATER IN THE MOON: IMPLICATIONS FOR LUNAR FORMATION AND GEOCHEMICAL EVOLUTION. G. Jeffrey Taylor, Hawaii Inst. of Geophys. and Planetology, UH NASA Astrobiology Program, 1680 East-West Rd., Honolulu, HI 96822; gjtaylor@higp.hawaii.edu

Introduction: Recent lunar sample analyses of pyroclastic glasses and apatite crystals in igneous rocks and breccias [1–5] have demonstrated the presence of water in the lunar interior. This overturned a four-decades-old conclusion that the Moon was anhydrous. This important discovery has implications for lunar origin and differentiation, and the ultimate sources of water to Earth and Moon. I summarize key issues here.

What is the water content of the bulk Moon? Although the Moon clearly has vastly more water than thought previously, its bulk water content is not known. Estimates range from tens of ppm based on pyroclastic magmas [1] to as low as 0.1 ppb determined on from fractionation of Cl isotopes [6]. The data imply that water is heterogeneously distributed in the Moon.

Water does not appear to be correlated with REE: Water behaves as an incompatible element during igneous processes, until low pressure allows it to escape from magma, so it ought to correlate with REE [7]. No such correlation is evident.

How did picritic glasses acquire water? The hundreds of ppm of water apparently present in the picritic magmas that produced pyroclastic eruptions [1] either came from source regions containing sufficient water (tens of ppm) or acquired it from hydrous regions as the magmas ascended to the surface. Magma ocean models [7] indicate that initial cumulates in the depth range (300-500 km) of picritic source regions contained only a few ppm or less if the initial lunar water content was ≤100 ppm. This has implications for lunar differentiation (nature of magma ocean turnover), magma interaction with rocks rich in incompatible-elements and/or water, and whether water was added to the Moon after it formed.

Does the Moon have inherently high D/H? Greenwood et al. [5] show that δD in lunar apatite crystals ranges from about -200 to 1000, with most values being clearly elevated compared to terrestrial D/H. It is critically important to determine if the high D/H in the lunar samples represents fractionation during loss of water from magmas or from the protolunar disk, or whether it represents the isotopic composition of bulk lunar water. If the latter, it could be a fingerprint of the objects that delivered water to the Moon [5].

Did the Earth and impactor have water when the moon-forming giant impact happened? A fundamental issue in planetary science is how and when Earth and the other terrestrial planets obtained their water [e.g., 8]. It is feasible to add water to both Moon and Earth after they formed, but it is also likely that Earth contained at least some water by chemisorption onto dust grains that ultimately accreted to form the Earth, and probably the moon-forming impactor [8].

How much water and other volatiles were lost from the protolunar disk? Desch and Taylor [9] suggest that the Moon retains about 2% of the water initially in the Earth and impactor. If the Earth and impactor had 500 ppm to begin with [10], lunar bulk water would be 10 ppm. Other volatiles would also be lost, in proportion to their solubility in the molten region of the protolunar disk. Loss of volatiles during volcanic eruptions can be quantified by an "emanation coefficient" [11]. Using this as a guide, lunar/terrestrial bulk abundances of volatile elements [12-13] can be compared to their emanation coefficients and to predicted abundances based on those coefficients. Abundances show a broad correlation with volatility, but there is considerable scatter.

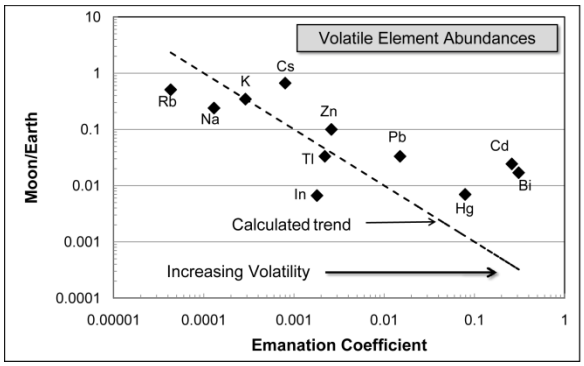

References: [1] Saal, A. E. et al. (2008) *Nature* **454**, 192-194. [2] McCubbin, F. M. et al. (2010) *PNAS* **107**, 11223-11228. [3] McCubbin, F. M. et al. (2010) *Am. Mineral.* **95**, 1141-1150. [4] Boyce, J.W. et al. (2010) *Nature* **466**, 466-469. [5] Greenwood, J.P. et al. (2011) *Nature Geosci.* 4**,** 79-82. [6] Sharp, Z.D. et al. (2010) *ScienceExpress*, 10.1126/science.1192606. [7] Elkins-Tanton, L. (2010) *LPSC 41st*, #1451. [8] Drake, M.J. (2005) *Meteor.Planet.Sci.* **40**, 1-9. [9] Desch, S.J. and Taylor, G.J. (2011) *LPSC 42nd*, #2005. [10] Mottl, M. et al. (2007) *Chem Erde* **67**, 253-282. [11] Rubin, K. (1997) *GCA* **61**, 3525-3542. [12] Taylor, S.R. and McLennan, S.M. (2009) *Planetary Crusts*, Cambridge. [13] McDonough, W.F. and Sun, S.-s. (1995) *Chem. Geol.* **120**, 223-253.

CONSTRAINING MODELS OF WATER MIGRATION IN THE LUNAR SUBSURFACE Luís F. A. Teodoro[1], Richard C. Elphic[2], Vincent R. Eke[3], Matthew Siegler[4], Norbert Schörghofer[5], [1]BAER Inst., NASA Ames Research Center, Moffett Field, CA 94035-1000, USA; luis@astro.gla.ac.uk; [2]NASA Ames Research Center, Moffett Field, CA 94035-1000, USA, [3]Department of Physics, Durham University, Science Laboratories, South Road, Durham DH1 3LE, UK, [4]Department of Earth and Space Sciences, UCLA, Los Angeles, CA 90095-1567, USA, [5] Institute of Astronomy, University of Hawaii at Manoa, Honolulu, Hawaii 96822, USA

The main aim of this research is to constrain models of the ice distribution with state-of-art lunar data and to gain a better understanding of water ice dynamics in the lunar sub-surface throughout the lunar history. Although controversial in its physical form (e.g., crystalline as opposed to amorphous), there is increasing evidence of water ice at the lunar poles "cold traps". Such locations plausibly hold not only water ice but also other volatiles of economic and scientific value. Future missions may include rovers with the ability to sample materials from the top metre of the surface. This requires the identification of regions to explore and sample with the highest likelihood of finding water ice. Cold traps, including those a few cm below the surface, are the most plausible candidates.

To understand the current distribution of water ice in the polar neighbourhoods, one needs to study the dynamics of water in the top layer of regolith throughout lunar history. In a seminal paper, [1] investigated the migration of H_2O molecules in the lunar regolith by random hops within the pores. In the current study, we propose to apply a more realistic diffusion model than the ones used in [1] to regions of the lunar surface where the measured temperatures (from LRO/Diviner) and the hydrogen maps (from Lunar Prospector) suggest that the water ice has been stable over the last few billion years.

Subsurface water ice migration and stability revisited: Water molecules move through the interstices in a porous regolith. In the Knudsen diffusion regime, the molecules do not interact with one another, but move in straight lines between points on the pore channel surface. Upon collision with the surface, a molecule adsorbs for some time, the residence time, that depends on the local temperature. An irregular surface can be considered as a perturbation on the top of a pore with a smooth surface. Along the pore, there are a large number of voids with a power law size distribution within the fractal range that describes the regolith at the Apollo sites [2]. In order to produce more realistic water ice distributions the effects of a fractal grain surface specifications are included in our novel analysis. We also study the implications of considering that the water molecules deposition and sublimation rates on the surface of a regolith grain to be the same [1]. This is justifiable if the water vapor is in equilibrium with the ice mono-layers on the grain surface. However, at locations where the density of water molecules in the vapor phase is larger (smaller) than the equilibrium vapor density [1] one expects deposition (sublimation) at a rate larger than the one predicted by equilibrium.

An accurate understanding of the temperature profile in the sub-surface is central to the modelling of the water ice distribution with depth since the molecules' mobility is controlled not only by the pore size and geometry but also by the residence time. We use temperature maps constrained by the latest LRO Diviner measurements [3]. However, besides the physical conditions for ice stability one needs also to consider the places where there had been a delivery of volatiles over the last two and half billion years. The best candidates are the regions that present the highest hydrogen concentrations as seen by the joint analysis of Lunar Prospector Neutron Spectrometer and topography data-sets [4]. Currently, we are considering including weathering and/or gardening in our models [5].

References: [1] N. Schörghofer, et al. (2007) *Journal of Geophysical Research (Planets)* 112(E11):2010 doi. [2] G. H. Heiken, et al. (1991) *Lunar sourcebook - A user's guide to the moon*. [3] D. A. Paige, et al. (2010) *Science* 330:479 doi. [4] L. F. A. Teodoro, et al. (2010) *Geophys. Res. Lett.* 37:12201 doi. [5] D. H. Crider, et al. (2003) *Advances in Space Research* 31:2293 doi.

THERMOCHEMISTRY OF APATITE AND ITS SOLID SOLUTIONS, APATITE-MELT PARTITIONING, AND IMPLICATIONS FOR THE MOON. A. H. Treiman[1] and J. W. Boyce[2], [1]Lunar and Planetary Institute, 3600 Bay Area Boulevard, Houston TX 77058 <treiman#lpi.usra.edu>. [2]Division of Geological and Planetary Sciences, Caltech, 1200 E. California Blvd. Pasadena, CA 91125 <jwboyce$caltech.edu>.

Introduction: Following the observation of H in lunar basaltic glasses [1], most of subsequent evidence has comes from analyses and interpretation of apatite grains in lunar igneous rocks [2-4]. Compositions of these apatites have been used to infer water contents of their parental magmas. To do this calculation properly requires knowing thermochemistry of volatile partitioning between apatite and melts, solid solution properties of apatites, and the effects of physical and chemical conditions on that partitioning.

Thermochemistry: To constrain the volatile compositions of phases associated with lunar apatite, one needs precise and accurate thermochemical data on apatite and its solid solutions. Literature data for end-member Ca-apatites are sufficient and mostly self-consistent (fluorapatite: [5-8]; chlorapatite: [5,9-12]; hydroxylapatite: [5,10,11,l3,14]). The thermochemistry of solid solutions in $Ca_5(PO_4)_3(F,Cl,OH)$ are not entirely clear. They may be ideal at the temperatures expected for lunar magmas and fluids [5,8,9], may also be non-ideal [15-17] consistent with evidence for anion ordering [18,19]. These apparent non-idealities have also been ascribed to solid solution of O^{2-} in place of OH & Cl [8,20].

Apatite-Melt Partitioning: Partition coefficients (as normally defined) like $D^{F}_{apat/basalt}$ are strongly dependent on compositions of both apatite and basalt. This dependency arises first because of closure: apatite must contain a fixed proportion of F+Cl+OH, while melts and fluids are not so constrained. Consider an OH-free, Cl-free, melt just saturated in F-apatite giving $D^{F}_{apat/basalt} = D_0$. The melt can accept more F, but the apatite cannot; thus $D^{F}_{apat/basalt}$ can vary, and be smaller than D_0! Thus, use of an experimental value for $D^{F}_{apat/basalt}$ can lead to an overestimate of the magma's proportion of F (or OH).

More proper is to consider exchange equilibria like $Ca_5(PO_4)_3Cl + F^-(melt) = Ca_5(PO_4)_3F + Cl^-(melt)$. For this, one can calculate an equilibrium constant K $\frac{x_{F-Ap}}{x_{Cl-Ap}} \cdot \frac{x_{Cl^-}}{x_{F^-}} = \exp\left(\frac{-\Delta G^0_{rxn}}{RT}\right) = K$ (here assuming ideal solid and melt solutions). Experimental data on anion partitioning are accommodated (to zero order) by this simple model: Fig. 1. Scatter in those fits can be ascribed to analytical undertainties [23], and to other compositional dependencies (e.g., F-Cl and F-OH partitionings are not identical [21,22], though they plot together in the Figure). Most of the literature data on apatite/basalt partitioning are for OH-rich systems, which may not be relevant for lunar magmas.

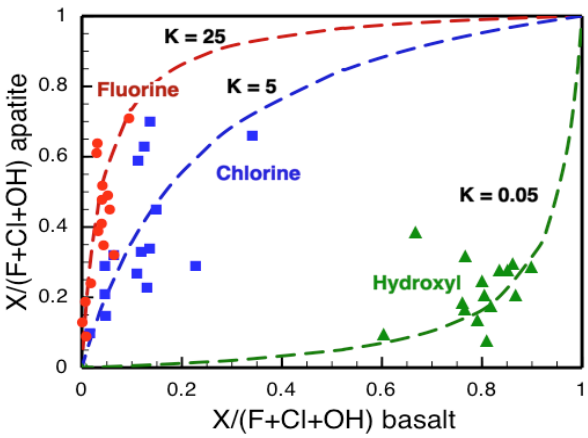

Fig. 1. Anion partitioning between apatite and basalt melt [21,22], and model fits with K values as in the equation.

Conclusions: Although the thermochemistry of Ca apatites is fairly certain, more data are needed on their solid solutions at magmatic temperatures. There is a critical need for apatite/melt partitioning experiments with lunar-relevant compositions. Use of single-element partition coefficients (e.g., $D^{F}_{apat/basalt}$) can lead to erroneous inferences. Apatite compositions can provide crucial clues to volatile abundances and proportions in lunar magmas, but must be interpreted with care.

References: [1] Saal A. et al. (2008) *Nature* **454**, 192-195. [2] Boyce J.W. et al. (2010) *Nature* **466**, 466-469. [3] McCubbin F.M. et al. (2010) *PNAS* **107**, 11223-11228. [4] Greenwood J.P. et al. (2011a) *Nature Geoscience* **4**, 79-82. - (2011b) *Lunar Planet. Sci.* **42nd**, Abstract #2753. [5] Zhu C. & Sverjensky D.A. (1991) *GCA* **55**, 1837-1858. [6] Robie R.A. & Hemingway B.S. (1995) *Thermodynamic properties of minerals and related substances at 298.15 K and 1 Bar (10^5 Pascals) pressure and at high temperatures.* U.S.G.S. Bulletin 2131. [7] Dachs (2010). [8] Hovis G.L. & Harlov D.E. (2010) *Amer. Mineral.* **95**, 946–952. [9] Tacker R.C. & Stormer J.C.Jr. (1989) *Amer. Mineral.* **74**, 877-888. [10] Jemal M. (2004) *Phosphorus Res. Bull.* 15, 119-124. [11] Cruz F.J.A.J. et al. (2005) *J. Chem. Thermo* **37,** 1061-1070. [12] Venkata Krishnan R. et al. (2008) *Thermochim. Acta* **478**, 13-16. [13] Egan E.P.Jr. et al. (1950) *J. Amer. Chem. Soc.* **72**, 2418-2421. [14] Jemal M. et al. (1995) *Thermochim. Acta* **259**, 13-21. [15] Duff E.J. (1972) *J. Inorg. Nucl. Chem.* **32**, 859-871. [16] Driessens F.C.M. (1979) *Ber. Bunsengesellschaft physical. Chemie* 83, 583-586. [17] deLeeuw N.H. (2002a) *Phys. Chem. Chem. Phys.* **4**, 3865–3871. - (2002b) *Chemistry Materials* **14**, 435-441. [18] Hughes J.M. & Rakovan J. (2002) Ch. 1 in *Phosphates, Rev. Mineral. Geochem.* 48. [19] Tacker R.C. (2004) *Amer. Mineral.* **89,** 1411–1421. [20] Schettler G. et al. (2011) *Amer. Mineral.* **96**, 138–152. [21] Mathez E.A. & Webster J.D. (2005) *GCA* **69**, 1275-1286. [22] Webster J.D. et al. (2009a) *GCA* **73**, 559-581. - (2009b) *Chem. Geol.* **263**, 19-36. [23] Boyce J.W. (2011) this meeting.

EXPERIMENTAL DETERMINATION OF DEGASSING PATH OF VOLATILES FROM LUNAR MAGMAS: NEW INSIGHTS FROM TIME STUDIES G. Ustunisik[1], H. Nekvasil[1], and D. H. Lindsley[1], [1]Department of Geosciences, Stony Brook University, Stony Brook, NY 11794-2100, Gokce.Ustunisik@stonybrook.edu, Hanna.Nekvasil@sunysb.edu.

Introduction: An essential part of the current lunar paradigm is that the lunar mantle contains very little water [1-4]. The primary line of reasoning behind this acceptance was perfectly consistent with the high-temperature, Moon-forming giant impact event [e.g., 5-7] until the recent evidence for water in the lunar interior by analysis of pyroclastic lunar glasses [8] as well as apatite grains in a variety of lunar lithologies [9-12]. These careful determinations have challenged the old paradigm of a "dry" mantle and opened the possibility that the strongly volatile depleted feature of lunar samples may not be correlated to volatility during the Moon-forming phase, but rather may have arisen by secondary magmatic processes at a much later stage.

Even though analysis of lunar apatites has provided invaluable information on instantaneous magmatic volatile contents, using this information to extract parental magmatic volatiles contents and source region volatile contents is not straightforward because apatite is commonly a late-crystallizing mineral and may reflect late-stage open system processes that have perturbed the magmatic volatile content. Therefore, the direct use of the inferred instantaneous volatile content of magmas co-existing with apatite to assess the bulk volatile content of the source regions was questioned by [13, 14] based on a set of mass balance calculations for the KREEP-bearing samples analyzed by [11]. These computations showed that the apatites record a degassing process that resulted in both loss of magmatic volatiles and in significant changes in the relative volatile contents of the residual liquids, which affected the composition of the apatites forming.

Recent degassing experiments [15,16] were conducted to determine the absolute and relative changes in abundance of volatiles (Cl, F, OH, and S) in the melt during the ascent of a lunar magma from 100 km depth to the surface without crystallizing. Based on the initial and final values for Cl, F, H_2O, and S (wt%), degassed samples with initially 2.2 and 2.5 wt% water lost 99-100% water, 89-84% Cl, 60-61% F, and 94-92% S. This percentage loss also affected the relative volatile contents of the melt with a strong decrease in water content and an increase in F:Cl ratio. In reflection of changes in melt volatile contents, hypothetical computed apatite compositions also show a strong reduction in OH content and a decrease in Cl:F ratio. While computed apatites from the initial (undegassed) magma had 20% Cl, 48% F, and 32% OH, computed apatites from degassed melts showed 10% Cl, 90% F, and 0% OH.

The mass balance computations of [13, 14] also indicated a two-stage degassing path consistent with the alkali halide-water systems in which a water and Cl-rich fluid vapor and aqueous liquid is lost first, followed by a more Cl-rich assemblage. Cl and F contents of apatite vary according to their lithologic type and these variations are not random but show a systematic path. The degassing experiments of [15,16] were designed to determine the composition of the bulk vapor and saline liquid assemblage from a synthetic 14053 composition [17] with added water, F, Cl, and S. However, these experiments did not provide insights in to the pathways taken by degassing. New experiments were designed as time studies and implemented to assess potential information on the degassing pathways.

Experimental Design and Details: The experiments are similar to those discussed by [15, 16, and in submission] but were designed to monitor changes in relative volatile content during successive intervals of low pressure degassing of a synthetic melt of 15043 with 0.5 wt% Cl, 0.5 wt% F, and 0.3 wt% S and 2.5 wt% water. The volatile-bearing glasses are prepared at 0.5 GPa in piston-cylinder apparatus then placed in Fe^o-capsules inserted into a long silica tube. After evacuation, the tubes are sealed and suspended by a Pt-wire into a vertical furnace and heated above the liquidus T for 2, 4, and 6 hours before quenching. Both the starting hydrous glasses and the degassed glasses at the end of each degassing interval are analyzed optically as well as by electron microprobe (at the AMNH) and by micro-FTIR (for water) at SUNY Stony Brook. The results of these experiments will be presented at the conference.

References: [1] Taylor, S.R. et al. (2006) *New Views of the Moon*, 657-704. [2] Fegley, B. and Swindle, T.D, (1993) *Resources of Near-Earth Space*, 367-426. [3] Papike et al. (1998) *Lunar Samples in Planetary Materials*, 5-1 - 5234. [4] Taylor (1992) *Solar System Evolution, A New Perspective*, 307p. [5] Albarede, F. (2009) *Nature*, 461, 1227–1233. [6] Canup, R. M. (2004) *Annu. Rev. Astron. Astr.*, 42, 441–475. [7] Lucey, P., et al. (2006) *Min. Soc. Am.*, 83–220. [8] Saal A. E. et al. (2008) *Nature*, 454,192–195. [9] Greenwood J. P. et al. (2011) *Nature Geosciences*, 4, 79-82. [10] McCubbin F. M. et al. (2010) *Am. Min*., 95. [11] McCubbin F. M. et al. (2010) *PNAS* 107, 11223. [12] Boyce J. W. et al. (2010) *Nature, 466*, 466-469. [13] Nekvasil et al. (2010) *AGU*, P41A05. [14] Nekvasil et al. (2011) *LPSC XLII ,2240*. [15] Ustunisik et al. (2010) *AGU*, P41A04. [16]Ustunisik et al. (2011) *LPSC XLII ,2643*. [17] Willis J. P. et al. (1972) *LPSC III*, 1269-1273.

CARBON SOLUBILITY IN LUNAR MAGMAS. D. T. Wetzel[1], M. J. Rutherford[1], S. D. Jacobsen[2], E. H. Hauri[3], and A. E. Saal[1], [1]Dept. of Geological Sciences, Brown University, Providence RI 02912 (Diane_Wetzel@brown.edu) , [2]Dept. of Earth and Planetary Sciences, Northwestern University, Evanston, IL 60208 (steven@earth.northwestern.edu) , [3]DTM Carnegie Institute of Washington, DC 20015 (hauri@DTM.ciw.edu).

Introduction: Available evidence suggests in the absence of water, carbon is the element responsible for generating the gas phase that drove lunar fire-fountain eruptions [1, 2]. The gas phase is generated by the oxidation of reduced C carried in the magma from depth [3]. Recent experiments have confirmed that C first forms a CO-rich gas phase in lunar picritic magmas at 40 MPa (~8.5km) [4]. A conduit flow model [5] predicted as little as 50 ppm C in the magma would create gas in sufficient quantities to drive the lunar eruptions. Recently, Saal et al. [6] identified indigenous H (H_2O), F, Cl, and S in a range of picritic glass compositions. Concentrations were found as residual diffusion-loss profiles in the lunar beads, which led to estimates for initial lunar volatile abundances. With new SIMS detection limits of 0.13 ppm C, Saal et al. [7] determined that picritic glass beads contained from 0-0.69 ppm C. Our study was designed to determine the solubility and speciation of C in H-bearing, graphite-saturated picritic lunar magmas, and the effect of H on the initial gas phase generated in these magmas at liquidus T's.

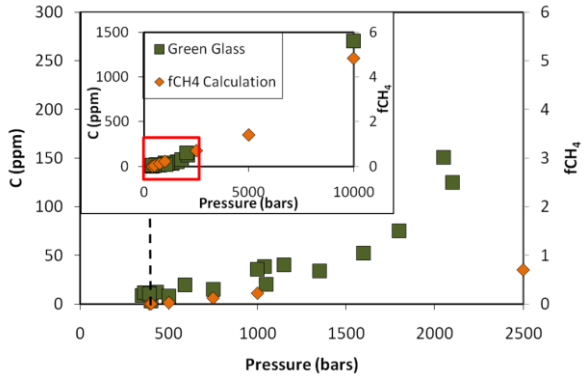

Fig 1: Carbon vs. pressure graph shows C increases with increasing P in the graphite-stable field at fO_2 ~IW. C decreases with the generation of CO-rich gas at P<400 bars (dashed line). CH_4 fugacity for the coexisting fluid phase was calculated [10].

Experimental and analytical methods: Experiments on synthetic A15 green glass compositions were carried out in an IHPV on pellets of powder, which were reduced to fO_2~IW. Samples were run with excess graphite in sealed Pt tubes as described by [4]. Temperatures were 1465°C, or ~15°C above the green glass liquidus T, at lower pressures and 1500°C for higher pressures (1 GPa). Pressures ranged from 30-1000 MPa. Samples were quenched to a glass and analyzed by EMP, SIMS, FTIR, and Raman spectroscopy.

Results: Experimental samples pre-set at IW and enclosed in graphite contained a glass with lower FeO due to the formation of Fe-metal at pressures below 40 MPa. At pressures greater than 40 MPa, C in the green glass has a strong positive correlation with pressure (Fig. 1). Abundances were determined by SIMS for all of the glasses, resulting in 3-150 ppm C at lower pressures and up to 1400 ppm C for a 1 GPa experiment. Analyses also show a positive correlation between dissolved C and H_2O in the experimental glasses. Raman spectroscopy indicates CH_4 present in the melt, which confirms the observed trend between C and H_2O in the lower pressure glasses.

Discussion and Conclusions: Analyses of the natural lunar samples [2] and our experimental green glasses suggest the formation of a CO-rich gas phase via C-oxidation at P< 40 MPa due to Fe metal present in these melts. With hydrogen present, Raman spectroscopy indicates CH_4 is the dominant C species dissolved in the melt. (Depending on the relative abundance of C and H in the magma, there may or may not be reduced C with CH_4 in ascending magma). Therefore, the solubility of C in picritic melt (Fig. 1) is directly proportional to the concentration of dissolved CH_4 and increases with increasing fCH_4. Experiments with water contents of 1000 ppm and excess graphite produced increasing maximum dissolved C in melts up to 1490 ppm at 1 GPa. Greater H_2O contents contribute to both CH_4 and water species (H_2O, OH^-, and H_2) present in the melt. If decompression-induced CH-gas saturation is reached at pressures greater than 40 MPa, methane could produce the first gas phase. These results are consistent with experiments on Na-silicate [8] and haplobasaltic [9] melts that indicate CH_4 dissolved in melts at fO_2~IW. Thermodynamic models [10] predict a CH_4- and H_2-rich gas phase in equilibrium with a melt at higher pressures and CO-rich gas phase at lower pressures (near 40 MPa C oxidation reaction).

References: [1] Sato M. (1976) *PLSC 7th*, p.1323-25. [2] Fogel R.F. and Rutherford M.J. (1995) *GCA, 59*, 201-15. [3] Heiken G.H. et al. (1974) *GCA, 38*, 1703-18. [4] Nicholis M.G. and Rutherford M.J. (2009) *GCA, 73*, 5905-17. [5] Rutherford M.J. and Papale P. (2009) *Geology, 37*, 219-22. [6] Saal A.E. et al. (2008) *Nature, 454*, p.192-95. [7] Saal A.E. et al. (2009) *Goldschmidt*, A1139. [8] Mysen et al. (2009) *GCA, 73*, 1696-1710. [9] Ardia P. et al. (2011) *LPSC XLII*, Abst. #1659. [10] Zhang C. and Duan Z. (2009) *GCA, 73*, 2089-2102.

DISCOVERY OF HEAVY ATOMS IN THE EXOSPHERE ABOVE THE PERMANENTLY SHADOWED REGION IN CABEUS. D. H. Wooden[1] , A. Colaprete[1], J. L. Heldmann[1], K. D. Retherford[2], R. M. Killen[3], R. Elphic[1] and K. Ennico[1], [1]NASA Ames Research Center, MS 245-3, Moffett Field, CA 94035-0001, Diane.Wooden@nasa.gov, [2]Southwest Research Institute, 6220 Culebra Rd., San Antonio, TX 78228, [3]NASA Goddard Space Flight Center, Code 695, Greenbelt MD 20771.

Introduction: The LCROSS (Lunar Crater Observation and Sensing Satellite) mission impacted the permanently shadowed region (PSR) of the Cabeus crater near the south pole of the Moon on 9 October 2009. A plume was created by the impact of the Centaur upper stage of the launch vehicle and observed by the LCROSS Shepherding Spacecraft (S-SC) instrument suite that allows us to characterize the water and volatile concentrations and to characterize the nature of the particulates released from the permanently shadowed region (PSR) on the floor of Cabeus crater [1, 2].

Emergence of UV Emission Lines as UV-Visible spectrometer FOV narrows in on Cabeus PSR: During the hour before impact, the LCROSS S-SC followed behind the Centaur by a distance of ~625 km and the LCROSS S-SC instrument suite took data to serve as a baseline for the study of the Centaur impact plume. Figure 1 shows the Radiance of the Mg I line growing in contrast to the solar reference spectrum as the spectrometer 1˚ nadir Field-of-View (FOV) narrows in on where the Centaur will hit the permanently shadowed region (PSR) of Cabeus.

During the last 125 [s] before Centaur impact, the spectrometer FOV no longer contains sunlit terrain. The "Cabeus PSR Exosphere" spectrum is derived from the last 19 spectra acquired before the S-SC observes the Centaur impact plume as follows. We remove the cosmic-ray hits from each of the 19 spectra prior to statistical analyses. The 19 spectra are then co-added to derive a mean and error in the mean without using those pixels identified as cosmic-ray hits. The result of subtracting a scaled solar reference spectrum from the mean of 19 scans is the high signal-to-noise emission line spectrum.

Cabeus PSR Exosphere: The UV spectrum of the nadir-view of Cabeus PSR at 900–625 km altitude is complex. These spectra reveal a forest of UV emission lines that we hypothesize are detection of new species in the lunar exosphere. Never before has the moon been investigated at these short wavelengths at such close distance. In the LCROSS UV spectra, we have identified Mg I (285.2 nm) with a high Signal-to-Noise Ratio (SNR=46). We tentatively identified lines of Ca, Fe, and Ti, where most but not all lines appear to be neutral species fluorescing from near the ground state. Specifically, the Fe I (372.1 nm) line (SNR=41) is present, which was predicted by [3]. Initial analyses of the Cabeus PSR Exosphere spectrum will be discussed during the Wet versus Dry Moon meeting.

Discussion: Studying the lunar exosphere can tell us generally about volatile transport processes, e.g., how the water and hydroxyl molecules seen by M3 and EPOXI at low latitudes are transported to the poles. Detection of heavy atoms above Cabeus PSR supports the goals of the LADEE Mission to detect heavy atoms in the Exosphere at mid-latitudes [4, 5].

References: [1] Colaprete A. et al. (2010) *Science, 330,* 463-468. [2] Schulz, P. et al. (2010) *Science 330*, 468. [3] Morgan T. H. and Killen R. M. (1997) *Planet. Space Sci. 45,* 81–94. [4] Sarantos M. et al. (2010) Lunar Exploration Analysis Group (LEAG) LPI Contrib. No. 1595, p. 62. [5] Author G. H. (1996) *LPS XXVII,* 1344–1345. [4] Killen R. M. et al. (2010) AGU Abstract #P42A-04.

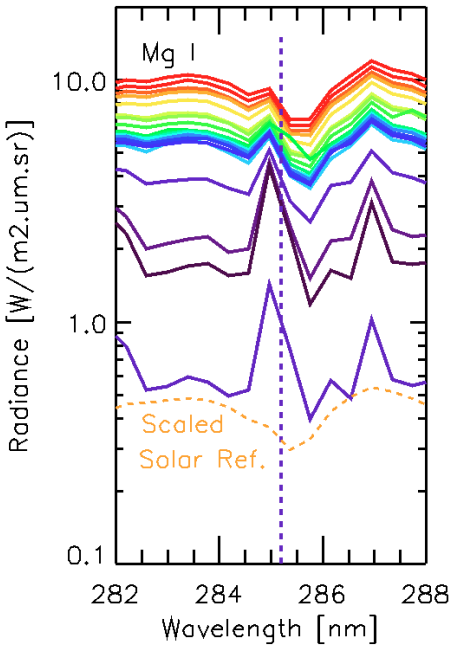

Figure 1. Mg I line revealed in the ~hour-long pre-impact descent of the LCROSS S-SC from 8100 km to 600 km. As less lit terrain is in the spectrometer's nadir 1˚ Field-of-View, the Radiance decreases and the Mg I line contrast increases with respect to a scaled solar reference spectrum, obtained from lit terrain at ~8000 km. A vertical line marks the rest wavelength of 285.2 [nm]; the LCROSS UV-Visible spectrometer wavelength scale has an uncertainty of +/- 0.25 [nm].

NOTES

NOTES